W.-Y. Cheng
H.-T. Lee
M.-H. Sun
C.-C. Shen

A Pterion Keyhole Approach for the Treatment of Anterior Circulation Aneurysms

257

Abstract

The supraorbital keyhole approach is most frequently used in treatment for lesions within the anterior cranial base. However, it has some drawbacks, including cosmetically poor appearance of the scar, forehead deformity, and difficulty in dealing with some kinds of middle cerebral artery (MCA) and internal carotid artery (ICA) aneurysms. Therefore, we have developed a small pterion keyhole approach for an alternative access to treat anterior circulation aneurysms. An oblique skin incision about 3–5 cm in length was made just from 1.0 cm anterior to the superficial temporal artery at the level of the zygomatic arch, curved just below the temporal line to the forehead, and stopped at the hairline over the sylvian fissure. Then a small craniotomy (2–3 cm) was made just over the sylvian fissure and the aneurysms were exposed through the lateral cerebral fissure. We used this approach to treat 40 patients with aneurysms located in posterior communicating arteries (n = 14), the MCA (n = 10), the anterior communicating arteries (n = 9), the anterior cerebral artery (n = 1), the ophthalmic arteries (n = 3), and the ICA (n = 3). The general outcome of all patients was good without serious complications from the surgical technique even though 3 cases underwent intraoperative premature rupture of the aneurysms. No approach-related complication occurred except that one patient had vasospasm 2 days after the aneurysm clipping. In conclusion, this pterion keyhole approach can achieve the best operative effect for the treatment of intracranial anterior circulation aneurysms in a selective group of patients with several advantages over traditional craniotomy including minor tissue damage, less brain retraction, a superior cosmetic result, and shorter duration of surgery. Moreover, the operative field becomes wider in the deep area, providing sufficient space for microscope-assisted surgery without the need for highly specialized instruments.

Key words

Intracranial aneurysms · keyhole · minimally invasive · pterion

Introduction

The most definitive treatment for intracranial aneurysms is surgical clipping. In most cases, a frontotemporal craniotomy is required. Although this is tolerated well by most patients, reducing the size of the opening would be beneficial. Recent advances in minimally invasive technique and instrumentation permit certain intracranial aneurysms to be treated using very small openings. These so-called "keyhole" openings have been used for exposure of lesions within the anterior cranial base [1–5]. Potential advantages of these approaches include reduced operative morbidity, expeditious patient recovery, and cost effectiveness in case management. However, the keyhole approach is not appropriate for every aneurysm. Only selected patients can benefit from this innovative approach. The mini-craniotomy used in these approaches sometimes requires the use of special instrumentation. In various keyhole procedures, the supraorbital approach is most frequently applied for the treatment of supratentorial aneurysms. However, this procedure has some problems including cosmetically poor appearance of the scar, forehead deformity, and difficulty in dealing some types

Table 1 Location of aneurysms in 40 patients						
Location of aneurysm	**ICA**	**ACA**	**ACoA**	**PCoA**	**MCA**	**Ophthalmic artery**
Number of patients	3	1	9	14	10	3

ICA = internal carotid artery; ACA = anterior cerebral artery; AcoA = anterior communicating artery; PcoA = posterior communicating artery; MCA = middle cerebral artery.

Table 2 Hunt and Hess grade and Fisher grade of the patients (n = 40)					
Grade	**I**	**II**	**III**	**IV**	**V**
Hunt and Hess	18	17	5	0	0
Fisher	22	14	4	0	–

of middle cerebral artery (MCA) and internal carotid artery (ICA) aneurysms. In this article, the authors present an interesting keyhole approach to treat anterior circulation aneurysms via a pterion minicraniotomy.

Patient and Methods

Patients and criteria
From March 1999 to December 2004, we clipped 40 intracranial aneurysms of the anterior circulation via a pterion keyhole approach. The aneurysmal locations included 14 posterior communicating arteries (PCoA), 10 MCAs, 9 anterior communicating arteries (ACoA), 1 anterior cerebral artery (ACA), 3 ophthalmic arteries, and 3 ICAs (Table 1). The patients were selected on the basis of the following criteria: Hunt and Hess Grades I through III, and subarachnoid hemorrhage evaluated as Fisher Grades I through III (Table 2). The patients comprised 24 females and 16 males with an average age of 57.4 years (ranged from 33 to 84 years). Twenty-five patients presented with subarachnoid hemorrhage (SAH), of whom twenty received early operation and five received delayed operation. Fifteen aneurysms without rupture received a regular operation. For releasing intracranial pressure and making the minicraniotomy easy, a lumbar drainage tube was inserted to drain the cerebrospinal fluid in some cases. The pterion keyhole approach was performed as we have previously described [6] and is detailed below.

Head position and skin incision
Under general anesthesia, the patient was placed in a supine position and immobilized with sandbags. The head was rotated to the side contralateral to the operative field so that the ipsilateral sylvian fissure and sphenoid ridge are oriented vertically. This rotation usually required turning of the patient's head by approximately 30–60 degrees according to the location of the aneurysm. In addition to rotation, the vertex of the head was placed downward, allowing the surgeon to see into the sylvian fissure later. Finally, the head and neck were elevated to improve venous drainage. The ipsilateral shoulder was elevated with a cushion beneath to keep the zygomatic arch horizontal. An oblique skin incision about 3–5 cm in length was made just from 1.0 cm anterior to the superficial temporal artery at the level of the zygomatic arch, anteriorly curved just below the temporal line to the forehead, and stopped at the hairline (Fig. 1a). To expose the skull, the scalp and temporal muscle were incised, dissected and fixed with elastic retraction. The temporal muscle near the edge of its insertion to the temporal bone was cut together with the skin flap. This procedure resulted in excellent exposure of the anterior and middle cranial base, even though this musculocutaneous flap may conceal a portion of the middle fossa.

Craniotomy
With a high-speed bone drill, a small burr hole was made at the temporal bone near the posterior margin of the zygomatic arch (Fig. 1b). Then a craniotomy was made with a width of 2–3.5 cm and height of 1.5–2 cm. It was limited by the sphenoid ridge anteriorly, the suprameatal crest posteriorly, the zygomatic arch inferiorly, and the squamosal suture superiorly. After craniotomy, a groove over the sphenoid ridge of the bone flap was made and fractured manually to remove the bone flap (Fig. 1c). This would allow easier control of bleeding from the middle meningeal artery. For access to the sylvian fissure, 1–2 cm of the temporal lobe was exposed by extending the craniotomy to the floor of the frontal fossa just above the orbital rim, exposing 2 cm of the frontal lobe (especially for ACA or ACoA aneurysm), and retracting the frontal lobe away from the MCA. If the extent of the frontal fossa exposure was inadequate, it might hamper visualization up into the sylvian fissure and force the surgeon to retract the temporal lobe inordinately. A rongeur or a high-speed drill was then used to remove the bones along the cranial base, including a portion of the squamous temporal bone and the sphenoid edge of the greater sphenoid wing. The dura was opened with an arched fashion around the sylvian fissure, flapped anteriorly, and tacked over the sphenoid ridge (Fig. 1d). Oozing from the pterion might be problematic and was usually reduced with tenting stitches and packing. Spinal drainage, if needed, was begun as the dura was opened.

Although a small portion of the incision extended to the forehead, it gave a more excellent cosmetic result than the supraorbital keyhole approach and provided sufficient frontal exposure for visualization deep into the sylvian fissure. This procedure allows the surgeon to work in the anterior and middle cranial fossa, the intracranial extradural space, and the subarachnoid space. Under the microscope, the neurosurgeon could easily gain a short access to the surgical targets in the suprasellar and tentorial areas, the circle of Willis, and the whole anterior cranial base. The pterion keyhole approach has the potential for access to aneurysms and related structures at the following sites: the ipsilateral ICA, the medial wall of the contralateral ICA, the ACoA, bilateral ophthalmic arteries, the M1, M2, and M3 segments of the ipsilateral MCA, the contralateral PCoA, the anterior choroidal artery, the P1 segment of the PCA, the suprasellar and tentorial areas, all the anterior cranial base structures, and the basilar apex. In some selected aneurysm cases, 0- and 30-degree endoscopic control was used (HSW Co., Tuttlingen, Germany) to confirm the patency of neighboring perforating arteries, the PCoA, and the anterior choroidal artery.
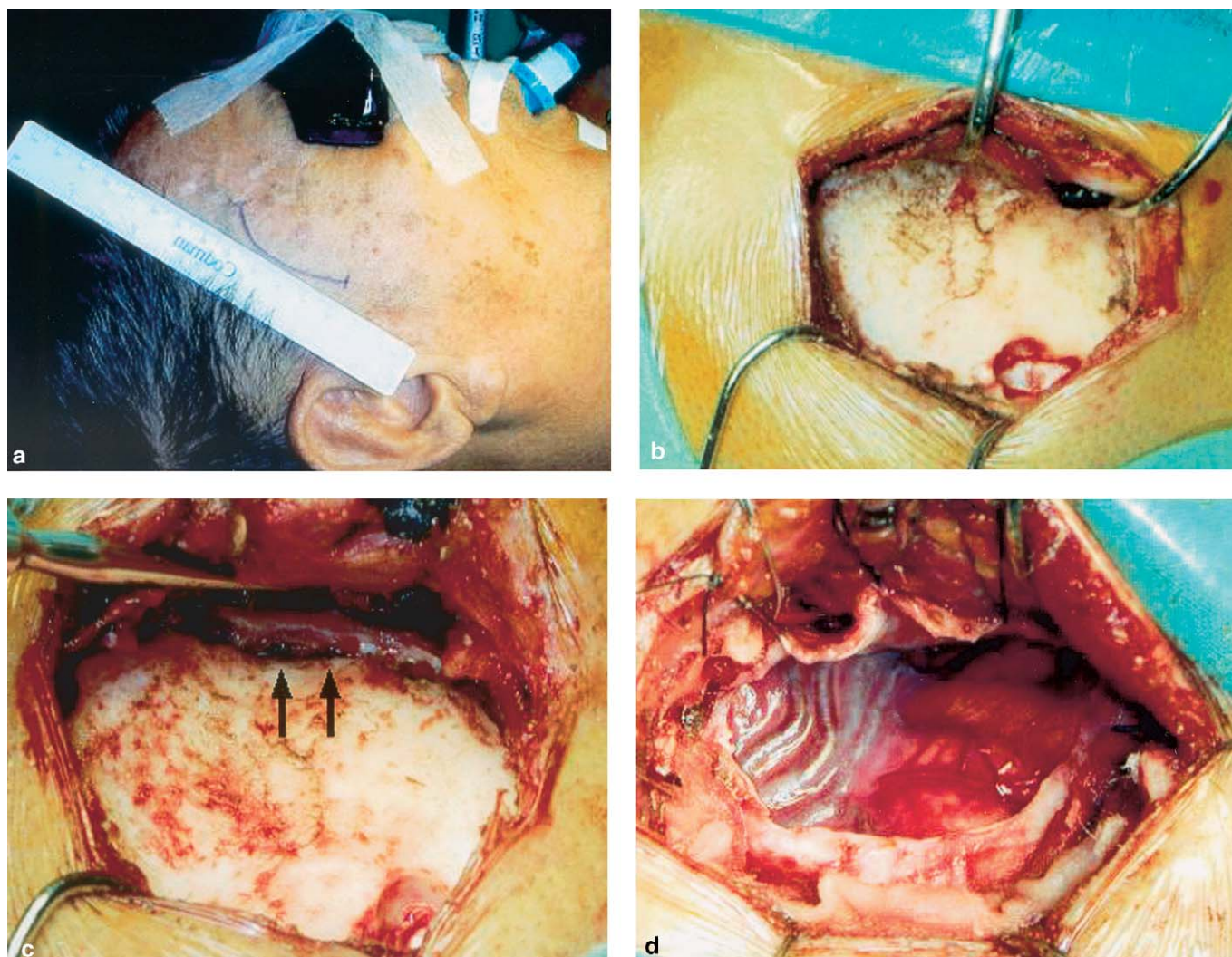
Fig. 1 Surgical procedure of pterion keyhole approach. **a** The skin incision line was 1.0 cm anterior to the superficial temporal artery at the level of the zygomatic arch, anteriorly curved just below the temporal line to the forehead, and stopped at the hairline. **b** A small burr hole was made at the temporal bone near the posterior margin of the zygomatic arch. **c** A groove (indicated by arrows) over the sphenoid ridge was made and the bony flap was removed. **d** The dura was opened in an arched fashion around the sylvian fissure and turned over anteriorly.

After clipping the aneurysms, the surgical wound was then closed layer by layer. It was noted that the temporal muscle must be reattached to the cranium otherwise it might produce a distinguishable bulge above the zygoma and postoperative forehead swelling and ecchymosis.

Results

All of the aneurysms were clipped successfully and uneventfully. The overall outcome was good (Table **3**), except for one patient who suffered complications of vasospasm and cerebral infarction 2 days after aneurysm clipping. No serious complications and mortality related to the surgical technique were noted. The surgical space afforded by use of this approach allows wide exploration of the anterior fossa, the orbital space, and the ipsilateral middle fossa structures without limitations. It also allowed access to portions of the contralateral ICA and its bifurcation. Three patients showed premature rupture during dissection of the aneurysmal neck including one each of the ACoA, PCoA and MCA. However, they were successfully clipped.

Table **3** Glasgow outcome scale of the patients (n = 40)

Score	5	4	3	2	1
Number of patients	37	2	0	1	0

No patient had postoperative visual or retinal disturbances with regard to either visual acuity or visual field impairment.

All patients sustained transient hypesthesia over the temporal region, which is expected and acceptable with the use of this approach and is not considered as a complication. The postoperative cosmetic result was excellent and the patients were satisfied with it (Fig. **2**). After 7 to 50 months of follow-up, we found that only 3 patients had temporomandibular dysfunction or signs of atrophy at the site of the craniotomy.

Discussion

Since Yasargil and Fox first described the frontotemporal craniotomy with a pterional approach, it has replaced bifrontal and

Fig. 2 The case of a right ophthalmic artery aneurysm treated by the pterion keyhole approach. **a** An aneurysm of the right ophthalmic artery under the microscope. **b** Clipping of the aneurysm. **c** Appearance of the incision one week after surgery. **d** Appearance of the incision two months after surgery. The cosmetic result was good.

frontolateral craniotomies for access to aneurysms of the anterior circulation. A common feature of all these conventional approaches is the relatively extensive brain exposure and brain retraction, causing an increase of surgical morbidity not related to the lesion itself. Occasionally, patients complain of the depressed deformities in the frontotemporal area due to craniotomy. Particularly, this occurs as a result of inappropriate repair of the bone defect at the burr holes. Although application of some biocompatible materials including hydroxyapatite ceramics [7], burr-hole buttons and miniplate systems [8, 9] can prevent this deformity to some extent, it does not fit well to a bone defect at the keyhole because of the complex curvature of the surrounding bone.

Since the implementation of the minimally invasive concept in neurosurgery is to avoid surgical trauma, many surgical approaches and technological advances have been made to facilitate this goal. The clinical results are overwhelming. Shorter hospital stay and less morbidity and mortality are achieved with minimally invasive approaches. Also, minimally invasive exploration through a small keyhole [10, 11] or endoscope-assisted supraorbital craniotomy [12–14], using an eyebrow or a superciliary skin incision, has become more widely performed with the improvement of diagnostic imaging and surgical techniques. Supraorbital keyhole craniotomy seems to cause less injury to soft tissue and offers excellent cosmetic results compared to the conventional frontotemporal craniotomy. The skin incision for a

frontotemporal craniotomy is always visible unless it is made within the eyebrow. Even for an incision within the eyebrow, hair loss at the margin of the incision may make it more visible. In contrast, a scalp incision for a pterion keyhole is entirely behind the hairline unless the patient is bald. Although any cosmetic problems caused by burr holes drilled during surgery have been largely eliminated by the use of plating systems and burr-hole covers, scalp and cosmetic deformities should be avoided. Additionally, the keyhole approach to cerebral aneurysms requires a slack brain and may be associated with a higher risk of devastating consequences due to unexpected conditions during surgery because of the narrower surgical fields than in a standard pterional craniotomy. This technique, therefore, is recommended for well-trained neurosurgeons having experience in conventional craniotomy techniques, because avoidance of brain injury should be more of a concern to a neurosurgeon than the length of the skin incision.

Advantages of the pterion keyhole approach

The pterion keyhole approach offers several advantages compared to a conventional frontotemporal craniotomy. First of all, brain exposure to air, accidental surgical trauma and brain retraction is minimal. This significantly decreases approach-related surgical morbidity and shortens hospitalization. Time spent in the surgical procedure is also significantly reduced when compared to standard techniques. The primary benefit of the pterion keyhole approach seems to be the avoidance of

resection of the orbital rim and roof, and frontal sinus, which would ultimately lead to a decreased incidence of cerebrospinal fluid leakage and may result in less cosmetic deformity and less discomfort than produced by supraorbital or transorbital approaches. The authors have demonstrated that, in a selected group of patients, the pterion keyhole approach is a viable alternative to the traditional pterion approach.

Disadvantages and limitations of the pterion keyhole approach

Due to the small craniotomy, there is less opportunity to change the surgical plan if unexpected conditions occur during surgery. Because brain swelling was difficult to manage with the pterion keyhole approach, we did not adopt this approach for patients with severe subarachnoid hemorrhage (Hess and Hunt grades IV – V) without hydrocephalus. Furthermore, an unexpected intraoperative serious rupture of the aneurysm would be extremely difficult to manage under the limited exposure of the brain by this approach. We prevented this catastrophic event by adequate exposure of the sylvian fissure and its vascular anatomy, as well as CSF drainage. Actually, for each patient, we had evaluated whether the pterion keyhole approach allowed for proximal control, dissection of the aneurysm, and application of the aneurysmal clip in advance. Multidirectional viewing through the keyhole was only achievable by use of intraoperative endoscopy. Therefore, preoperative diagnostic imaging is of paramount importance in reference to the surgical planning and for preventing the occurrence of unexpected intraoperative conditions in advance. The pterion keyhole approach for ACoA aneurysms has drawbacks. A limited resection of the gyrus rectus is often necessary for adequate control of the AcoA aneurysms [15].

Surgical flexibility

The pterion keyhole approach is an alternative in the treatment of patients with anterior circulation aneurysms in a wide anatomic area, either ipsilaterally or contralaterally. One of the important advantages of the approach is minimal brain retraction, which is achieved in three ways:

– changes of the approaching angle when the minicraniotomy is shifted to the frontal area, allowing access to the bilateral optic nerves;
– dissection and cistern drainage that is possible at all levels of the brain and, for approaching the sylvian fissure, is possible at the pre-pontine cistern; and
– modification of the head position with postural support of gravity permitting access to all of the natural spaces in this microsurgical corridor.

The pterion keyhole approach allowed for a craniotomy of up to 3.5 cm in diameter, approximately 1.5 cm wider than that obtained using the supraorbital keyhole approach. The larger craniotomy was particularly important because it increased the field of illumination and visualization under the surgical microscope, avoided total reliance on the endoscope, and decreased the potential obstruction of light by the surgical instruments.

The pterion keyhole approach required a 3- to 5-cm long oblique skin incision extending from the edge of the zygomatic arch to the center of the pterion just over the sylvian fissure. Such an incision method provided a superior postoperative cosmetic appearance, because the pterion keyhole was well covered by the temporal muscle. To avoid damage to the temporal muscle and the frontal branch of the facial nerve, we cut the temporal muscle near the edge of its insertion to the temporal bone. This prevented atrophy of the temporal muscle, temporomandibular joint problems, indentation of the temple, weakness of the frontal muscle, eyelid droop, and cosmetic anomalies likely caused by other cutting methods. Although the pterion keyhole approach requires a limited skin incision and a small trephinated bone opening, this approach allowed a short access to the suprasellar area through the keyhole. Moreover, the operative field became wider as it went deeper. Accordingly, sufficient operative space was obtained requiring no highly specialized instruments.

Application in neurovascular surgery

One of the commonest drawbacks of keyhole approaches in neurovascular surgery is the risk of bleeding. However, the keyhole procedures were carefully executed with consideration of the essential factors regarding aneurysm dissection, including individual anatomy, proximal vessels (flow control), distal vessels, neck and dome of the aneurysm, and perforating vessels. Thus, the usual microsurgical space of 20 mm at the site of the lesion is ultimately the same as that required in a large craniotomy, without compromising the manipulation of aneurysm clipping and, especially, without increasing the risk for the patient. Even though clinoid resection was not necessary for aneurysms in the paraclinoid segment or carotid cavum in some of our cases, the above point still works and has been documented in previous experimental studies [5, 11, 16, 17].

It is possible to gain access to the region of the tip of the basilar artery with appropriate microdrilling of the posterior clinoid. In those aneurysms with a ventral neck, a postural change to a more lateral angle allows better visualization than does the keyhole supraorbital approach. With regard to the limitation of axial illumination at 0-degree microscopic visualization, it is also possible to use an endoscope with 0 and 30 degree optics to verify the anatomic position of the neighboring arteries, the PCoA, the anterior choroidal artery, and the perforating arteries in the supraclinoid segment of the lCA. The procedure is safe under three-dimensional verification of the clip position. A second placement of the clip was necessary in only three of our cases.

Improvement of surgical technique

Perneczky and colleagues [1, 5] have advocated the keyhole concept in neurosurgery and have used the supraorbital minicraniotomy extensively for a variety of lesions. Recently, others have reported experience with this approach in the management of tumors and aneurysms of the anterior cranial fossa and the sellar and parasellar regions [2–5].

The drawbacks of supraorbital keyhole approach are:

– transient loss of supraorbital sensation that frequently occurs and is attributed to traction on the supraorbital nerve;

– prolonged paresis of the eyebrow in an elevated position probably due to the interrupted insertion of the frontal muscle on the eyebrow;
– alopecia of the eyebrow;
– unsatisfactory postoperative cosmetic results;
– contraindication for a large frontal sinus;
– injury of the temporal muscle by drilling a single burr hole at the orbital rim, causing a small indentation of the lateral aspect of the eyebrow.

A watertight dural closure and meticulous wound closure, particularly that of the brow skin incision, are important to attain a good cosmetic result.

As in the case with the standard pterional approach to aneurysms of the anterior circulation, atrophy of the anterior temporal muscle can occur and may cause a small indentation in the temporal region. The traditional large craniotomy needs significant brain retraction and may have associated morbidity. Instead, the pterion keyhole approach allows for a short and relatively safe access to the suprasellar area behind the optic chiasma and a ventrolateral entrance into the petroclival region [18].

The main advantage of the minicraniotomy for the pterion keyhole approach is the very low basal approach to the circle of Willis; particularly in the case of middle cerebral artery aneurysms, one can look directly into the sylvian fissure down to the suprasellar and petroclival region from an anterolateral direction, allowing minimal retraction for a temporofrontal approximation. This approach has also been found to be particularly easy, quick, and direct for other lesions of the perichiasmatic and suprachiasmatic region. As with any new procedure, familiarity brings a sense for properly determining its indications. We use a hairline incision instead of an eyebrow incision to facilitate harvesting a piece of temporal muscle or fascia for dural repair or preventing ecchymosis.

Conclusions

The pterion keyhole approach is effective for gaining access to the circle of Willis, and dissection of the sylvian fissure and MCA can be performed easily. A keyhole in the temporal bone may expose the middle fossa. Based on this concept, an extension of the craniotomy allows the surgeon to decrease the surgical distance and provides a more convenient microsurgical field for microscope-assisted and/or endoscope-assisted neurosurgery. In spite of any modification of this approach, the main purpose of the keyhole is not only to diminish the size of craniotomy but also to reduce brain retraction and simplify the subsequent intracranial procedure. A detailed preoperative study of standard and individual anatomy helps in determining the size and location of the keyhole craniotomy. It needs to be modified suitably in each case, not only according to the location and nature of the lesion, but also taking into account the treatment goal, the cosmetic implications, and the skills and experience of the surgeon.

References

1 Cohen AR, Perneczky A, Rodziewicz GS, Gingold SI. Endoscope-assisted craniotomy: approach to the rostral brain stem. Neurosurgery 1995; 36: 1128–1130

2 Jho HD. Orbital roof craniotomy via an eyebrow incision: a simplified anterior skull base approach. Minim Invas Neurosurg 1997; 40: 91–97

3 Sanchez-Vazquez MA, Barrera-Calatayud P, Mejia-Villela M, Palma-Silva JF, Juan-Carachure I, Gomez-Aguilar JM, Sanchez-Herrera F. Transciliary subfrontal craniotomy for anterior skull base lesions. Technical note. J Neurosurg 1999; 91: 892–896

4 Shanno G, Mans M, Bilyk J, Schwartz S, Savino P, Simeone F, Goldman HW. Image-guided transorbital roof craniotomy via a suprabrow approach: a surgical series of 72 patients. Neurosurgery 2001; 48: 559–568

5 van Lindert E, Perneczky A, Fries G, Pierangeli E. The supraorbital keyhole approach to supratentorial aneurysms: concept and technique. Surg Neurol 1998; 49: 481–490

6 Cheng WY, Shen CC. Minimally invasive approaches to treat simultaneous occurrence of glioblastoma multiforme and intracranial aneurysm – case report. Minim Invas Neurosurg 2004; 47: 181–185

7 Yamashima T. Reconstruction of surgical skull defects with hydroxylapatite ceramics button and granules. Acta Neurochir (Wien) 1998; 90: 157–162

8 Couldwell WT, Fukushima T. Cosmetic mastoidectomy for the combined supra/infratentorial transtemporal approach. Technical note. J Neurosurg 1993; 79: 460–461

9 Lerch KD. Reliability of cranial flap fixation techniques: comparative experimental evaluation of suturing, titanium miniplates, and a new rivet-like titanium clamp (CranioFix): technical note. Neurosurgery 1999; 44: 902–905

10 Czijak S, Szeifert GT. Surgical experience with frontolateral keyhole craniotomy through a superciliary skin incision. Neurosurgery 2001; 48: 145–150

11 Paladino J, Pirker N, Stimac D, Stem-Padovan R. Eyebrow keyhole approach in vascular neurosurgery. Minim Invas Neurosurg 1998; 41: 200–203

12 Fries G, Perneczky A. Endoscope-assisted brain surgery: part 2 – analysis of 380 procedures. Neurosurgery 1998; 42: 226–232

13 Menovsky T, Grotenhuis JA, de-Vries J, Bartels RH. Endoscope-assisted supraorbital craniotomy for lesions of the interpeduncular fossa. Neurosurgery 1999; 44: 106–112

14 Perneczky A, Fries G. Endoscope-assisted brain surgery: part 1 – evolution, basic concept, and current technique. Neurosurgery 1998; 42: 219–225

15 Horikoshi T, Nukui H, Mitsuka S, Kaneko M. Partial resection of the gyrus rectus in pterional approach to anterior communicating artery aneurysms. Neurol Med Chir (Tokyo) 1999; 32: 136–139

16 Evans JJ, Hwang YS, Lee JH. Pre-versus post-anterior clinoidectomy measurements of the optic nerve, internal carotid artery, and optico-carotid triangle: a cadaveric morphometric study. Neurosurgery 2000; 46: 1018–1023

17 Ramos-Zuniga R. The trans-supraorbital approach. Minim Invas Neurosurg 1999; 42: 133–136

18 Koos WTH, Spetzler RF, Lang J, Pendl G, Perneczky A. Tumors of the base of the skull. In: Color Atlas of Microneurosurgery: Microanatomy, Approaches, Techniques. New York: Thieme, 1993; vol 1, pp 275–283

A. Zohdi[1]
S. El Kheshin[2]

Endoscopic Approach to Colloid Cysts

263

Abstract

Objective: The aim of this study is to discuss the variations in the morbid anatomy of colloid cysts with its impact on the choice of endoscopic approach through a standard Kocher's burr hole. **Methods:** This study was conducted on 18 patients between 1996 and 2006. All patients were operated through a single burr hole at Kocher's point using a rigid endoscope with a single working channel. The anatomical variations of the cyst and the foramen of Monro dictated the use of the transforaminal approach, the transseptal interforniceal approach or both. **Results:** There were no mortalities or significant morbidities. The operative time ranged between 90 to 240 minutes (with a mean of 133 minutes). Five patients (27.7%) developed remediable postoperative chemical meningitis successfully controlled with steroids. Postoperative transient memory disturbance was observed in 3 patients (16.7%). One patient had a postoperative CSF leak that stopped spontaneously. Aspiration of the cyst's contents showed variable degrees of resistance to aspiration. The period of follow-up ranged between 5 months to 8 years and 3 months (mean: 4 years and 2 months). None of our patients showed radiological evidence of cyst recurrence during the follow-up period. **Conclusion:** Through a single right pre-coronal burr hole at Kocher's point, several endoscopic manoeuvres can be done. These include aspiration of the contents or its piecemeal removal, combined balloon squeeze and aspiration, foraminoplasty, pellucidotomy, coagulation of cyst capsule and ETV. The choice of the appropriate approach is largely dependent on the location of the cyst and the shape of the foramen of Monro. Coronal MRI may aid in preoperative evaluation of the tucked up retroforaminal growth of the cyst. We had no recurrence in our series with a follow-up reaching more than 8 years. This could be attributed to both the marsupialization and coagulation done for the remaining cyst capsule.

Key words

Neuroendoscopy · colloid cysts · transforaminal approach · transseptal interforniceal approach

Introduction

Third ventricular colloid cysts constitute about 0.5 to 1% of all intracranial tumors [1–3]. Surgery of this benign cystic lesion has challenged neurosurgeons since Dandy successfully removed a colloid cyst in 1921 [4]. Several therapeutic options have been proposed, ranging from shunting [5] to stereotactic aspiration [6–8]. In the past decade, microsurgical resection with the use of either a transcallosal [9–11] or a transcortical-transventricular [9,12,13] approach has been accepted as the "gold standard" treatment of colloid cysts. As this cystic lesion commonly induces obstructive hydrocephalus it is considered an attractive target for neuroendoscopic intervention. This has been supported in the past decade with the rapid advancement of neuroendoscopic equipment making endoscopic resection an effective, generally safe procedure with a favourable outcome [14–26]. The aim of this study is to discuss the impact of the variations in the morbid anatomy of colloid cysts on the choice of the endoscopic approach.

Affiliation
[1]Department of Neurosurgery, Kasr El Aini School of Medicine, Cairo University, Egypt
[2]Department of Neurosurgery, Tanta School of Medicine, Tanta University, Egypt

Correspondence
Prof. Ahmed Zohdi · Cairo Medical Tower · 55 Abdel Monem Riad St. · El Mohandeseen Giza · Postal code 12411 · Cairo · Egypt · Tel.: +20/12/210 33 20 · Fax: +20/2/363 43 93 · E-mail: azohdi54@yahoo.com

Patients and Methods

Patients

This study was conducted on 18 patients (10 males) treated in the University Hospitals of Kasr El Aini School of Medicine, Cairo and Tanta University Hospital, Tanta, between 1996 and 2006. The age ranged between 14 and 60 years (mean: 33.6) with the clinical presentations shown in Table **1** .

Endoscopic equipment

The rigid endoscope with a single working channel was used in all cases. The French 3 Fogarty catheter – whenever needed beside the instrument in the working channel **-** was inserted through the irrigation channel. The excess and outflow of the irrigation sufficiently welled out from around the catheter and the instrument.

Operative technique

Under general endotracheal anesthesia, in the supine position, a precoronal 1.5 cm. burr hole was done 3 cm lateral to the midline and jutting with the coronal suture. All the patients had moder-

Table **1**   Clinical presentations

Clinical features	No. of patients
Headache	17
Vomiting	2
Ataxia	2
Papilledema	13
Post–papilledemic optic atrophy	2
Urinary incontinence	5
Memory disturbance	3
Decreased level of consciousness	6
Bobble head doll syndrome	1

ate to severe hydrocephalus, hence free-hand insertion of the trocar followed by intraventricular endoscope loading was always done without any difficulty.

After careful endoscopic inspection of the anatomic structures and landmarks around the foramen of Monro, their relation to the colloid cyst was defined and the appropriate endoscopic approach chosen. These variations are shown in Fig. **1** and Table **2** .

The shape and size of the foramen of Monro dictated the use of the transforaminal approach (in 7 cases), the transseptal interforniceal approach (in 4 cases) and the combined approach (in 7 cases). Foraminoplasty was done in 10 patients who had a crescentic, coapted, displayed and glued foramina. Fogarty balloon squeeze of the cyst contents to facilitate its aspiration was done in 7 cases (Fig. **2**).

The transforaminal approach

We started the resection with initial bipolar coagulation of the cyst capsule and the overlying choroid plexus followed by fenestration of the cyst capsule. The contents of the cyst varied from mucoid suckable to solid difficult to aspirate and even mixed contents. A central venous cannula (CVC) was inserted and suction of the contents attempted. We initially used a 10-mL syringe followed by a 20-mL syringe if a forcible suction was required for the thick mucoid contents. Piecemeal removal of the solid contents with the biopsy forceps was done. Following evacuation of all the cyst contents, bipolar shrinkage of the inner and outer surfaces of the cyst capsule facilitated its maximum possible resection.

The transseptal-interforniceal approach

The cyst was approached through the septum pellucidum just behind the anterior septal vein. Initial coagulation and fenestration of the septum and underlying cyst capsule was performed. Using CVC, aspiration of the contents was first attempted apply-
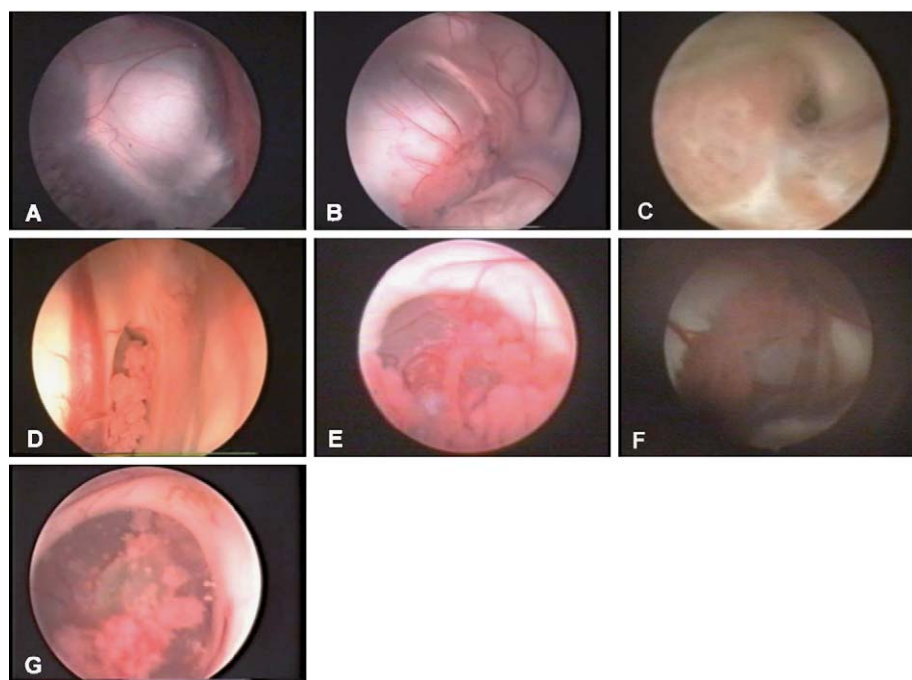

Fig. **1**   Endoscopic morbid anatomical variations showing the relationship of the colloid cysts to the foramen of Monro and related structures. The foramen of Monro is **A** "displayed", **B** "coapted", **C** "glued", **D** "crescentic", **E** "large" having enough space but with little choice of target area, **F** "divaricated" with the anterior septal vein running on cyst capsule, and **G** "dilated" permitting multiple points of entry.

Table 2 Types of foramina

Types of foramina	No. of patients
Displayed	2
Coapted	4
Glued	1
Crescentic	3
Large	4
Divaricated	1
Dilated	3
Total	18

Table 3 Size of cysts

Size of cyst in cm	No. of patients
< 1.5	5
1.5–3	8
> 3	5

Table 4 Endoscopic approaches

Approach	No. of patients	Shapes of foramina encountered
Transforaminal	7	1 divaricated, 3 dilated, 3 large
Trans–septal interforniceal	4	3 coapted, 1 glued
Combined	7	3 crescentic, 1 large, 1 coapted, 2 displayed
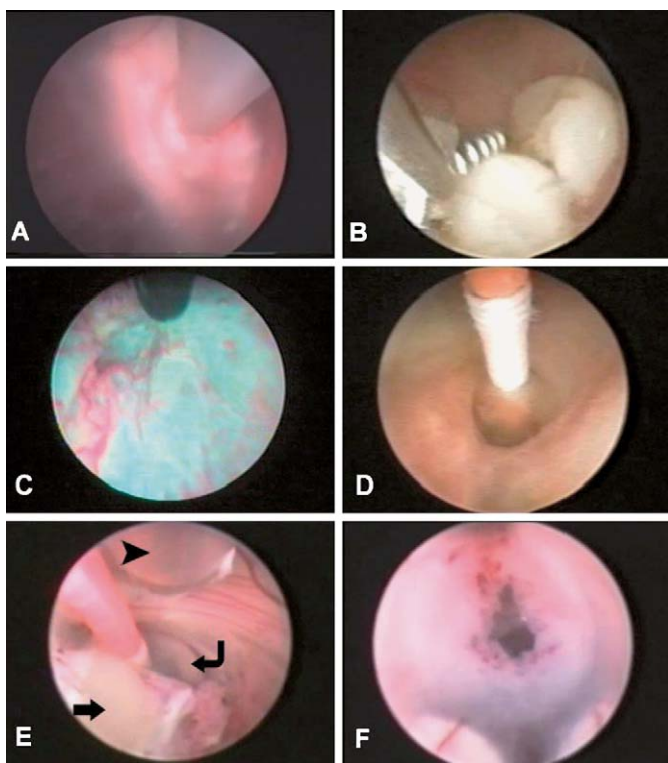
Fig. 2 **A** Aspiration of the cyst contents. **B** Removal of the solid contents with the biopsy forceps. **C** Cauterization of the inner surface of the capsule. **D** Balloon foraminoplasty of the amalgamated foramen. **E** Combined balloon squeeze and aspiration of contents. Note: the suction catheter (arrowhead), the inflated balloon catheter in the foramen of Monro (angled arrow) and the squeezed out contents (straight arrow). **F** ETV.

ing the same principle as mentioned above. A French 3 Fogarty catheter was then inflated around the fenestration to dilate it allowing better access to the remaining cyst contents. Balloon foraminoplasty was always performed to restore a patent foramen of Monro and squeeze the remaining cyst contents to facilitate removal with a suction catheter or a biopsy forceps.

The combined approach
Starting with the transforaminal approach, it would be possible to access the cyst capsule directly and deal with the contents. The bulging part behind the septum pellucidum is then approached through the transseptal-interforniceal approach.

We performed third ventriculocisternostomy as a last step in all of the cases. This was to ensure patency, free CSF circulation and prevent an unexpected rise in the intracranial pressure due to impaction of tissue debris or solid cyst fragments. Only in one patient, with a crescentic foramen of Monro, was a pellucidotomy done to inspect the contralateral foramen of Monro. Bleeding, although not frequently encountered, was controlled by profuse irrigation, Fogarty balloon tamponade and bipolar coagulation as a last resort (2 cases).

Results

In this series we successfully treated 18 patients with colloid cysts without any mortality or significant morbidity. None of our patients had any postoperative deterioration. The preoperative clinical manifestations improved postoperatively. The patients with preoperative decreased levels of consciousness (GCS 13–14), cleared up gradually.

The operative time ranged between 90 to 240 minutes (mean: 133 minutes). With the increase in learning curve the time needed accordingly decreased. Five patients (27.7%) developed remediable postoperative chemical meningitis that was successfully controlled with steroids. Postoperative transient memory disturbance was observed in 3 patients (16.7%). One patient had a postoperative CSF leak, with spontaneous cure 5 days later. The size of the cysts and the distribution of cases according to the approach used are shown in Tables **3** and **4**, respectively.

The contents of the cysts showed variable degrees of resistance to aspiration. One patient had a cyst content that was totally solid. Nine patients had mixed contents of thick mucoid that was difficult to aspirate and solid contents that were essentially removed with the biopsy forceps. Most of the previously mentioned ten patients with difficult aspiration had hypointense

265

lesions on T_2 MR imaging (9 out of 10 patients) (Figs. **3** and **4**). The period of follow-up ranged between 5 months to 8 years and 3 months (mean: 4 years and 2 months). None of our patients showed radiological evidence of any cyst recurrence during the follow-up period.

Discussion

The endoscopic approach to colloid cysts started in 1983 when Paul et al. [27] reported their successful endoscopic aspiration of a colloid cyst. Due to the advances achieved in endoscopic equipment and the experience of endoscopic neurosurgeons, endoscopic resection should be considered as the operative approach of choice.

In this study we are presenting different patterns of growth of colloid cysts seen on endoscopic navigation during cyst resection. These patterns of growth are not just typical for all cases. The velum interpositum appears to be the anatomic site of origin of third ventricular colloid cysts [28]. If the cyst slowly grows anteriorly, it tends to widen the foramen of Monro resulting in a foramen that is larger than normal with less choice of target area, a markedly dilated or divaricated foramen with a part of the cyst wall bulging into the lateral ventricle. The direct transforaminal approach was the preferred operative choice applied for these cases.

The cyst may grow posteriorly in the third ventricle medial to the septum pellucidum. This may compromise the foramen of Monro resulting in a coapted or glued foramen. This pattern of growth may also induce a displayed foramen that is hardly seen with narrowing of the anterior lateral ventricle. For all of these varieties, we essentially opened the septum pellucidum to get access to the cyst as a part of the transseptal interforniceal approach used.

An intermediate type of growth both medial to and bulging through the foramen of Monro gives it a crescent shape. We combined the mentioned approaches whenever any residue of the cyst remained.

Most authors presented their experience in endoscopic colloid cyst resection via a transforaminal approach. We reviewed the literature for reported cases in which the cyst was not visible through the foramen of Monro and how they were managed.

Abdou and Cohen [15] in their series on 13 patients had three patients with posteriorly placed lesions that were tucked up underneath the roof of the third ventricle; they described these cysts to be more difficult to evacuate endoscopically.

Decq et al. [19] and King W. A. et al. [24] described colloid cysts that were implanted too posteriorly. They believed that such cysts are not easily treatable endoscopically because a rigid endoscope is not physically able to reach a target behind the level of the interthalamic commissure without creating some damage to the foramen of Monro or the fornix.

Rodziewicz et al. [25] clearly mentioned that occasionally colloid cysts do not present at the foramen of Monro. In these cases, the cyst usually protrudes superiorly and splits the septum pellucidum. Such cysts can be approached transventricularly, but sur-
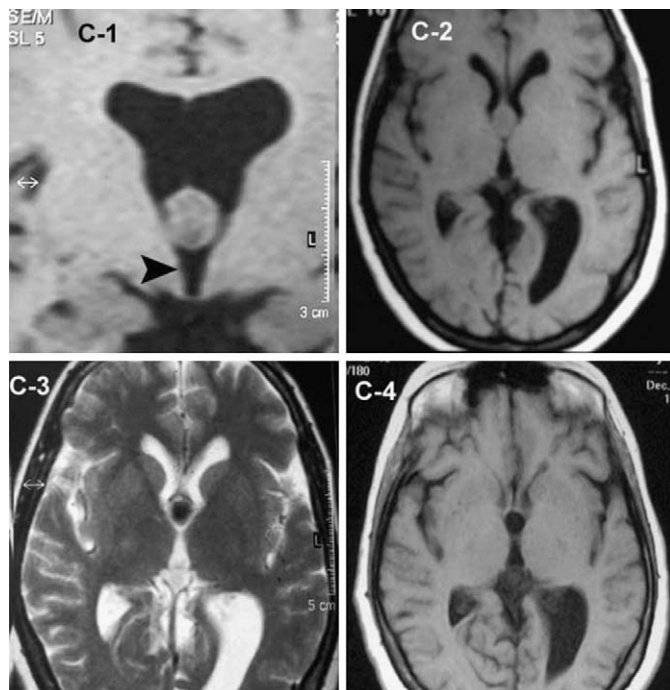
Fig. **3** A retroforaminal tucked up colloid cyst with a normal sized third ventricle in **C-1** image (arrowhead). **C-2** and **C-3** are preoperative axial T_1 and T_2 images respectively. Note: the hypointense lesion on image **C-3** (T_2) associated with intraoperative solid cyst contents. **C-4** is a postoperative axial T_1 image.
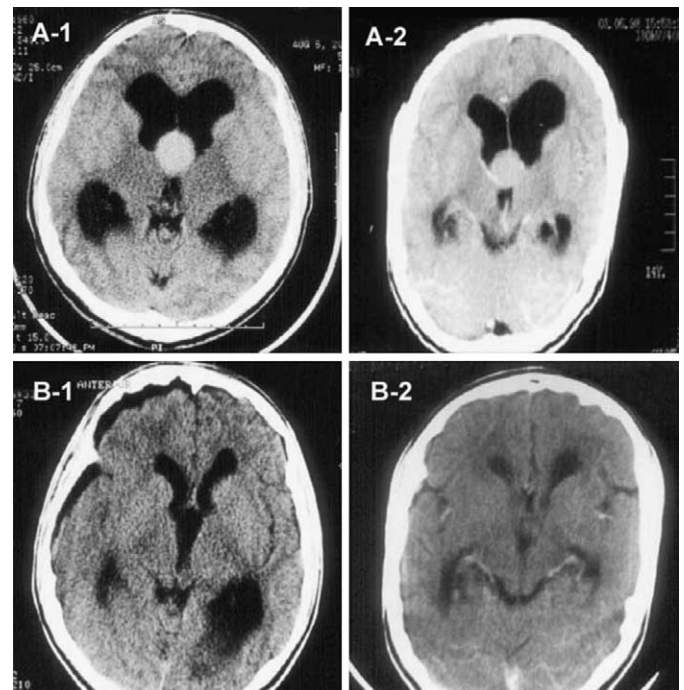

Fig. **4** **A-1** and **A-2** are preoperative CT scans of patients with coapted and displayed foramina of Monro. Both cysts lie higher than the third ventricle which is filled with CSF behind the lesion. **B-1** and **B-2** are their respective postoperative scans following resection through the transseptal interforniceal approach.

geons should anticipate the need to open the septum pellucidum to identify and reach the cyst, as in 7 cases of our series.

Vialogo [29] reported a case of colloid cyst located in a retroforaminal position, in the diencephalic roof, dissecting the raphe fornix, expanding superoposteriorly, inside the cavum of the septum pellucidum, and protruding on the floor of lateral ventricles. The cyst was approached with a rigid neuroendoscope, through a precoronal burr hole, 2.5 cm lateral to the midline (Kocher's point). Following a transventricular route, the right leaf of the septum pellucidum was endoscopically opened with bipolar, posterior to the septal vein. The two fornices were split apart by the uncommon expansion and location of the lesion, allowing a new endoscopic transventricular transseptointerforniceal approach. He also performed endoscopic septostomy and third ventriculostomy.

In our study of 18 patients we reported variations regarding visibility of the cyst at the foramen of Monro. The cyst was directly seen filling and widening the foramen of Monro in 8 cases, approached through a direct transforaminal route. Only three cases with crescentic foramina had both a small visible part of the cyst wall at the foramen of Monro and a retroforaminal bulge. In 7 patients we had a totally occluded foramen of Monro with no visible part of the cyst wall but a retroforaminal bulge pointing to the interseptal posteriorly tucked up lesion for which a transforaminal route was not feasible. We essentially opened the septum pellucidum as a part of the transseptal-interforniceal approach.

We believe that the transforaminal route is not the only approach to be used in endoscopic colloid cyst resection. The tucked up growth of the cyst in the posterior third ventricle can markedly approximate the edges of the foramen of Monro making a direct transforaminal route impossible. This direction of growth displaces the fornices, the leaves of the septum pellucidum and widens the interforniceal space. In this situation, the choice should not be to shift to open surgery as the interforniceal approach originally described in transcallosal microsurgery is still feasible with the endoscope.

The evacuation of the contents of the cyst behind the foramen of Monro will open it allowing a transforaminal approach to any remaining parts of the cyst. A combined approach should also be born in mind after transforaminal evacuation if any remnants of the cyst are still seen bulging behind the foramen of Monro and medial to the septum pellucidum.

Short-term memory disturbance due to forniceal trauma is a major disincentive to the transcallosal interforniceal approach to third ventricular lesions. A transient short-term memory loss was reported in 30% of patients in the series of Apuzzo and Amar using the interforniceal approach. The memory disturbance was maximal for the first 24 to 72 h and gradually settled, 75% resolved over 7 days and all resolved or returned to the preoperative status by 3 months [30].

We reported postoperative transient memory disturbances in 3 patients who gradually improved within 3 weeks. Two of these patients had preoperative memory disturbances that were mildly aggravated after surgery (both operated through combined approach) with preservation of the fornices. The third one had no preoperative memory complaint and showed an early return of normal memory within 5 days postoperatively and was operated by the direct transforaminal approach. This transient effect, which is still not higher than in the microsurgical approach, showed postoperative spontaneous improvement. It may be attributed to the manipulation of the fornices whether by the cyst itself or due to the balloon squeeze.

A total removal of the cyst capsule was not planned for in any of the patients. We removed as much as possible of the cyst wall and the remaining attached parts were coagulated and left in place to avoid any traction. We do believe, as others [14, 15, 24, 25], that a serious, endoscopically uncontrolled bleeding may follow this manoeuvre whose necessity is debatable.

In our series, there were no mortalities or permanent morbidities. The period of follow-up ranged between 5 months and 8 years and 3 months (mean: 4 years and 2 months). The regimen of radiological follow-up included a postoperative CT scan one day after surgery, MRI 3 months after surgery, one year after surgery, then every two years. We combined bipolar coagulation of the cyst capsule with cyst marsupialization, for continuous wash out of the formed colloid material if any by the circulating CSF. This combination could be the reason for the recurrence-free follow-up period amounting to 8 years and 3 months.

Conclusion

With an ascending learning curve, endoscopic colloid cyst resection could be the approach of choice. Through a single right precoronal burr hole at Kocher's point, several endoscopic manoeuvres can be done. These include aspiration of the contents or piecemeal removal, combined balloon squeeze and aspiration, foraminoplasty, pellucidotomy, coagulation of cyst capsule marsupialization of the cyst and ETV. The choice of the appropriate approach is largely dependent on the location of the cyst and the shape of the foramen of Monro.

References

1 Abernathey CD, Davis DH, Kelly PJ. Treatment of colloid cysts of the third ventricle by stereotaxic microsurgical laser craniotomy. J Neurosurg 1989; 70: 525–529
2 Campbell JR, Withfield R. Benign intraventricular tumors of the brain. NYSJ Med 1940; 40: 733–740
3 Little JR, MacCarty CS. Colloid cysts of the third ventricle. J Neurosurg 1974; 40: 230–235
4 Dandy WE. Benign tumors of the third ventricle: diagnosis and treatment. Springfield, IL., Charles C. Thomas, 1933, pp 1–37
5 Gutierrez-Lara F, Patino R, Hakim S. Treatment of tumors of the third ventricle: A new and simple technique. Surg Neurol 1975; 3: 323–325
6 Abernathey CD, Davis DH, Kelly PJ. Treatment of colloid cysts of the third ventricle by stereotaxic microsurgical laser craniotomy. J Neurosurg 1989; 70: 525–529
7 Desai SR, Sidhu PS, Dawson JM. An unusual consequence of stereotactic colloid cyst aspiration: Case report. Australas Radiol 1997; 41: 377–379
8 Hellwig D, Bauer BL, List-Hellwig E. Stereotactic interventions in cystic brain lesions. Acta Neurochir Suppl (Wien) 1995; 64: 59–63

9 Antunes JL, Louis KM, Ganti SR. Colloid cysts of the third ventricle. Neurosurgery 1980; 7: 450–455

10 Apuzzo MLJ, Chikovani OK, Gott PS, Teng EL, Zee CS, Giannotta SL, Weiss MH. Transcallosal, interfornicial approaches for lesions affecting the third ventricle: Surgical considerations and consequences. Neurosurgery 1982; 10: 547–554

11 Mathiesen T, Grane P, Lindgren L, Lindquist C. Third ventricle colloid cysts: A consecutive 12-year series. J Neurosurg 1997; 86: 5–12

12 Desai KI, Nadkarni TD, Muzumdar DP, Goel AH. Surgical management of colloid cyst of the third ventricle a study of 105 cases. Surg Neurol 2002; 57: 295–302

13 Chen TC, Krieger M, Hinton DR, Zee CS, Apuzzo LJ. The colloid cyst. In: Apuzzo MLJ (ed), Surgery of the Third Ventricle, 2nd edn. Philadelphia, Lippincott Williams & Wilkins, 1997, pp 1071–1131

14 Hellwig D, Bauer BL, Schulte M, Gatscher S, Riegel T, Bertalanffy H. Neuroendoscopic treatment for colloid cysts of the third ventricle: the experience of a decade. Neurosurgery 2003; 52: 525–533

15 Abdou MS, Cohen AR. Endoscopic treatment of colloid cysts of the third ventricle: Technical note and review of the literature. J Neurosurg 1998; 89: 1062–1068

16 Auer LM, Holzer P, Ascher PW, Heppner F. Endoscopic neurosurgery. Acta Neurochir (Wien) 1988; 90: 1–14

17 Bauer BL, Hellwig D. Minimally invasive endoscopic neurosurgery: A survey. Acta Neurochir Suppl (Wien) 1994; 61: 1–12

18 Caemaert J, Abdullah J, Calliauw L. Endoscopic diagnosis and treatment of para- and intraventricular cystic lesions. Acta Neurochir Suppl (Wien) 1994; 61: 69–75

19 Decq P, Le Guerinel C, Brugieres P, Djindjian M, Silva D, Keravel Y, Melon E, Nguyen JP. Endoscopic management of colloid cysts. Neurosurgery 1998; 42: 1288–1296

20 Deinsberger W, Böker DK, Bothe HW, Samii M. Stereotactic endoscopic treatment of colloid cysts of the third ventricle. Acta Neurochir (Wien) 1994; 131: 260–264

21 Deinsberger W, Böker DK, Samii M. Flexible endoscopes in treatment of colloid cysts of the third ventricle. Minim Invas Neurosurg 1994; 37: 12–16

22 Tirakotai W, Schulte DM, Bauer BL, Bertalanffy H, Hellwig D. Neuroendoscopic surgery of intracranial cysts in adults. Childs Nerv Syst 2004; 20: 842–851

23 Kehler U, Brunori A, Gliemroth J, Nowak G, Delitala A, Chiappetta F, Arnold H. Twenty colloid cysts: Comparison of endoscopic and microsurgical management. Minim Invas Neurosurg 2001; 44: 121–127

24 King WA, Ullman JS, Frazee JG, Post KD, Bergsneider M. Endoscopic resection of colloid cysts: Surgical considerations using the rigid endoscope. Neurosurgery 1999; 44: 1103–1111

25 Rodziewicz GS, Smith MV, Hodge Jr CJ. Endoscopic colloid cyst surgery. Neurosurgery 2000; 46: 655–662

26 Schroeder HW, Gaab MR. Endoscopic resection of colloid cysts. Neurosurgery 2002; 51: 1441–1444

27 Powell MP, Torrens MJ, Thomson JL, Hogan JG. Isodense colloid cysts of the third ventricle: A diagnostic and therapeutic problem resolved by ventriculoscopy. Neurosurgery 1983; 13: 234–237

28 Macaulay RJB, Felix I, Jay V, Becker LE. Histological and ultrastructural analysis of six colloid cysts in children. Acta Neuropathol 1997; 93: 271–276

29 Vialogo JG. Endoscopic transepto-interforniceal approach to colloid cysts: case report. Arq Neuropsiquiatr 2000; 58 (3B): 939–946

30 Apuzzo MLJ, Amar AP. Transcallosal interforniceal approach. In: Apuzzo MLJ (ed), Surgery of the Third Ventricle, 2nd edn. Williams and Wilkins, Baltimore, 1998, pp 421–452

H. J. Böhringer[1]
E. Lankenau[2]
V. Rohde[1]
G. Hüttmann[2]
A. Giese[1]

Optical Coherence Tomography for Experimental Neuroendoscopy

Abstract

Optical coherence tomography (OCT) is a non-invasive and non-contact imaging technology that has been applied to several biomedical applications. We have recently demonstrated that OCT allows discrimination of tumor adjacent brain, diffuse and solid tumor tissue and that this technology may be used to detect residual tumor within the resection cavity during resection of intrinsic brain tumors. Here we show that an OCT integrated endoscope can image the endoventricular anatomy and other endoscopically accessible structures in a human brain specimen. A Sirius 713 optical coherence tomography device was mounted to a modified rigid endoscope. A formalin-fixed human brain specimen was used to simulate endoscopic visualization of brain anatomy and two specimens of fixed malignant tumors with endoventricular growth patterns. Simultaneous OCT imaging and endoscopic video imaging of the visible spectrum was possible using a graded index rod endoscope. OCT imaging of a human brain specimen in water allowed an in-depth view into structures like the walls of the ventricular system, the choroid plexus or the thalamostriatal vein. OCT further allowed imaging of structures beyond tissue barriers or opaque media. In this fixed specimen OCT allowed discrimination of vascular structures down to a diameter of $50\,\mu m$. In vessels larger that $100\,\mu m$ the lumen could be discriminated and within larger blood vessels a layered structure of the vascular wall as well as endovascular plaques could be visualized. This in vitro pilot study has demonstrated that OCT integrated into neuroendoscopes may add information that cannot be obtained by the video imaging alone. This technology may provide an extra margin of safety by providing cross-sectional images of tissue barriers within optically opaque conditions.

Key words

Optical coherence tomography · intraoperative imaging · neuroendoscopy · ventriculoscopy

Introduction

Optical coherence tomography (OCT) is an imaging technology that uses reflected infrared light from tissue structures for reconstruction of tomographic images similar to ultrasound. The light from a super luminescence diode is split into a probe and a reference light beam. The reference light and the probe light are combined by a beam splitter and registered at a detector. Interference of low-coherence light only occurs when the optical path length of reference and probe are matched within the coherence length of the light source. Evaluating the interference for different path lengths of reference generates an A-scan image. Scanning the sample beam along a transverse axis can be used to create B-scan images. Implementation of this interferometer with fiber-optic couplers and beam scanning systems may be used to perform OCT measurements through hand-held probes [1], through the optical path of neurosurgical microscopes [2], or through fiber-optic catheters and endoscopes [3, 4, 5, 6]. Integration of OCT into specific applicators has en-

Affiliation

[1]Department of Neurosurgery, Georg-August-University of Göttingen, Göttingen, Germany
[2]Institute for Biomedical Optics, University of Lübeck, Lübeck, Germany

Correspondence

Alf Giese, M.D. · Department of Neurosurgery · Georg-August-University of Göttingen · Robert-Koch-Straße 40 · 37075 Göttingen · Germany · Tel.: +49/551/39 60 33 · Fax: +49/551/39 87 94 · E-mail: alf.giese@med.uni-goettingen.de
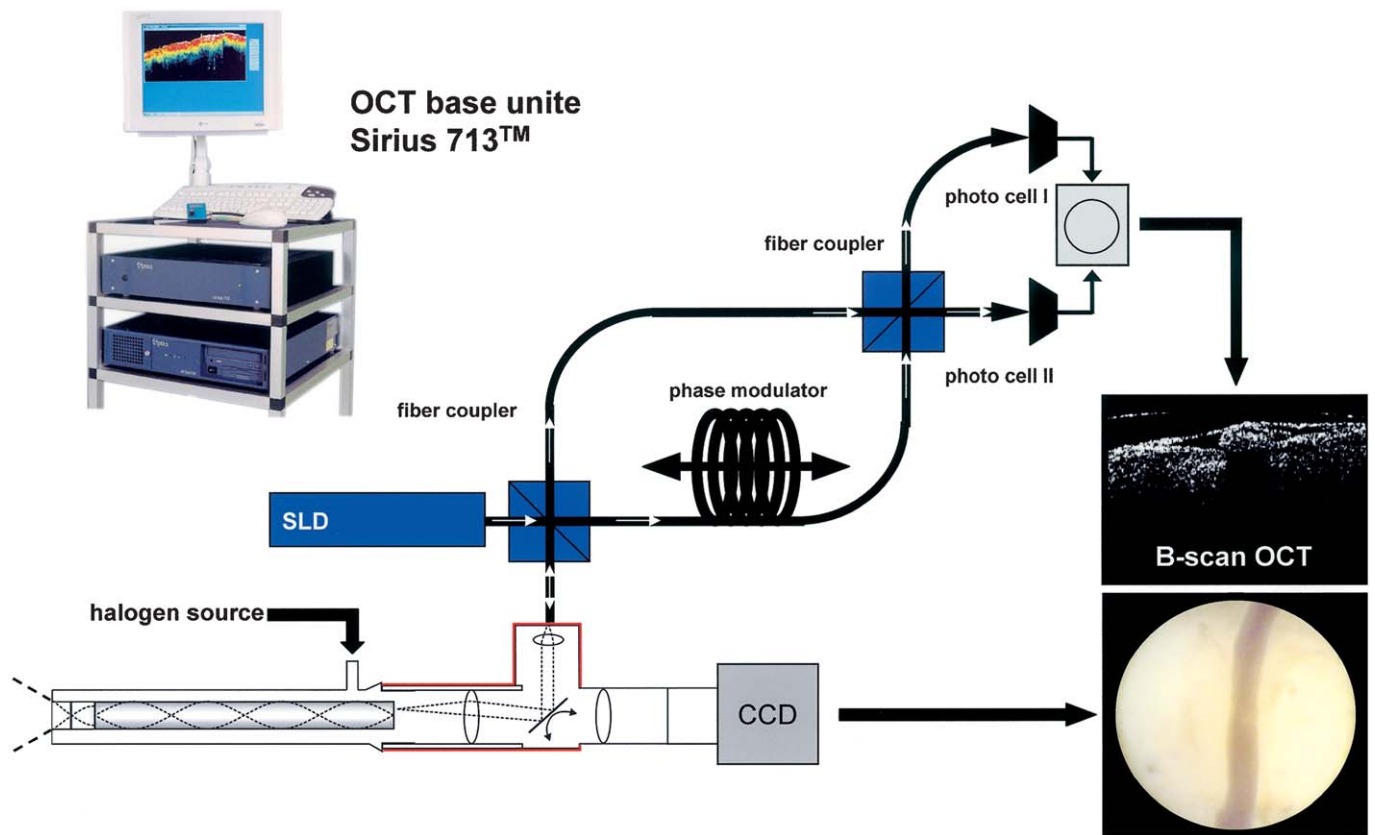
OCT base unite Sirius 713™

Fig. **1** Endoscope integrated optical coherence tomography. The sample beam of a fiber optic interferometer is passed through a GRIN rod endoscope via a galvo scanner. A superluminescence diode (SLD) with a central wavelength of 1300 nm was used as a light source. Interference of low-coherence light occurs when the optical path length of the phase modulator and the sample beam are matched. Scanning the sample beam along a transverse axis can be used to create B-scan images. For positioning of the endoscope both the video and OCT images may be used.

abled medical applications in ophthalmology [7], gastroenterology [8], urology [3-5], and dermatology [1].

Optical coherence tomography can achieve a spatial resolution of micrometers and has also been applied to imaging of central nervous system tissues. Interpretable B-scan information in highly scattering tissue such as brain can only be obtained to a tissue depth of approximately 2 millimeters [9]. Ultrahigh resolution optical coherence tomography has recently been demonstrated to resolve brain tissue morphology from a single cell level to a whole animal brain ex vivo and in vivo [10]. We have recently shown that optical coherence tomography may be used to image human brain tumor tissue in vivo. At a spatial resolution of 10 µm optical coherence tomography differentiates tumor from adjacent brain, the infiltration zone, as well as highly cellular tumor and necrotic areas of malignant gliomas [11]. These observations have raised the question whether optic tissue analysis may allow detection of residual tumor within the wall of the resection cavity during operations for intrinsic brain tumors. Using a high-resolution spectral-domain implementation of the OCT technology we have analyzed biopsies taken from the wall of macroscopically tumor-free resection edges during surgical removal of a malignant glioma. OCT analysis demonstrated residual microscopic tumor in what appeared macroscopically normal cortex or white matter [12]. Because OCT analysis can be performed as non-contact measurements over distances of several centimeters we have recently integrated this technology

into the optical path of an experimental neuronavigated operating microscope [2].

In this study we have used a rigid endoscope, which accepts an OCT applicator and allows display of a simultaneous endoscopic video image and an OCT B-scan tomographic image of the tissue in front of the endoscope. A fixed human brain was used to simulate a ventriculoscopy and endoscopic approaches to other brain regions. This feasibility study demonstrates that neuroanatomical imaging by OCT can be performed through rigid endoscopes. Optical tomography may be used to identify and measure anatomic structures through tissue barriers such as membranes and non-transparent media and may help to discriminate pathological tissues from normal brain specimens.

Material and Methods

Optical coherence tomography and endoscope integration

In this study a time-domain optical coherence tomography device (Sirius 713 Tomograph, 40ptics, Lübeck, Germany) was used, which was modified by the Medical Laser Center, Lübeck, Germany for use with an endoscope (Fig. **1**). The radiation of a super luminescence diode (SLD) emitting at a central wavelength of 1310 nm with a coherence length of 15 µm was launched into an optical monomode fiber, which guides the radiation to an OCT adapter connected to a modified rigid endoscope with an outer diameter of 3 mm containing an imaging graded index (GRIN)
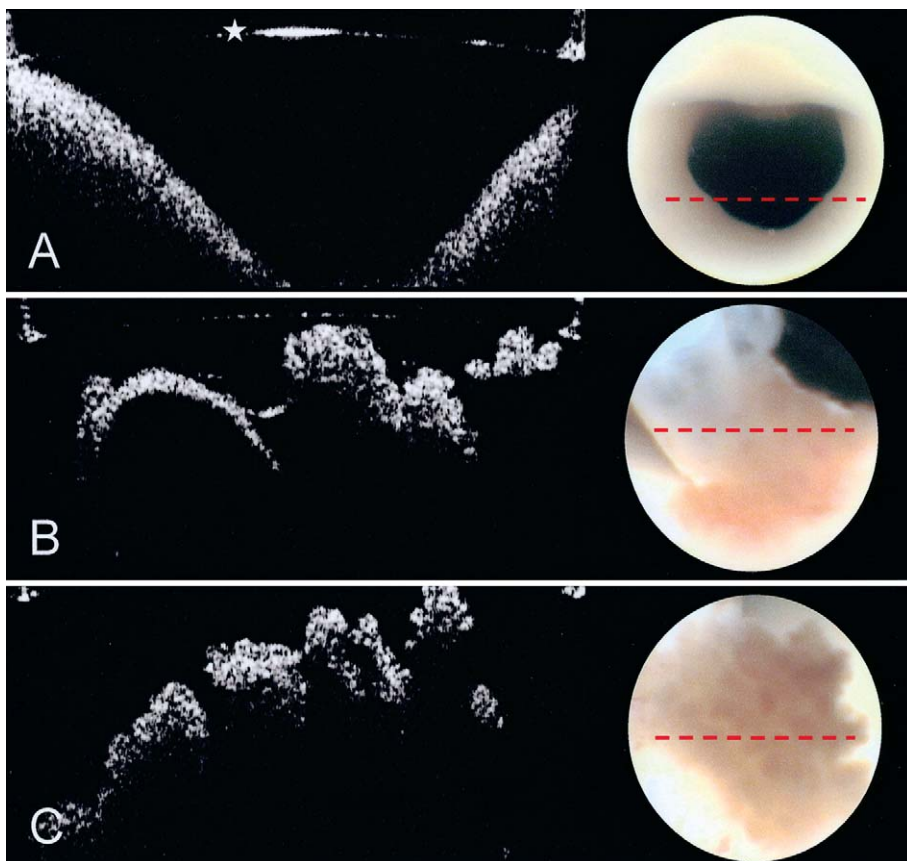
Fig. **2** Intraventricular OCT imaging. Cross-sectional image of the peri-aqueductal tissue (**A**). OCT imaging of the choroid plexus and the thalamostriatal vein (**B** and **C**).
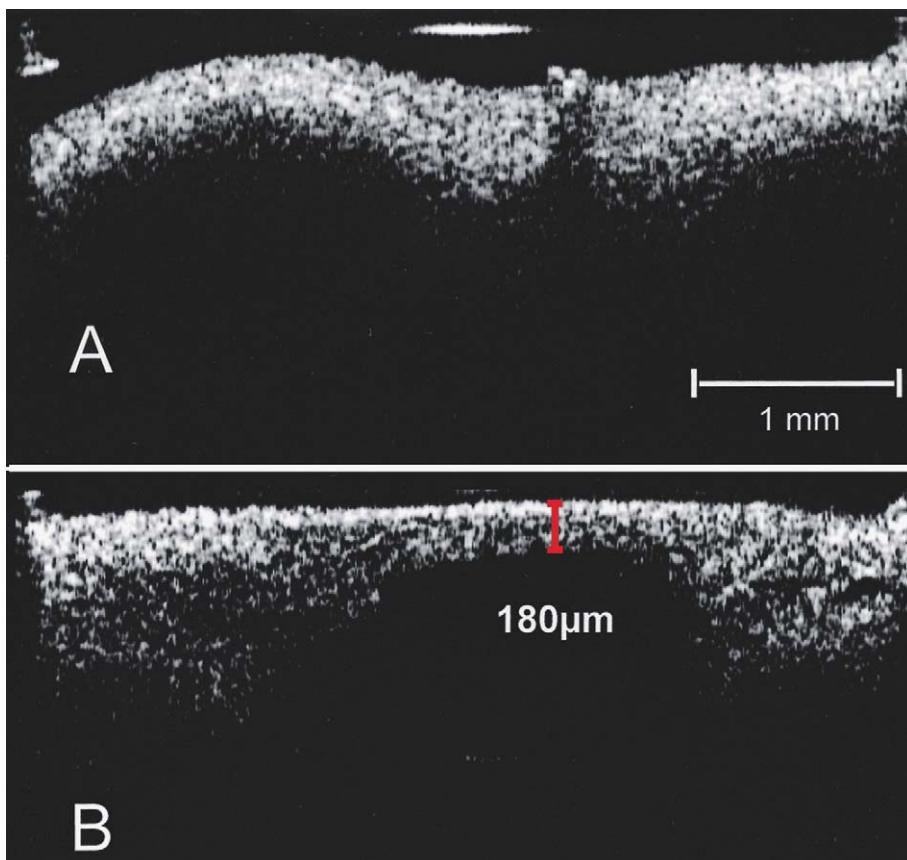
Fig. **3** OCT imaging of the floor of the third ventricle at the level of the corpora mamillaria (**A**) and approximately 4 millimeters rostral to the mamillary bodies (**B**).
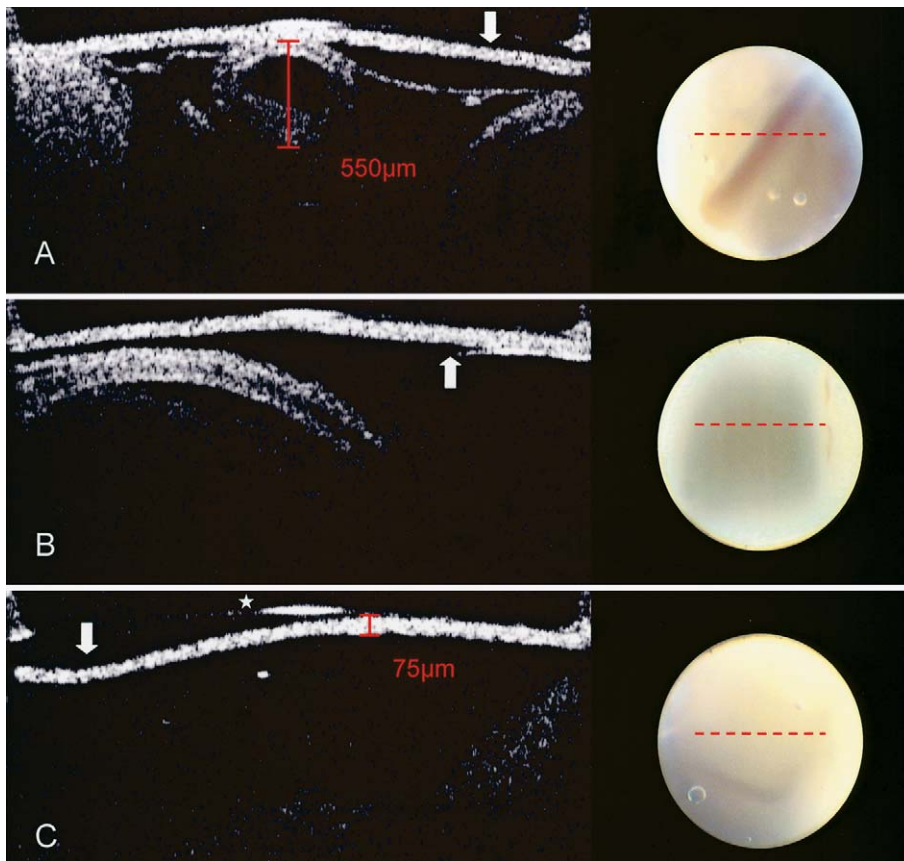
1 mm

180μm

Fig. 4 OCT imaging following perforation of the floor of the third ventricle. **A** Small blood vessel embedded in fine arachnoid membranes visualized through an arachnoid sheet of approximately 75 µm thickness. **B** The rostral wall of the basilar artery imaged through an arachnoidal barrier. **C** Fluid filled space between an arachnoid membrane and the anterior brain stem. Note, high signals represent direct geometric reflexes at the level of the front lens of the endoscope (star).

rod (Richard Wolf, Knittlingen, Germany). This allowed OCT measurements and conventional endoscopic visualization of endoscopically accessible brain tissue. The endoscope was placed close to structures of interest under visual guidance. In this configuration the OCT measurements of the tissue in front of the endoscope required positioning of the endoscope at a sub-millimeter distance to the region of interest, because of an OCT measurement window of 2 millimeters. This provided an optical tomography and B-scan image of a plain 90 degrees to the tissue surface and a 3 mm scan line [5]. The OCT image acquisition time at a resolution of 100 pixels/mm was about 2 seconds per 1 mm scan line. The OCT base unit used in this study allows an axial and lateral optical resolution of about 15 µm and has been used in other studies of imaging of central nervous system tissues and brain tumors by our group [9,11]. In this pilot study a formalin-fixed human brain and two formalin-fixed specimens of malignant tumors with endoventricular growth pattern were used in water to simulate ventriculoscopic imaging.

Results

OCT integrated endoscope

Traditionally endoscopes of 3 mm diameter are constructed using discrete lenses. Because of the inferior imaging quality GRIN rods are only used for very small diameters when the assembly of optical components is difficult. Unlike endoscopes constructed for the visible spectrum, endoscopes for OCT imaging must comply with low losses and low stray light as a consequence of reflections at the optical surfaces, in this case specifically at a wavelength of 1300 nm. In a GRIN endoscope the optical surfaces are minimized and a special antireflex coating for infrared spectra is not necessary. The rigid 0° GRIN endoscope used in this study was originally designed for cystoscopy. It allowed good visualization of the endoventricular anatomy similar to standards of conventional lens endoscopes. Simultaneously, an OCT B scan image was displayed on a second monitor providing a cross-sectional image of tissue within a 2 millimeter distance of the front lens (Fig. **2**). The OCT scan line of 3 millimeters was oriented horizontally in the center of the endoscopic field of view. Close range positioning of the endoscope to specific areas of interest was possible based on the on-line OCT image, which showed the distance of the target tissue volume from the front lens to the tissue surface.

Endoscopic OCT imaging of anatomical structures and tumor tissue

Simulation of a ventroculoscopy in a formalin-fixed human brain specimen in water demonstrated the possibility of a depth view into structures like the choroids plexus, or the thalamostriatal vein and the walls of the ventricular system (Fig. **2**). OCT imaging of the floor of the third ventricle was able to identify a fluid filled space underneath the ventricular floor. The tissue barrier prior to perforation was measured as 180 µm on post-acquisition OCT images (Fig. **3**). Hence, within a two millimeter window for OCT imaging not only intra-tissue structures but also structures underneath or beyond tissue barriers may be visualized. Within the basal and prepontine cisterns, OCT imaging was performed through arachnoid membranes. Whereas with decreasing distance to the arachnoid membrane the video image became increasingly opaque, OCT allowed measurements of structures behind the arachnoid membranes and showed detailed cross-
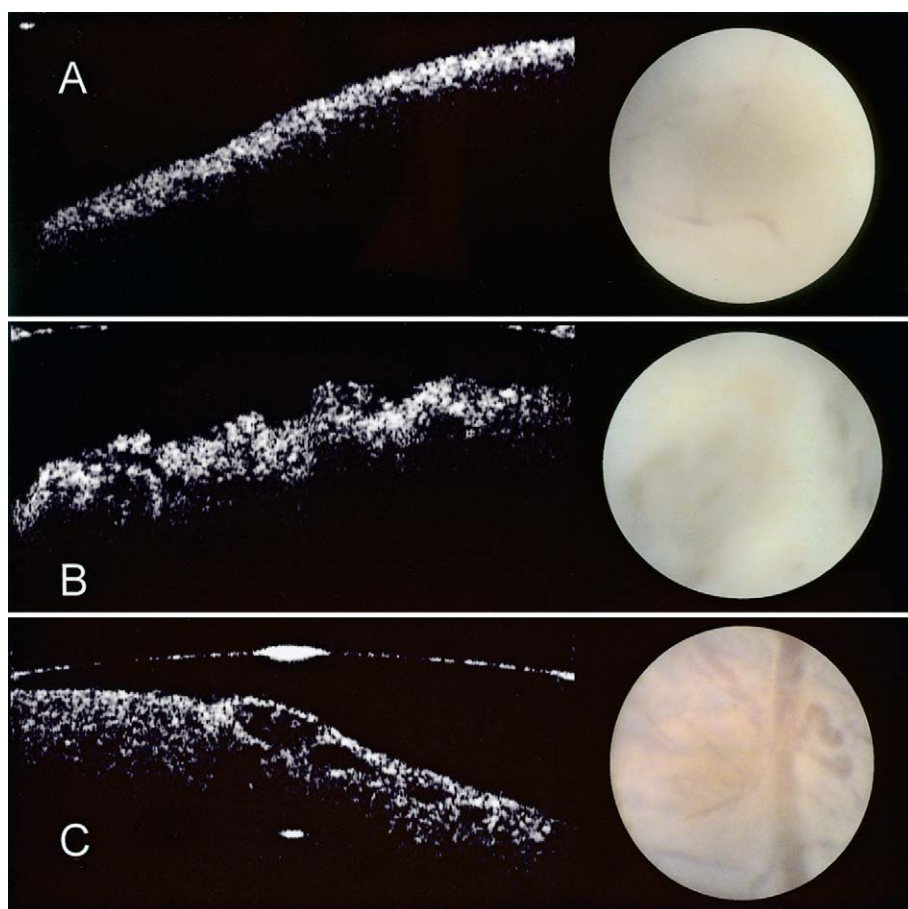
Fig. **5** OCT imaging of the normal ventricular ependyma in a fixed human brain specimen (**A**) and in fixed specimens of malignant tumors involving the walls of the ventricular system. **B** Glioblastoma WHO grade IV. **C** Vascularized capsule of a melanoma metastasis.

sectional images of, for example, vascular structures (Fig. **4**). This allowed visualization of the anterior wall of the basilar artery through an arachnoid membrane of 75 µm thickness. We have previously demonstrated that OCT differentiates tumor and normal brain based on the light attenuation profile and the intra-tissue microstructure [11,12]. For this in vitro study two specimens of tumors with intraventricular extensions were available as formalin-fixed tissue blocks. These specimens were OCT imaged in water. Similar to our previous findings for fixed normal human brain the ventricular walls of the fixed brain specimen showed little intra-tissue microstructure and a characteristic light attenuation profile with a signal intense tissue surface and a rapid continuous loss of signal with increasing tissue depth (Fig. **5**). In a specimen of a glioblastoma involving the ventricular wall, OCT imaging demonstrated a distinct microstructure and an altered light attenuation profile compared to the normal ventricular wall. Endoscopic OCT imaging of a melanoma metastasis showed the vascularization of the tumor capsule. The loss of signal in this specimen occurred at a greater distance from the tissue surface than in normal brain.

OCT imaging of cerebral blood vessels

The endoscope-integrated OCT was used to image cerebral blood vessels of different size. Small arachnoid vessels were imaged by placing the endoscope into the basal cistern. B-scan images identified vascular structures as small as 50 µm in diameter. For arachnoid vessel larger than 100 µm the lumen could be visualized (Fig. **6A**). Moving the OCT-B scan plain along vascular structures displayed branching of smaller vessels from parent vessels (Fig. **6B**). OCT showed a layered structure of vascular

walls of different size blood vessels (Fig. **6C**). For vessels up to a diameter of approximately 1.5 millimeters the entire lumen could be displayed within the imaging window (Fig. **6E**). Larger vessels only allowed imaging of sectors of the vascular wall and the lumen (Fig. **6F**). However, analysis of the basilar artery showed that details of the vascular anatomy may be studied by OCT. OCT showed that the rostral wall of the basilar artery showed a layered structure characteristic for large vessels (Fig. **4B**). The posterior wall of the basilar artery in this specimen was significantly larger in diameter than the vascular wall and did not show a defined structure. A heterogeneous signal of low and high intensity was found within the vascular wall. Histology demonstrated a large plaque distorting the vascular anatomy in this area (Fig. **6F**).

Discussion

Optical coherence tomography is a high-resolution, cross-sectional optical imaging technique that allows real-time imaging for some applications approaching histological resolution without the need to remove tissue. Different strategies have been followed to permit OCT imaging through endoscopes. OCT imaging may be performed through fiber-optic catheters that can be passed through the instrument channel of conventional endoscopes. This approach has demonstrated visualization of the gastrointestinal epithelium and has been applied to imaging of esophageal adenocarcinoma and colonic polyps. Currently, in gastroenterology OCT provides visualization at the same imaging depth as conventional mucosal biopsy and may prove to become
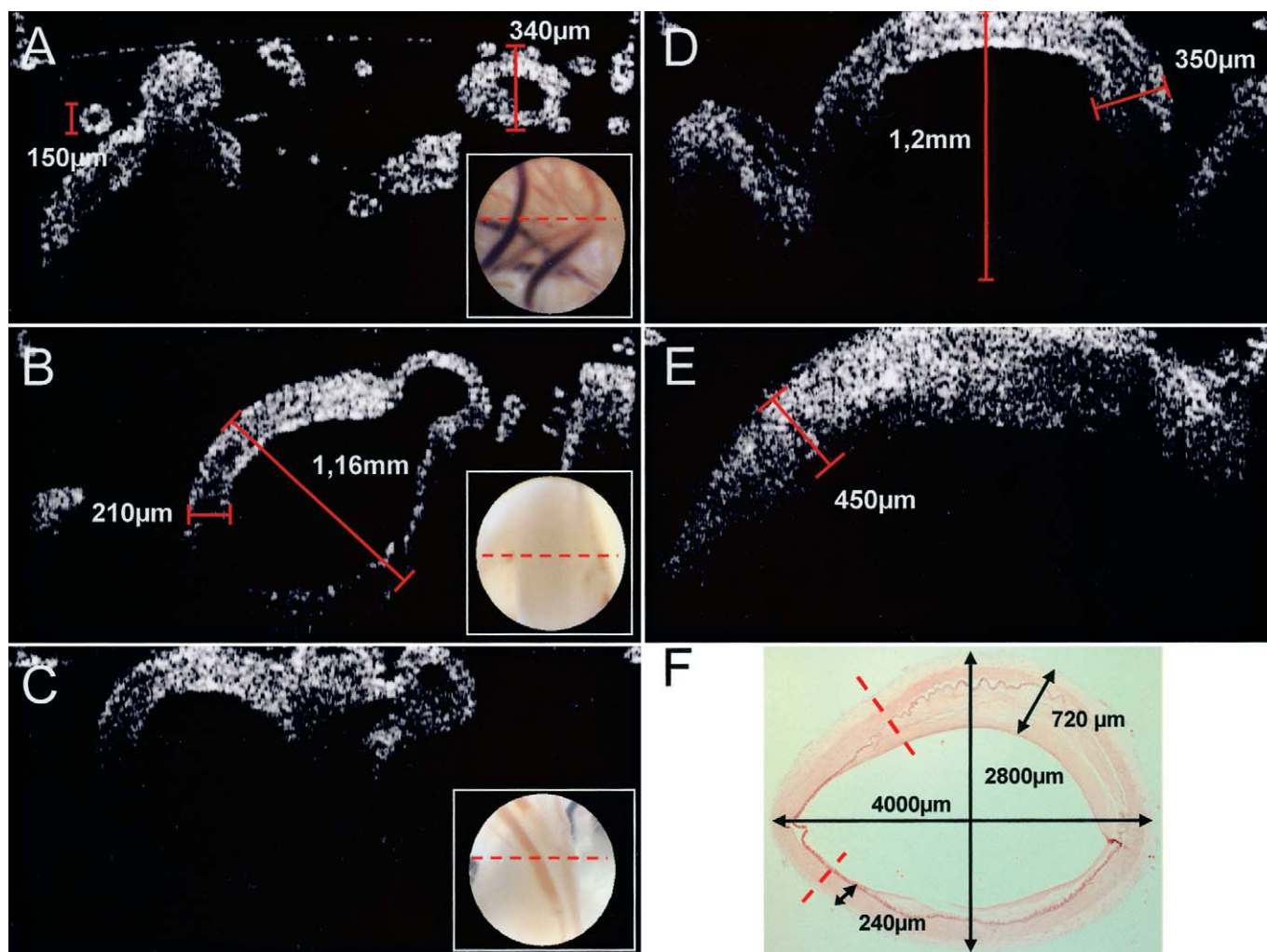
Fig. **6**   Endoscopic OCT imaging of intracranial blood vessels. **A** Arachnoidal vessels within the prepontine cistern. **B** Branching point of a small vessel from the M2 segment of the middle cerebral artery. **C** and **D** M1 segment of the middle cerebral artery showing the layered structure of larger arteries. **E** OCT image of the posterior wall of the basilar artery showing a thickened vascular wall with a low intensity signal within the vascular wall. **F** Corresponding H&E staining of the basilar artery.

a useful minimally invasive technique for evaluation of early neoplastic changes [13]. Diagnostic cystoscopy frequently faces the challenge that structural alterations of the bladder wall below the surface can only be characterized by excisional biopsy. Using fiber-optic catheters through the instrument channel of a cystoscope, characteristic OCT patterns of non-proliferative and proliferative inflammation, dysplasia and transitional cell carcinoma could be obtained in vivo [6]. Because OCT provides a cross-sectional analysis, neoplastic lesions may be discriminated based on the loss of tissue layering. Daniltchenko et al. have demonstrated that OCT imaging can be performed through the optic path of a rigid cystoscope, eliminating the need for shared or dedicated instrument channels [5]. In this study we have used a similar OCT integration in a rigid GRIN endoscope to simulate endoscopic procedures in formalin-fixed whole brain specimens. Similar to our previous findings of non-contact central nervous system tissue and brain tumor OCT tissue analysis through air, interpretable B-scan image information could be obtained in up to 1.5–2.0 millimeter depth depending on the tissue characteristics [11].

Several details of the intraventricular anatomy could be identified by OCT. Further, OCT allowed visualization of structures

through arachnoid membranes and other structures obscuring the view of the endoscope. The preliminary analysis of two tumor specimens with endoventricular growth demonstrated that, based on the light attenuation and the intra-tissue structure, these neoplastic tissues showed a distinct appearance to normal ependyma. However, this analysis was done in fixed specimens. We have previously shown that formalin fixation results in a loss of intra-tissue structure and carries less diagnostic information. In fixed brain interpretable OCT B-scan information can be obtained at lower tissue depth compared to the in vivo situation [9]. Further studies of endoscope integrated in vivo OCT will have to show whether endoscopic OCT imaging of tumor tissue may contribute to a safer identification of the target tissue volume. However, in vivo OCT imaging of normal brain and intrinsic brain tumors of different histological grade through air facilitates non-invasive imaging of tumor to adjacent brain, the infiltration zone, solid tumor and necrosis at high definition based on both the light attenuation profile and the appearance on B-scan images [12].

A feasibility study using OCT analysis of clinical biopsy specimens from solid tumor and the wall of the resection cavity ex vivo has demonstrated that OCT allows identification of micro-

scopic tumor in what appeared macroscopically normal cortex and white matter [12]. However, non-contact imaging of brain tissue during neurosurgical procedures has to take into account that the target volume follows the respiratory and arterial cycle resulting in movements of several millimeters in amplitude, which results in a characteristic distortion of the OCT image. Post-acquisition image processing and automated detection of the air to tissue intensity change at the tissue surface allowed realignment of the A scans, which allowed easy interpretation of changes in the intra-tissue light attenuation profile in vivo [11]. These findings illustrate that optical technologies offer the potential of a high resolution imaging modality of the structure and optical properties of brain and brain tumor tissue, which has lead to integration of OCT into the optic path of a neurosurgical operating microscope. This has fully integrated OCT into the workflow of experimental microsurgical procedures [2]. In this early phase of evaluation OCT has already demonstrated an interesting potential as an aid to neurosurgical procedures.

Regardless of the OCT applicator, endoscope, free probe, or microscope integration, OCT offers perspectives for further developments. Recent development of Doppler OCT offers the potential of functional optical tissue imaging. These technologies are largely software-based and theoretically can be implemented into both endoscopic and microscopic OCT integrated instruments. In this study we have shown that OCT provides cross-sectional images of brain blood vessels of varying calibers. Doppler optical coherence tomography (D-OCT) images the flow velocity of moving particles in highly scattering media [14]. Recently, a fast-scanning D-OCT system has been presented that uses the phase information derived from a Hilbert transformation demonstrating accurate measurements of the blood flow velocity in blood vessels of $10-30\,\mu m$ diameter in human skin up to a tissue depth of $600\,\mu m$ [15]. Measurements of blood flow in small vessels in which red blood cells move at low velocity is difficult because the high imaging frame rates required for real-time D-OCT reduce the sensitivity due to very short A-scan times. However, at A-scan rates of $400\,Hz$ a minimum velocity of $10\,\mu m/s$ could be detected at a spatial resolution of $10\,\mu m$ [15]. For potential neurosurgical applications this would suggest that both blood flow analysis of larger vessels in neurovascular procedures as well as measurements of tissue perfusion based on the flow velocity of capillary-size vessels can be obtained. We have demonstrated here that imaging of the lumen of large cerebral blood vessels by endoscope-integrated OCT is feasible, suggesting that D-OCT integration may allow a non-contact analysis of vessels of all sizes relevant to neurosurgical procedures.

OCT may carry some potential as a tool in neuroendoscopy. To improve the image definition and image acquisition rates of an OCT-integrated neuroendoscope our group is currently working on a high-resolution spectral-domain OCT-integrated GRIN endoscope. Further in vivo studies will have to demonstrate the value of this technology.

References

1 Welzel J, Reinhardt C, Lankenau E, Winter C, Wolff HH. Changes in function and morphology of normal human skin: evaluation using optical coherence tomography. Br J Dermatol 2004; 150: 220–225

2 Giese A, Böhringer HJ, Leppert J, Kantelhardt SR, Lankenau E, Koch P, Hüttmann G. Non-invasive intraoperative optical coherence tomography of the resection cavity during surgery of intrinsic brain tumors. Spie Bios 2006, in press

3 Tearney GJ, Brezinski ME, Southern JF, Bouma BE, Boppart SA, Fujimoto JG. Optical biopsy in human urologic tissue using optical coherence tomography. J Urol 1997; 157: 1915–1919

4 Tearney GJ, Brezinski ME, Bouma BE, Boppart SA, Pitris C, Southern JF, Fujimoto JG. In vivo endoscopic optical biopsy with optical coherence tomography. Science 1997; 276: 2037–2039

5 Daniltchenko D, König F, Lankenau E, Sachs M, Kristiansen G, Huettmann G, Schnorr D. Utilizing optical coherence tomography (OCT) for visualization of urothelial diseases of the urinary bladder. Radiologe 2005, Aug 6 [Epub ahead of print]

6 Zagaynova EV, Streltsova OS, Gladkova ND, Snopova LB, Gelikonov GV, Feldchtein FI, Morozov AN. In vivo optical coherence tomography feasibility for bladder disease. J Urol 2002; 167: 1492–1496

7 Puliafito CA, Hee MR, Lin CP, Reichel E, Schuman JS, Duker JS, Izatt JA, Swanson EA, Fujimoto JG. Imaging of macular diseases with optical coherence tomography. J Biomed Opt 2004; 9: 47–74

8 Bouma BE, Tearney GJ, Compton CC, Nishioka NS. High-resolution imaging of the human esophagus and stomach in vivo using optical coherence tomography. Gastrointestinal Endoscopy 2000; 51: 467–474

9 Böhringer HJ, Boller D, Leppert J, Knopp U, Lankenau E, Reusche E, Hüttmann G, Giese A. Time domain and spectral domain optical coherence tomography in the analysis of brain tumor tissue. Lasers in Surgery and Medicine, in press 2006

10 Bizheva K, Unterhuber A, Hermann B, Povazay B, Sattmann H, Drexler W, Stingl A, Le T, Mei M, Holzwarth R, Reitsamer HA, Morgan JE, Cowey A. Imaging ex vivo and in vitro brain morphology in animal models with ultrahigh resolution optical coherence tomography. J Biomed Opt 2004; 9: 719–724

11 Böhringer HJ, Leppert J, Lankenau E, Reusche E, Hüttmann G, Giese A. Analysis of human brain tumor tissue by optical coherence tomography. 2005, submitted

12 Böhringer HJ, Leppert J, Wüstenberg R, Bodensteiner C, Reusche E, Stellmacher F, Lankenau E, Winter C, Koch P, Hüttmann G, Giese A. Analysis of glioma tissue by high resolution spectral-domain optical coherence tomography. 2005, submitted

13 Brand S, Poneros JM, Bouma BE, Teamey GJ, Compton CC, Nishioka NS. Optical coherence tomography in the gastrointestinal tract. Endoscopy 2000; 32: 796–803

14 Tomlins PH, Wang RK. Theory, development and applications of optical coherence tomography. J Phys D: Appl Phys 2005; 38: 2519–2535

15 Zhao Y, Chen Z, Saxer C, Xiang S, de Boer JF, Nelson S. Phase-resolved optical coherence tomography and optical Doppler tomography for imaging blood flow in human skin with fast scanning speed and high velocity sensitivity. Optics Letters 2000; 25: 114–116

Original Article

275

Review of Radiosurgery of Pineal Parenchymal Tumors. Long Survival Following 125-Iodine Brachytherapy of Pineoblastomas in 2 Cases

J. Julow[1]
Á. Viola[1,2]
T. Major[3]

276

Abstract

Objective: The aim of the present work is to report the volumetric changes of tumor in two pineoblastoma patients treated with stereotactic interstitial irradiation and to present a review on radiosurgery of pineal parenchymal tumors. **Methods:** Two of our patients with pineoblastoma were treated with CT and image-fusion guided 125-iodine brachytherapy. The tumor volumes were determined with outlined contours on planning and control CT/MRI images and were compared. **Results:** Until January 2006, there were 61- and 58-month follow-up periods in the two cases. 56 and 53 months after irradiation the MRI images showed significant tumor shrinkage. In case 1 tumor volume was $0.76\ cm^3$ on the last control MRI image, compared to the $2.87\ cm^3$ at the time of interstitial irradiation, which means 73% shrinkage. In case 2, tumor volume measured with the last control MRI examination was $0.29\ cm^3$, which represents 77% shrinkage of the original tumor volume. In both Cases 1 and 2, PET examinations using ^{11}C-methionine showed no active tumor mass 56 and 53 months following brachytherapy. **Conclusion:** Two successful treatments of pineoblastoma are reported. The interstitial irradiation of the tumors decreased their volumes significantly. The CT and image fusion-guided 125-iodine stereotactic brachytherapy can be planned well dosimetrically and is surgically precise.

Key words

Pineoblastoma · brachytherapy · 125-iodine interstitial irradiation · shrinkage · image fusion

Introduction

The frequency of pineal region tumors (PRTs) shows regional differences. From a global perspective PRTs make up 0.4–1% of all brain tumors and 3–11% of childhood brain tumors in the USA and Europe compared to 2.2–8.8% of all brain tumors and 12.5% of childhood tumors in Japan and Taiwan [1–5]. PRTs can be divided into 4 main groups, 50% of these tumors appear in people under 20 years of age (Table **1**) [6–8].

The pineal parenchymal tumors (PPT) can be further differentiated according to their types. Their frequency is not gender biased (Table **2**) [2, 7].

Symptoms caused by PRTs can be a result of increased intracranial pressure provoked by obstructive hydrocephalus, pressure on the tectum mesencephali and more rarely, pressure on the hypothalamus. Hormonal changes can be caused by the hormonal activity of the tumor, or by the damage to the surrounding tissues [2, 9, 10].

Today, biopsy is a standard procedure and can be readily performed to support the diagnosis of PRT [11–13]. Regis et al. have reported 1.3% mortality and 0.8% morbidity following the biopsy of 370 PRTs. The tumors were correctly identified in 94% of the cases [13]. Dempsey et al. reported 0% mortality and less than 2% morbidity while performing biopsies of PRTs [14, 15].

Table 1 Types and frequency of pineal region tumors	
Type	*Frequency (%)*
I. Germinomas	*33–71*
II. Pineal parenchymal tumors (PPT)	*14–30*
III. Neuroectodermal tumors	*0–10*
IV. Other tumors, cysts and vascular malformations	*0–10*

Table 2 Types and frequency of pineal parenchymal tumors	
Type	*Frequency (%)*
1. Pineocytomas	*45*
2. Pineoblastomas	*45.5*
3. Pineal parenchymal tumors with intermediate differentiation	*8.5*
4. Mixed pineocytoma/pineoblastoma	*10*

Patients and Methods

In the treatment of two cases of pineoblastoma tumor, we used CT and image-fusion guided 125-iodine (^{125}I)-stereotactic brachytherapy. The image fusion was performed by the BrainLab-Target 1.19 software on an Alfa 430 (Digital) workstation before, during and after interstitial irradiation of pineoblastoma with 125-iodine seeds. This method has been described in a previous publication [16,17].

Case Reports

Case 1

K. Cs., female patient born in 1952, complained of headaches and vertigo for one year in February 2000. The CT examination confirmed hydrocephalus and a space-occupying lesion in the pineal region. Because of the hydrocephalus, a ventriculo-antral shunt was implanted in February 2000. Ten months later in December 2000, following a stereotactic biopsy which showed a pineoblastoma, a catheter was stereotactically introduced into the tumor through a right-side parieto-occipital burr hole, followed by a CT-guided computerized treatment planning and interstitial irradiation. The placement of the catheter was confirmed by intraoperative CT-CT image fusion. Two ^{125}I isotope seeds, each with 4.6 mCi activity, were introduced into the catheter, so the total activity was 9.2 mCi. As a result, 94 % of the tumor volume (2.87 cm^3) was irradiated by the dose of 60 Gy or more.

The catheter with the isotope seeds was removed 522 hours after the implantation. The patient reported no complaints and exhibited no neurological changes. The general state of the patient corresponds to level 100 of the Karnofsky scale in January 2006.

Case 2

Cs. L. a female patient, born in 1937, complained of unsteady gait, vertigo and loss of memory of 3 weeks duration in January 2001. The neurological examination revealed bilateral horizontal nystagmus. The CT examination revealed a space-occupying lesion located in the pineal region that caused obstructive hydrocephalus. A ventriculo-peritoneal shunt was implanted in February 2001. This procedure significantly reduced the unsteady gait and vertigo. In March 2001 a stereotactic biopsy was performed confirming a pineoblastoma. A CT-guided stereotactic target volume determination and computerized treatment planning of the interstitial irradiation was completed. A catheter was introduced into the tumor from the right-side centro-parietal burr hole. The location of the catheter was confirmed with an intra-operative CT-CT image fusion. One ^{125}I isotope seed of 17.1 mCi activity in the catheter was placed into the tumor, and 92 % of the
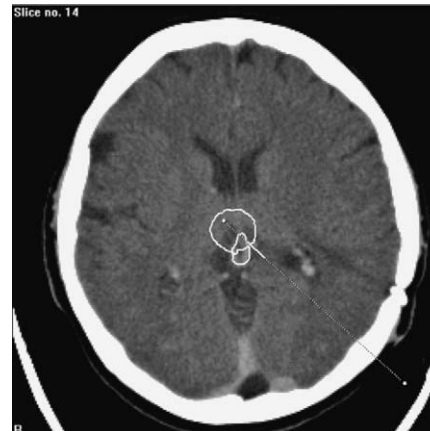

Fig. 1 The fusion of planning CT images with the control CT images obtained 56 months after the brachytherapy of the 1st case. The green contour indicates the tumor contour before and the yellow one 56 months after the brachytherapy. The examination shows a 73 % decrease of the original tumor volume.

tumor volume (1.27 cm^3) was irradiated with a dose of 54 Gy or more. The catheter with the seed was removed 192 hours following the implant procedure. The complaints of the patient ceased and no change has occurred in her neurological status. In January 2006, the general state of the patient corresponded to level 90 of the Karnofsky scale.

Results

In January 2006, the follow-up period after the brachytherapy was 61 months in case 1 and 58 months in case 2. We have repeatedly performed control MRI and PET examinations on both patients. The last MRI and PET examinations were done in August 2005. In case 1, the measured tumor volume was 0.76 cm^3 on the control MR images, which means a 73 % shrinkage compared to 2.87 cm^3 tumor volume at the time of brachytherapy (Fig. 1). In case 2, the tumor volume measured on the control MRI images was 0.29 cm^3, which demonstrated 77 % shrinkage of the initial 1.27 cm^3 tumor volume at the time of brachytherapy (Fig. 2). In case 1, as well as in case 2, PET examinations using ^{11}C-methionine were showing no active tumor mass 56 and 53 months following brachytherapy.

Discussion

The surgical treatment of PRT goes back to the first two decades of the 20th century. The first attempts are attributed to Krause (1907), Horsley (1910), Bruhner (1913) and Pusepp (1914). In 1913, Oppenheim and Krause performed the first successful
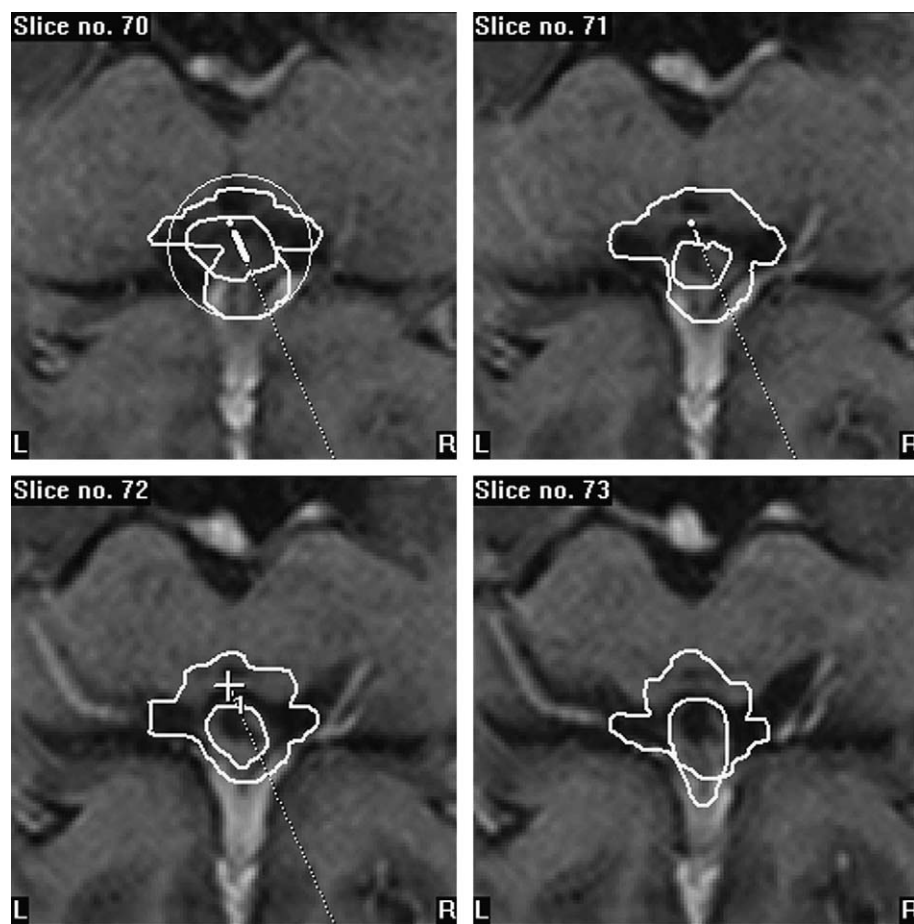
Fig. **2** The fusion of planning CT images with the control MRI images obtained 53 months after the brachytherapy of the 1st case. The red contour indicates the tumor contour before and the white one 53 months after the brachytherapy. The examination shows a 77 % decrease of the original tumor volume.

exposure of the infratentorial supracerebellar pineal region on a ten-year-old boy in the sitting position. Dandy reported 3 parieto-occipital transcallosal exposures in 1921. Right-side parieto-occipital transcortical translateral ventricular exposure was introduced by Van Wagenen in 1928. The occipital interhemispherial transtentorial exposure is associated with Poppen and Jameison [18–22].

The mortality rate for surgical procedures by excision was 50–70 % at the beginning and therefore less radical procedures were introduced later. In the period between 1948–1968 Torkildsen began to use ventriculo-cisternostomia. Radiotherapy was practiced by Kahn [23]. Thanks to these new methods, the survival rate at one year reached 50 %, while the rate of survival at five years reached 30 %. Stein (1971), one of the forerunners of microsurgery of the pineal region, reported on 6 PRTs using infratentorial supracebellar exposure with a 0 % morbidity rate [22, 24].

Hoffmann et al. reported on the surgical mortality rate of PRTs in a retrospective study, showing a decrease from 75 % to 25 % between 1950–1960, and a further decrease to 4 % between 1967–1974, and finally reaching 0 % between 1975 and 1982. This significant decrease in mortality was found to be a direct result of the use of microsurgical techniques, the development and use of improved anesthesia coupled with the advancement in intensive care and management of patients [4, 25, 26].

The utilization of radiotherapy (gamma knife, LINAC, brachytherapy, frameless stereotactic radiosurgery and the combination of these with external irradiation) with PRTs increased in the decades between the 1960 and 1990 [14, 27–33]. Many studies showing the results of the treatment of PRTs have been published in the last few decades [13, 26, 34, 35]. The effectiveness of the individual types of treatments has not yet been studied. Based on information from previous publications, we were able to demonstrate that our radiological method used in the treatment of histologically confirmed PPT was efficacious (Tables **3**–**5**) [2, 11, 15, 23, 26–28, 34–45].

Wara reports a survival of 3 years after the external irradiation administered locally on the tumor [32]. Sung et al. report a 3–6 year follow-up period following the introduction of a VP shunt and external irradiation administered locally on the tumor [44].

According to Fuller, the PPT has a more frequent reoccurrence than any other type of tumor of the pineal region. The incidence of spinal metastases is significantly increased in patients undergoing surgical biopsy and in patients without surgical biopsy of the PPT. Fuller did not find any correlation between the quantity of the dose administered to the tumor, the frequency of relapse and the length of survival [35].

As for Schild, relapses were more frequent when the radiotherapeutic dose was less than 50 Gy–in 6 of 7 cases. Using doses higher than 50 Gy, the frequency of relapse was 0 in 12 cases [46].

Table 3 Treatment results of external irradiation of pineal parenchymal tumors

Author (year)	Histology	Number of cases	Number of hydrocephalus treatment	RT – Number of cases/Type/Dose (Gy)	Other therapy – Number of cases/Type	Relapse – Number of cases/Time after RT	Leptomeningeal and spinal disease – Number of cases/Time after RT	Death – Number of cases/Time after RT	Follow up from RT
Fuller (1993)	PNB	3	ND	3/L, CS/54–55.8, 30.6–39	ND	2/10 Mo, 1 Yr	–	–	1–6 Yr
Chao (1993)	PNC	1	1	1/L, WB/36, 20	1/SR	–	–	–	41 Mo
Linggood (1992)	PNB	4	3	4/L, WB, CS/10–15, 30–50 30	3/SR	ND	ND	3/16, 20, 27 Mo	16 Mo–6 Yr
D'Andrea (1987)	PNC	6	3	6/L, WB, CS, S/40–61, 32.5, 36–40, 30	3/K, 5/SR	4/0.5–3.5 Yr	2/0.5, 2 Yr	4/1–5.5 Yr	1–5.5 Yr
Chapman (1980)	PNB	3	2	3/L, WB, S/50, 30–50, 15.5–20	2/SR	1/ND	2/ND	3/16, 27, 28 Mo	16–28 Mo
Borit (1980)	PNC	1	–	1/ND/60	–	–	–	1/1 Yr	1 Yr
	PNB	1	–	1/ND/50, 30, 35	1/SR	ND	1/ND	1/24 Mo	24 Mo
Neuwelt (1979)	PNC	2	2	2/L, WB, S/10, 40, 40–43	2/SR	–	–	–	1 Mo, 2 Yr
	PNB	2	2	2/L, WB, S/15, 40–50, 22.5–34	1/SR	–	1/10 Mo	1/13 Mo	6–13 Mo
Pecker (1979)	PNC	1	1	1/ND	–	ND	–	–	29 Mo
	PNB	1	1	1/ND	–	ND	1/ND	–	42 Mo
Sung (1978)	PNB	1	1	1/L/50	ND	ND	ND	–	6 Yr
	MIX	1	1	1/L/50	ND	ND	ND	–	3 Yr
Wara (1977)	PNB	1	ND	1/L/42.5	ND	ND	ND	1/3 Yr	3 Yr

CS = cerebrospinal, K = chemotherapy, L = local, MIX = mixed pineocytoma/pineoblastoma, Mo = month, ND = no data, PNB = pineoblastoma, PNC = pineocytoma, RT = radiotherapy, S = spine, SR = surgery, WB = whole brain, Yr = year.

Table 4 Treatment results of stereotactic radiosurgery of pineal parenchymal tumors

Author (year)	Histology	Number of cases	Stereotactic radiosurgery Marginal dose (Gy)	Number of hydrocephalus treatment	RS – Number of cases/Type/Dose (Gy)	Other therapy – Number of cases/Type	Death – Number of cases/Time after RS	Follow up from RS
Hasegawa (2002)	PNC	10	12–20	8	1/WB/ND	1/K, 1/SR	1/14 LM	
	PNB	4	13–16	3	2/WB, S/24–30	3/K		
					1/WB, L, S/32, 19.8, 36	1/SR	4/LM, NL, S, ND	52 Mo
	MIX	2	14	2	1/L/56	2/SR	–	
Manera (1996)	PNC	3	12–20	2	–	1/K	–	4, 10, 12 Mo
	PNB	2	12–20	2	–	2/K	–	1, 33 Mo
Dempsey (1992)	PNC	1	20	NA	–	–	–	14 Mo
Backlund (1974)	PNC	2	ND	1	–	–	–	1, 3 Mo

K = chemotherapy, L = local, LM = leptomeningeal disease, MIX = mixed pineocytoma/pineoblastoma, Mo = month, ND = no data, NL = new lesion, PNB = pineoblastoma, PNC = pineocytoma, RS = radiosurgery, S = spine, SR = surgery, WB = whole brain, Yr = year.

Abay performed radiotherapy on 27 tumors of the pineal region, and found a direct correlation between the size of the irradiated field and the local tumor control. The larger the irradiated field the better the tumor control [9].

Bradfield pursued radiotherapeutic treatment on 20 PRTs and reported on longer survival when having irradiated larger fields [47]. Similar results were given by Rao, however, he found no correlation between the intensity of the administered dose and the survival length [48].

Mincer found an absence of symptoms in patients who had been irradiated in smaller field rather than in those irradiated in larger field [49].

Table 5 Treatment results of brachytherapy of pineal parenchymal tumors

Author (year)	Histology	Number of cases	Brachytherapy – Number of cases/Type of isotope/Marginal dose (Gy)	Number of hydrocephalus treatment	Radiotherapy – Number of cases/Type/Dose (Gy)	Other therapy – Number of cases/Type	Relapse – Number of cases/Time after BT	Death – Number of cases/Time after RS	Follow up from BT
Barlas (2000)	PNB	2	4/^{125}I/50–60	ND	2/L, CS/50.4, 36	1/K	24, 18* 13, 27** 20, –***	–	50 Mo, 70 Mo
Kreth (1996)	PNC	8	4/^{125}I/60	–	3/L/60	1/OB	–	– 1/8 Mo	41 Mo
Tada (1996)	PNB	1	1/^{192}Ir/40	1	1/ND	1/K, SR	ND	–	24 Mo
Matsumoto (1995)	MIX	1	1/^{192}Ir/36	1	–	–	–	–	8 Mo
Frank (1985)	PNC	1	1/^{125}I/100–120	ND	–	–	–	–	3 Yr
Borit (1980)	PNC	1	1/^{198}Au/ND	1	–	–	ND	1/9 Mo	4 Yr
	PNB	3	1/^{198}Au/ND	2	–	–	2/ND	2/9 Mo, 7 Yr	9 Mo, 20 Mo, 7 Yr

BT = Brachytherapy, CS = cerebrospinal, K = chemotherapy, L = local, MIX = mixed pineocytoma/pineoblastoma, Mo = month, ND = no data, OB = observation, PNB = pineoblastoma, PNC = pineocytoma, SR = surgery, Yr = year, * = after radiotherapy, ** = after 1st brachytherapy, *** = after 2nd brachytherapy.

The first stereotactic radiosurgery of histologically verified PPTs was performed by Backlund in 1974. He administered 50 Gy irradiation on each tumor. One year later, 2 irradiated pineocytomas disappeared completely, or shrunk significantly [27].

Hasegawa et al. utilized gamma knife irradiation on 16 PPTs. They proceeded as follows. pineocytomas of less than 3 cm in diameter were treated with stereotactic irradiation; pineocytomas of more than 3 cm in diameter were resected, and in the case of other types of PPTs the treatment procedure was craniospinal radiotherapy, chemotherapy and stereotactic boost irradiation. The marginal dose was 12–20 Gy, the average follow-up period was 52 months (7–108 months), and the highest mortality was recorded in the case of pineoblastomas (4/4) with 7–47 months survival [11].

The first brachytherapy of a histologically verified pineal parenchymal tumor was associated with the name of Borit. He used the ^{198}Au isotope for the implantation and the follow-up period was 7 years [28]. Kreth performed brachytherapy of PPT on the largest number of cases, the average follow-up period for the 8 PPTs irradiated with 125-iodine isotopes was 41 months. He reported a mortality rate only for 1 patient 8 months following the brachytherapy [26].

Barlas recorded relapses at 3 months after pineoblastomas excision, and at 13–27 months following interstitial irradiation with 125 iodine isotopes [2].

In the case of our two patients with pineoblastomas, confirmed with biopsy and histological diagnosis, we opted for the interstitial irradiation to be performed during a single session, thus saving our patients an additional stereotactic procedure. The ^{125}I brachytherapy revealed 73 % tumor shrinkage at 56 months after the irradiation in case 1, and 77 % tumor shrinkage at 53 months after the irradiation in case 2. In both cases, PET examinations using ^{11}C-methionine were showing no active tumor mass 56 and 53 months following brachytherapy, respectively. The patients are now essentially symptom-free and without complaints. The CT and image fusion guided ^{125}I stereotactic brachytherapy can be planned well dosimetrically and is surgically precise.

References

1 Araki C, Matsumoto S. Statistical re-evaluation of pinealoma and related tumors in Japan. J Neurosurg 1969; 30: 146–149
2 Barlas O, Bayindir Ç, İmer M et al. Non-resective management of pineoblastoma. Minim Invas Neurosurg 2000; 43: 163–170
3 Edward MAB, Hudgins RJ, Wilson CB. Pineal region tumors in children. J Neurosurg 1988; 68: 689–697
4 Hoffman HJ. Pineal region tumors. Prog Exp Tumor Res 1987; 30: 281–288
5 Packer RJ, Sutton LN, Rosenstock JE et al. Pineal region tumors of childhood. Pediatrics 1984; 74: 97–101
6 Kersh CR, Constable CW, Eisert DR et al. Primary central nervous system germ cell tumors. Cancer 1988; 61: 2148–2152
7 Mena H, Scheithauer BW, Nakazato Y. Pineal parenchymal tmours. In: Kleihues P, Cavenee WK. Pathology and genetics of tumours of the nervous system. International Agency for Research on Cancer, Lyon, 1997, pp 83–88
8 Rubenstein LD. Tumors of the central nervous system. Atlas of tumor pathology. Washington, DC. AFIP, 1972, pp 269–284
9 Abay EO, Laws ER, Grado GL et al. Pineal tumors in children and adolescents. J Neurosurg 1981; 55: 889–895
10 El-Mahdi AM, Philips E, Lott S. The role of radiation therapy in pinealoma. Radiology 1972; 103: 407–412
11 Hasegawa T, Kondziolka D, Hadjipanayis CG et al. The role of radiosurgery for the treatment of pineal parenchymal tumors. Neurosurgery 2002; 51: 880–889
12 Ostertag C. Pineal region management – A stereotactic perspective. Pan Arab-Journals 1999; 3: 2–12
13 Regis J, Bouillot P, Rouby-Volot F et al. Pineal region tumors and the role of stereotactic biopsy. Review of the mortality, morbidity, and diagnostic rates in 370 cases. Neurosurgesry 1996; 39: 907–911
14 Dempsey PK, Kondziolka D, Lunsford LD. Stereotactic diagnosis and treatment of pineal region tumours and vascular malformations. Acta Neurochir 1992; 116: 14–22
15 Dempsey PK, Lunsford LD. Stereotactic radiosurgery for pineal region tumors. Neurosurg Clin N Am 1992; 3: 245–253

16 Julow J, Major T, Emri M et al. The application of image fusion in stereotactic brachytherapy of brain tumours. Acta Neurochir 2000; 142: 1253–1258

17 Viola A, Major T, Julow J. The importance of postoperative CT image fusion verification of stereotactic interstitial irradiation for brain tumors. Int J Radiat Oncol Bilo Phys 2004; 60: 322–328

18 Dandy WE. Operative experiences incases of pineal tumors. Arch Surg 1936; 33: 19–46

19 Jamieson KG. Excision of pineal tumors. J Neurosurg 1971; 35: 550–553

20 Pendl G. The surgery of pineal lesions – historical perspective. In: Neuwelt ER (ed), Diagnosis and treatment of pineal region tumours. Williams and Wilkins, Baltimore, 1984, pp 139–154

21 Poppen JL. The right occipital approach to a pinealoma. J Neurosurg 1966; 25: 706–710

22 Rosenfeld JF. Supratentorial approaches to pineal tumors. In: Kaye AH, Black PMcL (eds), Operative neurosurgery. Harcourt Publishers Limited, London, New York, Philadelphia, St. Luis, Sydney, Toronto, 2000, pp 825–840

23 Pecker J, Scarabin JM, Vallee B et al. Treatment in tumours of the pineal region. Value of stereotaxic biopsy. Surg Neurol 1979; 12: 341–348

24 Shibamoto Y, Abe M, Yamashita J et al. Treatment results of intracranial germinoma as a function of the irradiated volume. Int J Radiat Oncol Biol Phys 1988; 15: 285–290

25 Herrmann HD, Winkler D, Westphal M. Treatment of tumours of the pineal region and posterior part of the third ventricle. Acta Neurochir 1992; 116: 137–146

26 Kreth FW, Schatz CR, Pagenstecher A et al. Stereotactic management of lesions of the pineal region. Neurosurgery 1996; 39: 280–291

27 Backlund EO, Rähn T, Sarby B. Treatment of pinealomas by stereotaxic radiation surgery. Acta Radiol Ther Phys Biol 1974; 13: 368–376

28 Borit A, Blackwood W, Mair WGP. The separation of pineocytoma from pineoblastoma. Cancer 1980; 45: 1408–1418

29 Buatti JM, Bova FJ, Friedman WA et al. Preliminary experience with frameless stereotactic radiotherapy. Int J Radiat Oncol Biol Phys 1998; 42: 591–599

30 Casentini L, Colombo F, Pozza F et al. Combined radiosurgery and external radiotherapy of intracranial germinomas. Surg Neurol 1990; 34: 79–86

31 Regine WF, Hodes JE, Patchell RA. Intracranial germinoma. Treatment with radiosurgery alone. J Neurooncol 1998; 37: 75–77

32 Wara WM, Jenkin RDT, Evans A et al. Tumors of the pineal and suprasellar region. Children's Cancer Study Group treatment results 1960–1975. Cancer 1979; 43: 698–701

33 Zeng-min T, Zong-hui L, Gui-quan K et al. CT-guided stereotactic injection of radionuclide for treatment of brain tumors. Stereotact Funct Neurosurg 1992; 59: 169–173

34 Chao CKS, Lee STL, Lin FJ et al. A multivariate analysis of prognostic factors in management of pineal tumor. Int J Radiat Oncol Biol Phys 1993; 27: 1185–1191

35 Fuller BG, Kapp DS, Cox R. Radiation therapy of pineal region tumors. 25 new cases and a review of 208 previously reported cases. Int J Radiat Oncol Biol Phys 1994; 28: 229–245

36 Chapman PH, Linggood RM. The management of pineal area tumors. A recent reappraisal. Cancer 1980; 46: 1253–1257

37 D'Andrea AD, Packer RJ, Rorke LB et al. Pineocytomas of childhood. A reappraisal of natural history and response to therapy. Cancer 1987; 59: 1353–1357

38 Frank F, Gaist G, Piazza G et al. Stereotaxic biopsy and radioactive implantation for interstitial therapy of tumors of the pineal region. Surg Neurol 1985; 23: 275–280

39 Linggood RM, Chapman PH. Pineal tumors. J Neuro-Oncol 1992; 12: 85–91

40 Manera L, Régis J, Chinot O et al. Pineal region tumors. The role of stereotactic radiosurgery. Stereotact Funct Neurosurg 1996; 66: 164–173

41 Matsumoto K, Higashi H, Tomita S et al. Pineal region tumours treated with interstitial brachytherapy with low activity sources (192-iridium). Acta Neurochir 1995; 136: 21–28

42 Neuwelt EA, Glasberg M, Frenkel E et al. Malignant pineal region tumors. A clinico-pathological study. J Neurosurg 1979; 51: 597–607

43 Stein BM. The infratentorial supracerebellar approach to pineal lesions. J Neurosurg 1971; 35: 197–202

44 Sung DII, Harisiadis L, Chang CH. Midline pineal tumors and suprasellar germinomas. Highly curable by irradiation. Radiology 1978; 128: 745–751

45 Van Wagenen WP. A surgical approach for the removal of certain pineal tumors. Report of a case. Surg Gynecol Obstet 1931; 53: 216–220

46 Schild SE, Scheithauer BW, Schomberg PJ et al. Pineal parenchymal tumours. Cancer 1993; 72: 870–879

47 Bradfield JS, Perez CA. Pineal tumors and ectopic pinealomas. Radiology 1972; 103: 399–406

48 Rao YTR, Medini E, Haselow RE et al. Pineal and ectopic pineal tumors. The role of radiation therapy. Cancer 1981; 48: 708–713

49 Mincer F, Meltzer J, Botstein C. Pinealoma. A report of twelve irradiated cases. Cancer 1976; 37: 2713–2718

Y. Nakagawa
M. Yoshida
M. Kawakami
M. Ando
H. Hashizume
A. Minamide
K. Maio
Y. Enyo
M. Okada

Posterior Endoscopic Surgery for Lumbar Disc Herniation with Contralateral Symptoms – A Report of Two Cases

Original Article

282

Abstract

We report two cases of lumbar disc herniation with contralateral nerve root involvement, surgically treated with a microendoscopic disectomy system (METRx™-MED system). The nerve root of the symptomatic side (contralateral to the side of the disc herniation) had been compressed to the superior facet by herniated disc from the opposite side. Endoscopic observation revealed inflammatory findings of the nerve root on the symptomatic side, such as fibrosis, adhesion, redness and swelling. In contrast, on the non-symptomatic side (ipsilateral side of the disc herniation), the nerve root had been merely compressed by the herniated disc but did not demonstrate any inflammatory findings. Excision of the herniated disc and decompression of the non-symptomatic nerve root should be done first, approaching from the disc herniation side. After that, through the same approach, the nerve root of the opposite (symptomatic) side should be decompressed.

Key words

Minimally invasive surgery · posterior endoscopic surgery · lumbar disc herniation · contralateral symptoms

Introduction

Lumbar disc herniation with symptoms to the contralateral side of the disc herniation is uncommon [1, 2]. Wide exploration and exposure of the pathologies and anatomical findings have been required to operatively treat such a case. Technical progress in minimally invasive surgery has reduced the problem of morbidity following surgery. Endoscopic surgery can provide a wide visualization through the oblique lens and reduce tissue damage. In this article, we report intraoperative endoscopic findings of lumbar disc herniations with contralateral symptoms, and discuss the surgical strategy with a minimally invasive technique.

Case Reports

Patient 1

The patient was a 45-year-old male with a history of right lower extremity radiculopathy and weakness of dorsiflexion in his big toe. He had received physical therapy, which did not help him with his pain and motor weakness. His past history was not significant. Physical examination revealed a sensory deficit of the right L5 segment. He had right extensor hallucis longus weakness (2/5) and right tibialis anterior weakness (3/5), but the rest of his motor and sensory examination was normal. The straight leg raising (SLR) test was positive at 45 degrees in his right leg. Magnetic resonance imaging (MRI) revealed a left side dominant herniation at L4-L5 disc (Figs. **1A** and **B**). The patient underwent microendoscopic discectomy (MED) using the METRx-MED system (Medtronic Sofamor Danek, Memphis, TN). First, the patient had decompression of the right L5 nerve root (symptomatic side) by a right-sided approach. Next, discectomy was performed by a left-sided approach. Both approaches required different muscle splitting through the same incision of skin. The right L5 nerve root (symptomatic side) had been compressed to the superior facet by herniated disc from the opposite side. Endoscopic
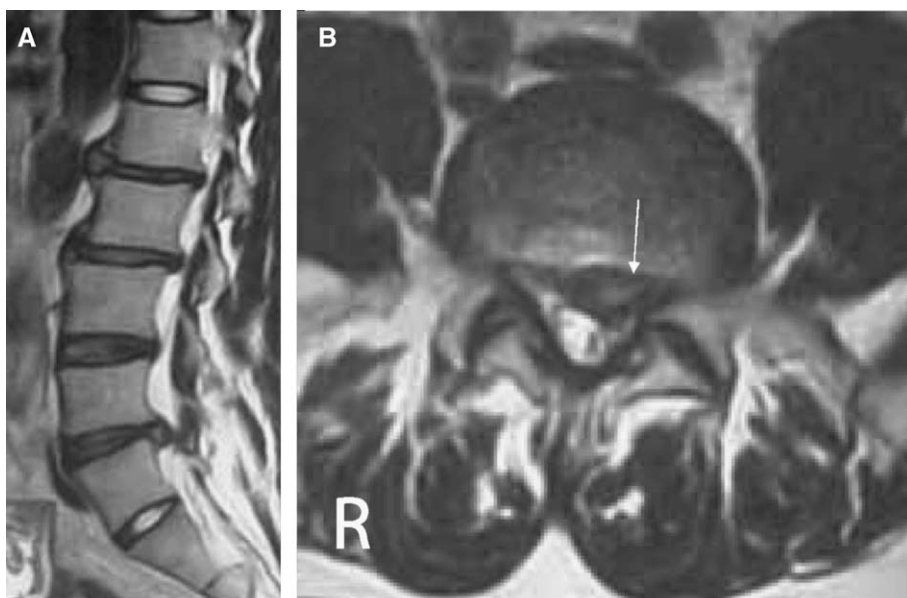
Fig. 1 Case 1: Preoperative magnetic resonance images (MRI). Sagittal (A) and axial (B) T$_2$-weighted images demonstrate left-sided lumbar disc herniation (arrow) at L4-L5.
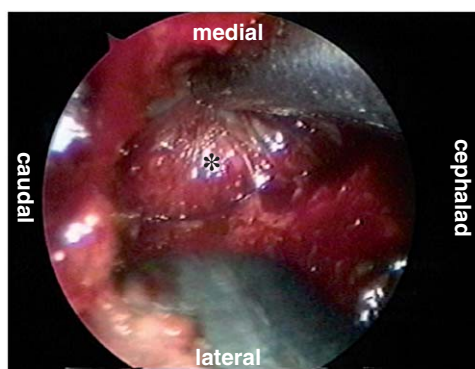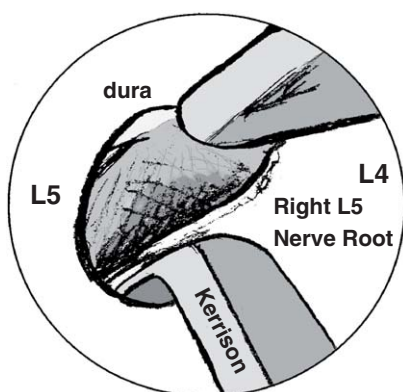
283

Fig. 2 Case 1: Endoscopic view of the right (approach side; symptomatic) L5 nerve root (*) following medial facetectomy. The nerve root was swollen and covered with fibrous tissue, with adhesions around the tissue. It also had been compressed from the contralateral side (herniation side).
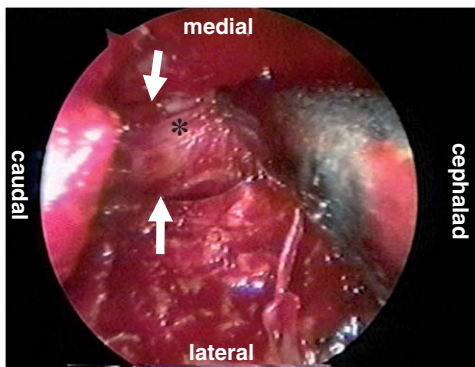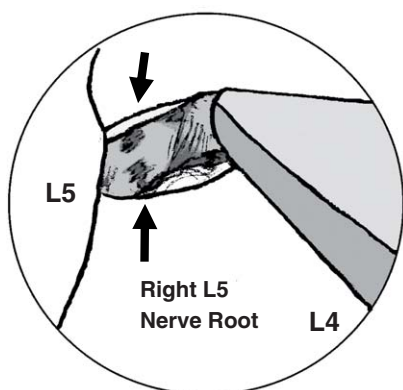

Fig. 3 Case 1: Endoscopic view of the right (approach side) L5 nerve root (*), following further decompression. The nerve root became slack, and red spots (arrows) were found on the surface of the nerve root, which indicated compression at the superior facet.

observation revealed inflammatory findings including fibrosis, adhesion, redness and swelling of the right L5 nerve root (Figs. 2 and 3), while the left nerve root was without inflammatory signs. On the first post-operative day, the right L5 radiculopathy was relieved, and he started to walk. Muscle weakness of right extensor hallucis longus and tibialis anterior recovered gradually. He did not have any symptoms or muscle weakness at 2-year follow-up.

Patient 2
The patient was an 18-year-old female with a history of left leg pain and low back pain. She had had conservative therapies such as physical therapy, pain medication and epidural injection of steroids, which did not help her with her pain. Physical examination revealed a left L5 sensory deficit and muscle weakness of the left extensor hallucis longus (3/5), but the rest of her motor and sensory examination was normal. The SLR test was positive
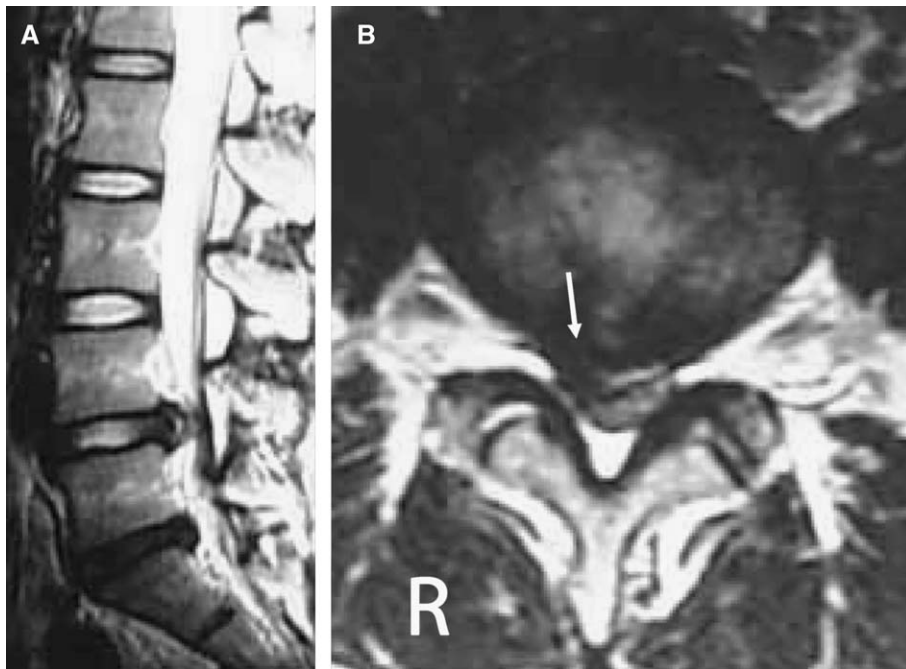
Fig. **4** Case 2: Preoperative magnetic resonance images (MRI). Sagittal (**A**) and axial (**B**) T$_2$-weighted images demonstrate the right-sided lumbar disc herniation (arrow) at L4-L5.
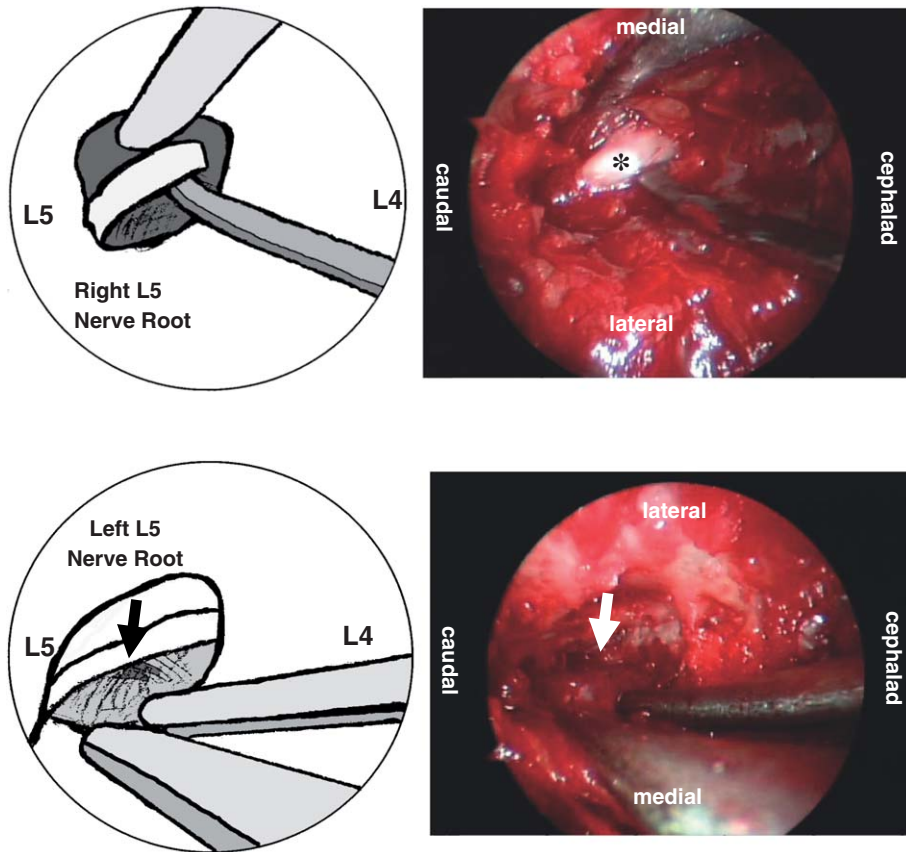
284

Right L5
Nerve Root

Fig. **5** Case 2: Endoscopic view of the right (approach side; asymptomatic) L5 nerve root (*), which had been compressed by disc herniation on the same side. The nerve root did not demonstrate inflammatory findings.

Left L5
Nerve Root

Fig. **6** Case 2: Endoscopic view of the left (contralateral side) L5 nerve root (arrow) from a right-sided approach. The nerve root had been compressed under the superior facet, and showed adhesion, redness and fibrous tissue developments.

at 60 degrees in both legs, but produced only left leg pain. MRI showed a disc herniation at the L4-L5 level, which was right side dominant (Figs. **4A** and **B**). The patient underwent MED via a right side (asymptomatic with herniated side) approach. With regard to this patient, discectomy was performed first. After excision of the herniated disc, the tubular retractor was angled medially to visualize the contralateral side, and decompression of left L5 nerve root was carried out. This maneuver is a so-called unilateral approach and bilateral decompression technique. The left L5 nerve root (symptomatic side) had been compressed by the superior facet due to the herniated disc from the opposite side. Endoscopic observation showed inflammatory findings of the left L5 nerve root, such as fibrosis, adhesion, redness and swelling (Fig. **5**). On the contrary, the right L5 nerve root simply had compression without inflammation (Fig. **6**). On the first post-operative day, the left L5 radiculopathy was relieved, and she started to walk. At the final follow-up, 2 years after surgery, she had no symptoms.

Discussion

There are a few reports about contralateral symptoms from lumbar disc herniation [1, 2]. Nerve root anomaly and contralateral compression of the nerve root at the site of a hypertrophied facet or the pedicle were supposed to be the cause of the contralateral symptoms. In the case of surgery for lumbar disc herniation with a discrepancy between the clinical symptoms and the preoperative MRI findings, confirmation of anatomy and pathology and complete decompression of bilateral nerve roots should be required. Hence, a wide laminectomy and extensive exploration had been used. Recent progress in posterior endoscopic surgery allows surgeons to obtain a wide and clear view of the pathology, and to perform minimally invasive decompression of bilateral nerve roots.

MED was originally introduced as a minimally invasive surgery for lumbar disc herniation by Foley and Smith in 1997 [3]. Since then, this endoscopic decompressive technique has been further developed and applied to various spine pathologies including lumbar spinal stenosis and cervical radiculopathy and myelopathy [4–13]. This procedure also may allow surgeons to perform bilateral decompression via a unilateral approach, the so-called "unilateral approach and bilateral decompression" [14]. This is also one of the most widely used techniques of minimally invasive decompressive spine surgery.

In our cases, endoscopy revealed the compression of the nerve root at the superior facet on the opposite side to the herniation. It also revealed inflammatory findings such as fibrosis, adhesion, redness and swelling of the nerve root on the symptomatic side (contralateral side to the disc herniation). On the contrary, the nerve root on the asymptomatic side (disc herniation side) had simply been compressed by disc herniation and was not inflamed.

With regard to operation in cases that demonstrate symptoms to the contralateral side of the herniation, the surgeon must decompress the nerve roots bilaterally and confirm their anatomy and pathology. Deciding which side should be done first might be a problem. In our cases, we took different approaches to each of them. Patient 1 had decompression of the symptomatic nerve root first, followed by discectomy on the asymptomatic side by another MED approach. In patient 2, discectomy was achieved first, and decompression of the contralateral symptopmatic nerve root was carried out using the unilateral approach and bilateral decompression technique. In our experience, ipsilateral discectomy and subsequent contralateral nerve root decompression using the unilateral approach and bilateral decompression technique is a reasonable approach of posterior endoscopic surgery.

Completing this procedure under endoscopy requires some experience, however, and there is a steep learning curve to obtain the necessary endoscopic surgical skill. If the unilateral approach and bilateral decompression technique proves difficult, bilateral approaches should be used.

In conclusion, posterior endoscopic decompressive surgery can be applied to such a complicated case with a discrepancy between the clinical symptoms and the findings of imaging techniques, and has been successfully performed.

Acknowledgements

References

1 Choudhury AR, Taylor JC, Worthington BS, Whitaker R. Lumbar radiculopathy contralateral to upper disc herniation: report of 3 cases. Br J Surg 1978; 65: 842–844
2 Auld AW, Dewall JG. Myelographic defect on the side opposite the leg pain. Spine 1979; 4: 174–175
3 Foley KT, Smith MM. Microendoscopic discectomy. Tech Neurosurg 1997; 301–307
4 Yoshida M, Maio K, Sumiya H, Kawai M, Yamada H, Nakagawa Y. Indications and clinical outcome of posterior endoscopic surgery for lumbar and cervical radiculopathy. Rinsho Seikei Geka 2004; 39: 563–569 (in Japanese)
5 Yoshida M, Nakagawa Y, Maio K, Kawakami M, Ando M, Hashizume H, Minamide A. Indications and clinical outcomes of microendoscopic discectomy for lumbar disc herniation. Rinsho Seikei Geka 2005; 40: 371–377 (in Japanese)
6 Khoo LT, Fessler RG. Microendoscopic decompressive laminotomy for the treatment of lumbar stenosis. Neurosurgery 2002; 51 (Suppl 2): 146–154
7 Guiot BH, Khoo LT, Fessler RG. A minimally invasive technique for decompression of the lumbar spine. Spine 2002; 27: 432–438
8 Yoshida M, Ueyoshi A, Maio K, Kawai M, Nakagawa Y. Surgical procedures and clinical results of endoscopic decompression for lumbar canal stenosis. In: Dezawa A, Chen PQ, Chung JY (eds), State of the Art for Minimally Invasive Spine Surgery. Springer-Verlag, Tokyo, 2005, 15–24
9 Sairyo K, Katoh S, Sakamaki T, Komatsubara S, Yasui N. A new endoscopic technique to decompress lumbar nerve roots affected by spondylolysis. J Neurosurg (Spine 3) 2003; 98: 290–293
10 Ikuta K, Arima J, Tanaka T, Oga M, Nakano S, Sasaki K, Goshi K, Yo M, Fukagawa S. Short-term results of microendoscopic posterior decompression for lumbar spinal stenosis. J Neurosurg (Spine 2) 2005; 624–633
11 Adamson TE. Microendoscopic posterior cervical laminoforaminotomy for unilateral radiculopathy; results of a new technique in 100 cases. J Neurosurg (Spine 1) 2001; 95: 51–57
12 Adamson TE. The impact of minimally invasive cervical spine surgery. J Neurosurg (Spine 1) 2004; 1: 43–46
13 Yabuki S, Kikuchi S. Endoscopic partial laminectomy for cervical myelopathy. J Neurosurg (Spine 2) 2005; 98: 170–174
14 Young S, Veerapen R, O'Laoire SA. Relief of lumbar canal stenosis using multilevel subarticular fenestrations as an alternative to wide laminectomy: preliminary report. Neurosurgery 1988; 23: 628–632

Clinical Utility of Multislice Computed Tomographic Angiography for Detection of Cerebral Vasospasm in Acute Subarachnoid Hemorrhage

S. P. Joo
T. S. Kim
Y. S. Kim
K. S. Moon
J. K. Lee
J. H. Kim
S. H. Kim

286

Abstract

Digital subtraction angiography (DSA) has been used as the standard method for detecting cerebral vasospasm after subarachnoid hemorrhage (SAH). Multislice computed tomographic angiography (CTA) is a relatively recent method used for evaluating the vasculature of the intracranial arteries. The purpose of this study was to compare multislice CTA and DSA for the detection and quantification of cerebral vasospasm after SAH, and to analyze the usefulness of multislice CTA. Eight patients with SAH underwent initial CTA with DSA within 72 hours after the onset of symptoms and follow-up multislice CTA and DSA 8 to 48 days after SAH. Five arterial locations were established in the A1 and A2 segments of the anterior cerebral artery, the M1 and M2 segments of the middle cerebral artery and the posterior cerebral artery (PCA) on both multislice CTA and DSA images. Vasospasm was classified as none, mild (up to 30 % reduction in luminal diameter), moderate (31–60 % reduction), and marked (at least 60 % reduction) using the scale of Schneck and Kricheff. The multislice CT system used the following parameters: 1.25 mm collimation and 3.75 pitch with a 4-channel system. The degree of vasospasm revealed by the multislice CTA was significantly correlated with the degree of vasospasm revealed by DSA. In general, most discrepancies between CTA and DSA were in the detection of mild and moderate vasospasm. We found that the consistency between multislice CTA and DSA was greater for mild (100 %, n = 3) or moderate (100 %, n = 3) vasospasm than none (n = 1) or marked vasospasm (n = 1). However, it was unclear whether multislice CTA was more specific for a proximal location (A1, M1, PCA) or distal location (A2, M2) for evaluation of cerebral arteries. Multislice CTA can detect angiographic vasospasm after SAH with an accuracy similar to that of DSA. Multislice CTA is highly sensitive, specific and accurate in detecting mild and moderate cerebral vasospasm. It is less accurate for detecting no vasospasm and marked vasospasm. Therefore, the authors propose that multislice CTA be considered as a useful tool for the detection and management of intracranial vasospasm after SAH.

Key words

Multislice computed tomographic angiography · digital subtraction angiography · subarachnoid hemorrhage · vasospasm

Abbreviations

A1 and A2	proximal and distal segment of the anterior cerebral artery
ACA	anterior cerebral artery
Acom	anterior communicating artery
CTA	computed tomographic angiography
DSA	digital subtraction angiography
ICAB	internal cerebral artery bifurcation
M1 and M2	proximal and distal segment of the middle cerebral artery
MCA	middle cerebral artery
MCAB	middle cerebral artery bifurcation
PCA	posterior cerebral artery
Pcom	posterior communicating artery

SAH   subarachnoid hemorrhage
TCD   transcranial Doppler sonography.

Introduction

Cerebral vasospasm is one of the major causes of mortality and morbidity in patients with subarachnoid hemorrhage [1]. Vasospasm typically occurs 7 to 10 days after hemorrhage, and its prompt diagnosis is required to initiate appropriate therapy to avoid ischemic insults. Digital subtraction angiography (DSA) is accepted as the standard method used to confirm the diagnosis of vasospasm [1]; however, it carries a total complication rate of approximately 5 % and a permanent stroke rate of approximately 0.5 to 1 % [2–6]. In addition, it cannot be performed repeatedly in critically ill patients because of its invasive nature. Transcranial Doppler ultrasonography is widely used to evaluate cerebral vasospasm [7, 8]; however, its operator dependence, and difficulty in accurately detecting vasospasm at sites other than the proximal middle cerebral artery (MCA) limit its use to a screening method only with the definitive diagnosis being made by DSA.

CT angiography (CTA) does not carry the neurological risks associated with DSA. Moreover, it is less expensive and requires less time than DSA. CTA has been shown to depict the intracranial vasculature well in the setting of SAH [9–13]. The purpose of this study was to compare CTA with DSA in its ability to detect cerebral vasospasm in patients with SAH.

Patients and Methods

Between January 2003 and December 2003, 216 patients underwent surgery at our institution for SAH. Of these patients, eight patients had an initial CTA with DSA within 72 hours after the onset of symptoms, and a follow-up multislice CTA and DSA 8 to 48 days after the SAH. In this prospective study, there were 3 men and 5 women whose ages ranged from 48–74 years (mean: 57.8 years). The multislice CT system (General Electric, Co, Milwaukee, USA) used had the following parameters: 1.25 mm collimation and 3.75 pitch (mm per rotation table increment) with a 4-channel system. The formal CTA examination consisted of 140 mL of non-ionic iodinated contrast agent (ultravist 300, Schering AG, Berlin, Germany) infused at a rate of 3.45–5 mL/s via an antecubital intravenous catheter. Helical scanning was performed from the craniocervical junction to 30 mm above the floor of the sella turcica. The pitch was 3.1, with 220 mA. The CT value was measured in the circular regions of interest (ROIs) in bilateral carotid arteries. Axial slices were reconstructed with a 1.25 mm slice thickness at 0.5 mm intervals, and the reconstructed images were transferred to a computer workstation for 3D reconstruction. The DSA studies were performed using the transfemoral Seldinger technique and anteroposterior and lateral views were obtained. The CTA and DSA examinations were compared retrospectively by two neurosurgeons. The initial and delayed CTA examinations were reviewed for the presence of spasm by comparing the corresponding vessel diameters on the initial and follow-up studies. These results were then compared with findings on the corresponding DSA images. A total of five arterial locations were established in the A1 and A2 segments of

Table **1**   Scale for grading intracranial vasospasm

Grade	Definition
None	Normal
Mild	< 30 % reduction
Moderate	30 < 60 % reduction
Severe	60 % reduction

the anterior cerebral artery, the M1 and M2 segments of the middle cerebral artery and the posterior cerebral artery (PCA) on both multislice CTA and DSA images. Vasospasm was classified as none, mild (up to 30 % reduction in luminal diameter), moderate (31–60 % reduction), and marked (at least 60 % reduction) using the scale of Schneck and Kricheff (Table **1**) [14].

Results

The patients' CTA and DSA findings are summarized in Table **2**. The ruptured aneurysms were located at the anterior cerebral artery in three patients, the posterior communicating artery in two patients, the internal carotid artery in one patient, the middle cerebral artery in one patient and the vertebrobasilar artery in one patient. The degree of vasospasm revealed by multislice CTA was significantly correlated with the degree of vasospasm by DSA. Discrepancies between CTA and DSA have been, in general, a result of detecting mild and moderate degrees of vasospasm. Our findings showed that the consistency between multislice CTA and DSA was greater for mild (100 %, n = 3) or moderate (100 %, n = 3) vasospasm than none (n = 1) or marked or severe vasospasm (n = 1). At all locations, agreement between CTA and DSA was greater for mild and moderate degrees of vasospasm (Figs. **1** and **2**). However, CTA was not highly sensitive and accurate for detecting no or marked spasm (Fig. **3** and **4**). However, it was unclear whether multislice CTA was more specific for proximal locations (A1, M1, PCA) or distal locations (A2, M2) of the cerebral arteries.

Discussion

Transcranial Doppler sonography (TCD) is the most commonly used method for the detection of cerebral vasospasm. This tool has been shown to be 84 % to 85 % sensitive and 89 % to 98 % specific for detection of spasms at proximal middle cerebral artery locations [7, 8, 15, 16]. TCD can be used on a daily basis with minimal cost and risk to the patient; however, its operator dependence and limited application to the whole intracerebral vasculature limits its effectiveness in making a definitive diagnosis. Thus TCD alone is inadequate for the detection of vasospasm, and other methods are required [16].

Magnetic resonance angiography (MRA) has been used for the diagnosis of intracranial aneurysms [17, 18]. The advantages of MRA include reduced invasiveness, lack of exposure to ionizing radiation and no requirement for intravenous contrast administration. However, its sensitivity and specificity for the detection

Table **2** Demographic and clinical data, 3D-CTA and DSA findings

Case	Age/Sex	Site of aneurysm	Arterial narrowing on 3D-CTA Site	Grade	Arterial narrowing on DSA Site	Grade
1	52/M	ICAB, Lt	A1, A2, M1, M2	Moderate	A1, A2, M1, M2	Moderate
2	63/F	Pcom, Rt	A1, M1	Mild		None
3	50/F	MCAB, Rt	A1, A2, M1, M2	Mild	M1, M2	Mild
4	48/F	A1, Rt	A1, A2, M1, M2	Moderate	A1, A2, M1, M2	Marked
5	74/F	Pcom, Rt	A1, M1, M2	Mild	A1, A2	Mild
6	66/M	Basilar top	PCA, A1	Moderate	A1, A2, M1, M2, PCA	Moderate
7	48/F	Acom	A1, A2, M1, M2	Moderate	A1, A2, M1, M2	Moderate
8	61/M	Acom	A1	Mild	A1, A2, M2	Mild

CTA = computed tomographic angiography; DSA = digital subtraction angiography; ICAB = internal cerebral artery bifurcation; Pcom = posterior communicating artery; MCAB = middle cerebral artery bifurcation; M1 and M2 = proximal and distal segment of the middle cerebral artery; Acomm = anterior communicating artery; A1 and A2 = proximal and distal segment of the anterior cerebral artery; PCA = posterior cerebral artery; Lt = left; Rt = right.
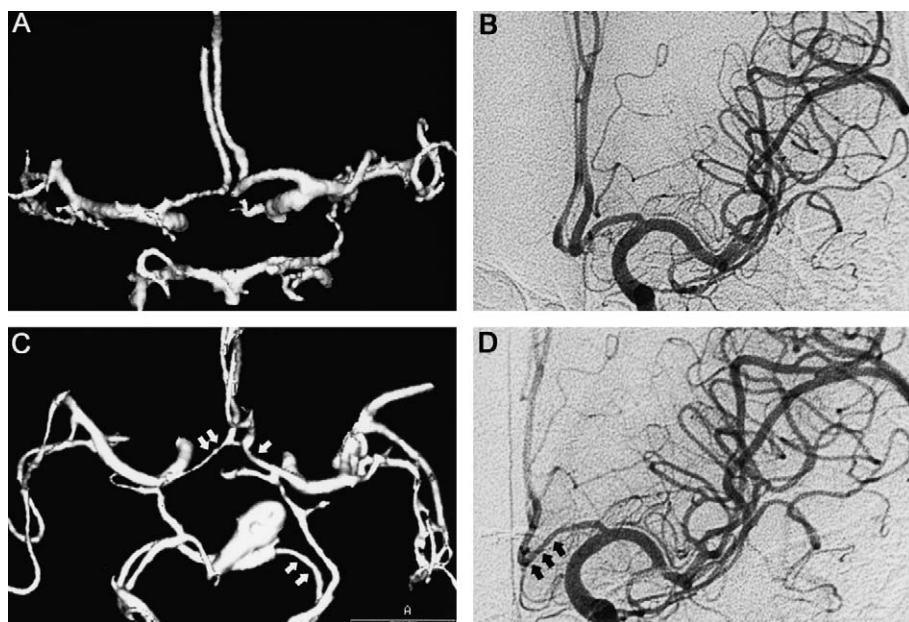
Fig. **1** Angiograms obtained in a 61-year-old man with SAH due to rupture of an anterior communicating artery aneurysm (Case 8). **A** Preoperative computed tomographic angiogram, anteroposterior view. **B** Preoperative digital subtraction angiogram, anteroposterior view. **C** Postoperative computed tomographic angiogram, anteroposterior view, demonstrating mild narrowing of the distal segment of the anterior cerebral artery (arrow). **D** Postoperative digital subtraction angiogram, anteroposterior view, demonstrating mild narrowing of the distal segment of the anterior cerebral artery (arrow).
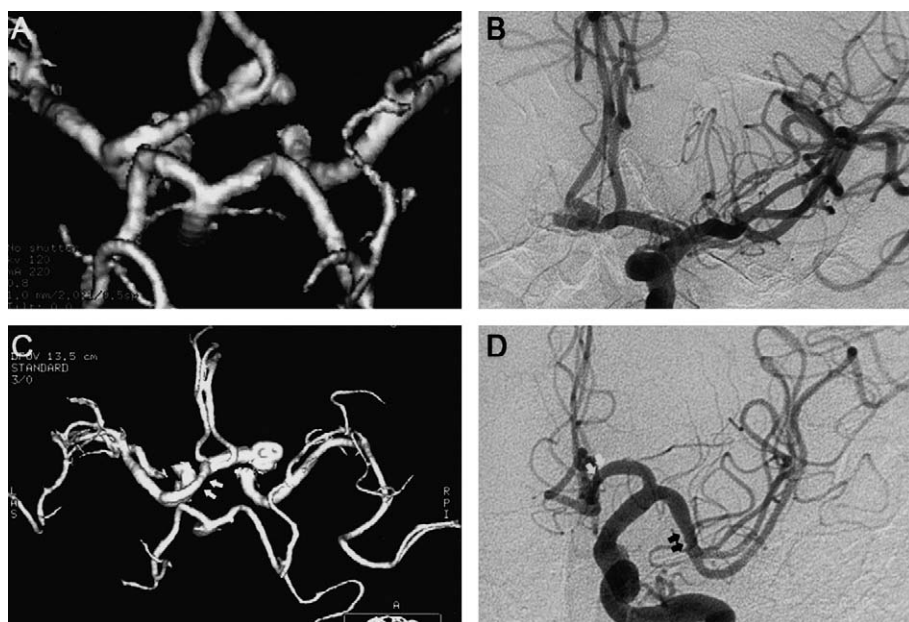

Fig. **2** Angiograms obtained in a 66-year-old man with SAH due to rupture of a basilar top aneurysm (Case 6). **A** Preoperative computed tomographic angiogram, anteroposterior view. **B** Preoperative digital subtraction angiogram, anteroposterior view. **C** Postoperative computed tomographic angiogram, anteroposterior view, showing moderate narrowing of the proximal segment of the anterior and posterior cerebral artery (arrow). **D** Postoperative digital subtraction angiogram, anteroposterior view, showing moderate narrowing of the proximal segment of the anterior cerebral artery (arrow).
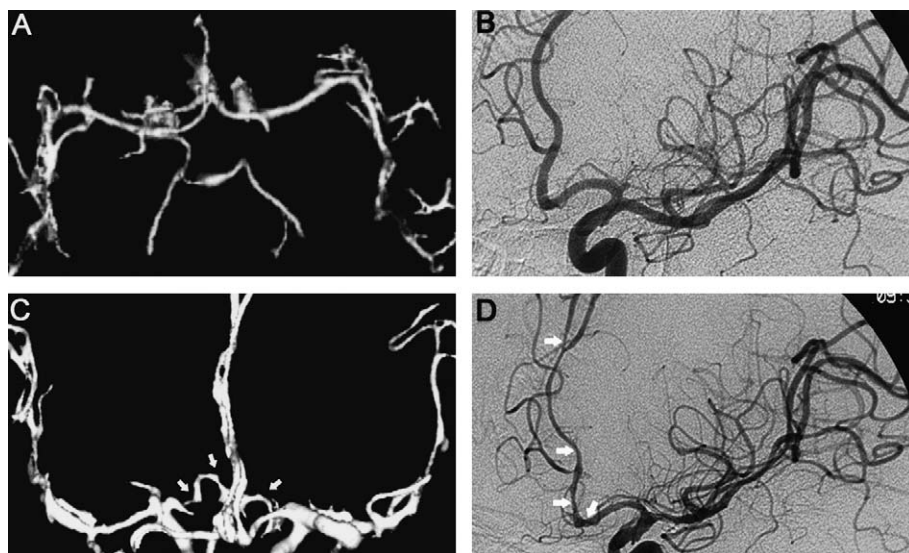
Fig. 3 Angiograms obtained in a 48-year-old woman with SAH due to rupture of the right proximal segment (A1) of the anterior cerebral artery (Case 4). A Preoperative computed tomographic angiogram, anteroposterior view. B Preoperative digital subtraction angiogram, oblique view. C Postoperative computed tomographic angiogram, anteroposterior view, showing moderate narrowing of the proximal segment of the anterior cerebral artery (arrow). D Postoperative digital subtraction angiogram, oblique view, showing severe narrowing of the proximal and distal segment of the anterior cerebral artery (arrow).
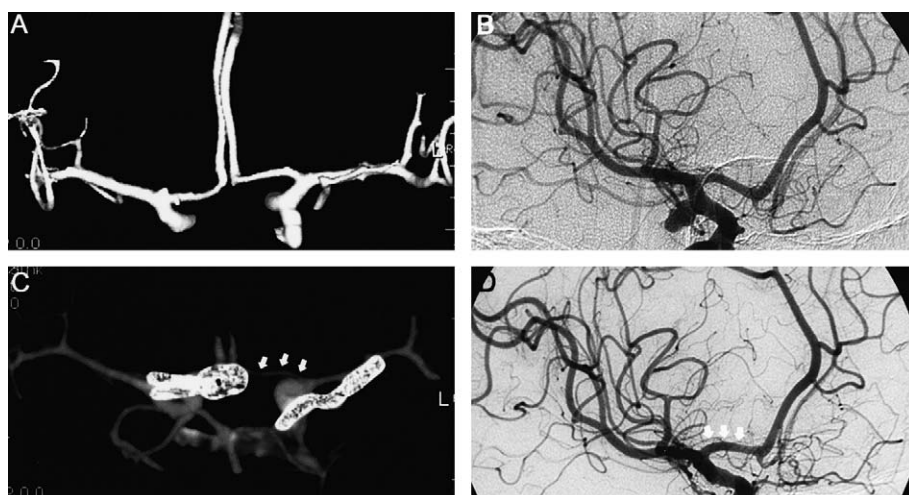

Fig. 4 Angiograms obtained in a 63-year-old woman with SAH due to rupture of the right posterior communicating artery (Case 2). A Preoperative computed tomographic angiogram, anteroposterior view. B Preoperative digital subtraction angiogram, oblique view. C Postoperative computed tomographic angiogram, anteroposterior view, showing mild narrowing of the proximal segment of the anterior cerebral artery (arrow). D Postoperative digital subtraction angiogram, oblique view, showing no vasospasm of the proximal segment of the anterior cerebral artery (arrow).

of vasospasm after SAH remain relatively low [19, 20]. MRA has limitations for detecting the severity of vasospasm and visualization of the distal arteries [20]. In addition, for obtunded, often mechanically ventilated, critically ill patients, MRA may not be ideal owing to the relatively prolonged acquisition times and limited patient access. Electric and metallic devices, such as aneurysmal clips, also preclude its routine use in the postoperative patient [21]. Furthermore, MRA tends to lead to an overestimation of stenotic changes because of dephasing [22]. Therefore, MRA has not been shown to be a useful examination for patients with vasospasm after SAH.

DSA is the reference standard for demonstrating intracranial vasospasm and is commonly performed for suspected delayed cerebral ischemia. The risks for performing this procedure, in a critically ill patient, however, can limit its application; central nervous system complications from this procedure are reported to be as least as high as 0.9% in healthy persons [6]. Less serious, but more common complications associated with DSA include: nausea, vomiting, puncture site hematoma and hypotension which may have a greater clinical significance in the critically ill. DSA cannot therefore be performed repeatedly.

Three-dimensional CTA has proved useful in screening for intracranial aneurysms [9, 23 – 25] and in assessing acute SAH for planning surgery [26, 27]. Its usefulness in the diagnosis of intracranial vasospasm was reported by Ochi et al. in 1997 [11]. Multislice CTA has several advantages. The examination time is short, the ability to rotate the 3D images through 360 degrees may provide a better view of the anatomy of the aneurysm and the surrounding vessels, and a selective arterial cannulation with the risk of stroke can be avoided. Furthermore, multislice CTA seems to be relatively inexpensive compared with MRA and DSA [28]; in addition, CTA can visualize the distal cerebral arteries, which resulted in a high possibility of agreement between DSA and CTA for detection of cerebral vasospasm. The disadvantages include the relatively large amount of contrast medium needed to obtain optimal axial source images and the slightly increased risk of immediately performing subsequent DSA in a patient with an abnormal finding (remnant of the neck, vasospasm), the time-consuming effort of excluding bone structures at the cranial base, the time required to perform the 3D reconstructions and clip artifacts. For multislice CTA, the artifacts were small and limited to the extension of the axis of the clip, so they only rarely interfered with the interpretation of the images and more

information could be obtained. Anderson et al. [29] found CTA to be perfect in detecting severe spasm (> 50 % luminal reduction) and to be highly sensitive and accurate in detecting normal vessels in the absence of spasm. Vasospasm was best detected in proximal arterial locations (ICA, M A1, M1, and basilar arteries) and when categorized as either absent or severe. Mild or moderate spasm (1 % to 50 % luminal reduction) was less well detected, especially at distal locations (A2 and M2). In our study, the discrepancies between CTA and DSA were in detecting mild and moderate degrees of vasospasm. However, the consistency between multislice CTA and DSA was greater for mild or moderate vasospasm than none or marked vasospasm. Our findings support that multislice CTA, such as 16- or 64-channel acquisition, will allow for improved quality of the vascular images with time; however, its role in the management of patients with aneurysmal SAH requires further study.

Conclusion

Although a valuable statistical analysis is not possible because of the relatively small number of patients, multislice CTA can detect angiographic vasospasm after SAH with accuracy similar to that of DSA. Multislice CTA is highly sensitive, specific and accurate in detecting mild and moderate cerebral vasospasm. It is less accurate for detecting no vasospasm and marked vasospasm. Therefore, multislice CTA is a suitable alternative to conventional angiography for the diagnosis and treatment of patients with intracranial vasospasm.

References

1 Weir B, Grace M, Hansen J, Rothberg C. Time course of vasospasm in man. J Neurosurg 1978; 48: 173–178
2 Earnest F, Forbes G, Sandok BA, Piepgras DG, Faust RJ, Ilstrup DM, Arndt LJ. Complications of cerebral angiography: prospective assessment of risk. AJR Am J Roentgenol 1984; 142: 247–253
3 Dorsch NW, Young N, Kingston RJ, Compton JS. Early experience with spiral CT in the diagnosis of intracranial aneurysms. Neurosurgery 1995; 36: 230–236
4 Pryor JC, Setton A, Nelson PK, Berenstein A. Complications of diagnostic cerebral angiography and tips on avoidance. Neuroimaging Clin N Am 1996; 6: 751–758
5 Heiserman JE, Dean BL, Hodak JA, Flom RA, Bird CR, Drayer BP, Fram EK. Neurologic complications of cerebral angiography. AJNR Am J Neuroradiol 1994; 15: 1401–1407
6 Waugh JR, Sacharias N. Arteriographic complications in the DSA era. Radiology 1992; 182: 243–246
7 Lindegaard KF, Nornes H, Bakke SJ, Sorteberg W, Nakstad P. Cerebral vasospasm diagnosis by means of angiography and blood velocity measurements. Acta Neurochir (Wien) 1989; 100: 12–24
8 Sloan MA, Haley Jr EC, Kassell NF, Henry ML, Stewart SR, Beskin RR, Sevilla EA, Torner JC. Sensitivity and specificity of transcranial Doppler ultrasonography in the diagnosis of vasospasm following subarachnoid hemorrhage. Neurology 1989; 39: 1514–1518
9 Aoki S, Sasaki Y, Machida T, Ohkubo T, Minami M. Cerebral aneurysms: detection and delineation using 3-D-CT angiography. AJNR Am J Neuroradiol 1992; 13: 1115–1120
10 Dillon EH, van Leeuwen MS, Fernandez MA, Mali WP. Spiral CT angiography. AJR Am J Roentgenol 1993; 160: 1273–1278
11 Ochi RP, Vieco PT, Gross CE. CT angiography of cerebral vasospasm with conventional angiographic comparison. AJNR Am J Neuroradiol 1997; 18: 265–269
12 Hsiang JN, Liang EY, Lam JM, Zhu XL, Poon WS. The role of computed tomographic angiography in the diagnosis of intracranial aneurysms and emergent aneurysm clipping. Neurosurgery 1996; 38: 481–487
13 Zouaoui A, Sahel M, Marro B, Clemenceau S, Dargent N, Bitar A, Faillot T, Capelle L, Marsault C. Three-dimensional computed tomographic angiography in detection of cerebral aneurysms in acute subarachnoid hemorrhage. Neurosurgery 1997; 41: 125–130
14 Schneck SA, Kricheff II. Intracranial aneurysm rupture, vasospasm, and infarction. Arch Neurol 1964; 11: 668–680
15 Vora YY, Suarez-Almazor M, Steinke DE, Martin ML, Findlay JM. Role of transcranial Doppler monitoring in the diagnosis of cerebral vasospasm after subarachnoid hemorrhage. Neurosurgery 1999; 44: 1237–1247
16 Okada Y, Shima T, Nishida M, Yamane K, Hatayama T, Yamanaka C, Yoshida A. Comparison of transcranial Doppler investigation of aneurysmal vasospasm with digital subtraction angiographic and clinical findings. Neurosurgery 1999; 45: 443–449
17 Gouliamos A, Gotsis E, Vlahos L, Samara C, Kapsalaki E, Rologis D, Kapsalakis Z, Papavasiliou C. Magnetic resonance angiography compared to intra-arterial digital subtraction angiography in patients with subarachnoid haemorrhage. Neuroradiology 1992; 35: 46–49
18 Huston J 3rd, Nichols DA, Luetmer PH, Goodwin JT, Meyer FB, Wiebers DO, Weaver AL. Blinded prospective evaluation of sensitivity of MR angiography to known intracranial aneurysms: importance of aneurysm size. AJNR Am J Neuroradiol 1994; 15: 1607–1614
19 Grandin CB, Cosnard G, Hammer F, Duprez TP, Stroobandt G, Mathurin P. Vasospasm after subarachnoid hemorrhage: diagnosis with MR angiography. AJNR Am J Neuroradiol 2000; 21: 1611–1617
20 Tamatani S, Sasaki O, Takeuchi S, Fujii Y, Koike T, Tanaka R. Detection of delayed cerebral vasospasm, after rupture of intracranial aneurysms, by magnetic resonance angiography. Neurosurgery 1997; 40: 748–753
21 Klucznik RP, Carrier DA, Pyka R, Haid RW. Placement of a ferromagnetic intracerebral aneurysm clip in a magnetic field with a fatal outcome. Radiology 1993; 187: 855–856
22 Dumoulin CL, Hart Jr HR. Magnetic resonance angiography. Radiology 1986; 161: 717–720
23 Schwartz RB, Tice HM, Hooten SM, Hsu L, Stieg PE. Evaluation of cerebral aneurysms with helical CT: correlation with conventional angiography and MR angiography. Radiology 1994; 192: 717–722
24 Alberico RA, Patel M, Casey S, Jacobs B, Maguire W, Decker R. Evaluation of the circle of Willis with three-dimensional CT angiography in patients with suspected intracranial aneurysms. AJNR Am J Neuroradiol 1995; 16: 1571–1578
25 Wilms G, Guffens M, Gryspeerdt S, Bosmans H, Maaly M, Boulanger T, Van Hoe L, Marchal G, Baert A. Spiral CT of intracranial aneurysms: correlation with digital subtraction and magnetic resonance angiography. Neuroradiology (Suppl) 1996; 38: S20–25
26 Vieco PT, Shuman WP, Alsofrom GF, Gross CE. Detection of circle of Willis aneurysms in patients with acute subarachnoid hemorrhage: a comparison of CT angiography and digital subtraction angiography. AJR Am J Roentgenol 1995; 165: 425–430
27 Zeman RK, Silverman PM, Vieco PT, Costello P. CT angiography. AJR Am J Roentgenol 1995; 165: 1079–1088
28 Harbaugh RE, Schlusselberg DS, Jeffery R, Hayden S, Cromwell LD, Pluta D, English RA. Three-dimensional computed tomographic angiography in the preoperative evaluation of cerebrovascular lesions. Neurosurgery 1995; 36: 320–326
29 Anderson GB, Ashforth R, Steinke DE, Findlay JM. CT angiography for the detection of cerebral vasospasm in patients with acute subarachnoid hemorrhage. AJNR Am J Neuroradiol 2000; 21: 1011–1015

N. Mikuni
N. Hashimoto

A Minimally Invasive Transsulcal Approach to the Paracentral Inner Lesion

Abstract

Objective: Surgical options to remove lesions located deep in the sulcus at the paracentral area are limited. To minimize therapeutic morbidities, such as cortical injuries before the removal, a transsulcal approach was applied by taking the results of neuroimaging and functional mapping into consideration. **Methods:** Four patients with paracentral inner lesions including anaplastic astrocytoma, cortical dysplasia, and cavernous angioma were operated on. All lesions were located deep in the paracentral sulci. According to the outcome of MRI and functional mapping of the cortex over the lesion, the central or the postcentral sulcus was opened toward the lesion. Immediately after complete dissection of the sulcus to remove the lesion, neurological findings were evaluated in the awake state. **Results:** All lesions were situated beneath the hand or foot area. The transsulcal approach was successfully conducted without any neurological deficits in all cases. **Conclusion:** Microsurgical techniques based on anatomic and functional information allow surgeons to reach the lesions deep in the paracentral area safely.

Key words

Functional mapping · paracentral area · motor evoked potential · awake surgery · transsulcal approach

Introduction

With the recent developments of neuroimaging, functional mapping, and anesthesia, lesions in eloquent areas are often resectable without neurological deficits [1–3]. Even so, paracentral lesions, especially located deep in the brain, are still one of the most challenging therapeutic obstacles in neurosurgery due to risks associated with the surgical procedures. Brain injuries during the approach to a deeply situated lesion cause immediate clinical deficits in motor and/or sensory function, as well as decreases in evoked potentials (i.e., motor evoked potential [MEP] and/or somatosensory evoked potential [SEP]). Since transsylvian or transsulcal approaches are usually selected for deeply located lesions in our institute [4], this paper reports a transsulcal approach to lesions deep in the sulcus at the paracentral area. Technical considerations of this approach as a minimally invasive way are discussed by taking the results of preoperative MRI and functional mapping into account.

Patients and Methods

Patients

Four right-handed patients (Table **1**) including one with an anaplastic astrocytoma, one with medically intractable epilepsy due to cortical dysplasia, and two with cavernous angiomas accompanied by hematomas, aged 31 to 53 years, were operated on by this approach. Patient 1 had mild central facial palsy and

Affiliation
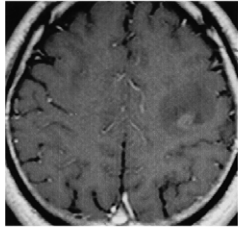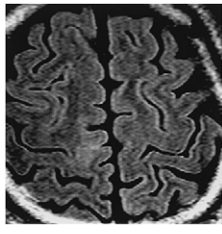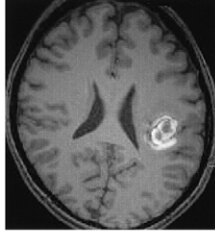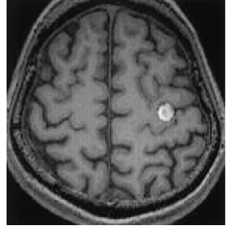Department of Neurosurgery, Kyoto University Graduate School of Medicine, Kyoto, Japan

Correspondence
Nobuhiro Mikuni, M.D., Ph.D. · Department of Neurosurgery · Kyoto University Graduate School of Medicine · 54 Kawahara-cho · Shogoin · Sakyo-ku · Kyoto 6068507 · Japan · Tel.: + 81/75/751 34 59 · Fax: + 81/75/752 95 01 · E-mail: mikunin@kuhp.kyoto-u.ac.jp

Patient	1	2	3	4
Age (yr)	53	31	38	46
Preoperative deficits	Dysarthria, Clumsiness of the right hand	None	None	None
Function (modality)	Hand (Cortical stimulation)	Foot (Cortical stimulation)	Hand (SEP, Cortical stimulation)	Hand (Cortical stimulation)
Sulcus	Lt. central sulcus	Rt. central sulcus	Lt. post-central gyrus	Lt. central sulcus
Histology	Anaplastic astrocytoma	Cortical dysplasia	Cavernous angioma	Cavernous angioma
MRI				

Rt.: right, Lt: left

clumsiness on his right hand. Patient 2 had no clinical deficits interictally. In patients 3 and 4, motor and sensory deficits in the upper extremities due to hemorrhage had recovered completely before surgery.

MRI

Preoperative imaging was performed on a 3 Tesla MR scanner (Trio, Siemens, Erlangen, Germany) equipped with a receiver only 8 channels of phased-array head coil.

In all patients, the lesions were located deep in the paracentral sulcus (the central sulcus in patients 1, 2, and 4 and the postcentral sulcus in patient 3) and did not extend to the brain surface. We obtained T_1-weighted volume data using 3-D magnetization prepared rapid gradient echo (MPRAGE) sequence with 1 mm thickness. Near isotropic voxels were acquired with an image matrix of 256×240 and $240\,mm \times 225\,mm$ field of view, providing $0.9\,mm \times 0.9\,mm \times 1\,mm$ resolution. After stripping the skull and scalp from the T_1-weighted volume data with brain extraction tools (Oxford Centre for Functional Magnetic Resonance of the Brain, Oxford University, Oxford, UK), a volume-rendered image of extracted brain was created.

Functional mapping

Functional mapping was performed with magnetoencephalography (MEG), functional MRI, and electric stimulation. Additionally, the MPRAGE images and DICOM-format tractography images of the pyramidal tracts together with the results of functional MRI were transferred to the navigation system (Vector Vision Compact Navigation System, Brain LAB AG, Heimstetten, Germany). In patients 1 and 2, subdural electrode grids were placed on the paracentral cortex to define the epileptogenic areas as well as to examine cortical functions. Electric stimula-

tion for functional mapping was done with approval by the Ethical Committee of Kyoto University Graduate School of Medicine (No. 79) and written informed consent was obtained from the patients. All contacts used for cortical stimulation were made of platinum of 3 mm in diameter, and the center-to-center interelectrode distance was 1 cm. Details about the methods of electric stimulation have been described elsewhere [5]. Electric currents in square waves of alternating polarity each with duration of 0.3 ms were delivered to a pair of subdural electrodes at a frequency of 50 Hz for 1 s, and the currents were increased in 1 mA increments to a maximum of 15 IDA. The duration of electric stimulation was then increased in 1-s increments until a maximum of 5 s. Whenever after-discharges were induced, the test was repeated with the same or lower currents.

Opening of the sulcus

In all patients, transsulcal approaches (transcentral sulcus in three and transpostcentral sulcus in one patient) were applied to reach the lesions. In accordance with the shape of the sulcus and the function of surrounding cortex, the initial part for dissection on the sulcus was determined. If the sulcus above the lesion was tight due to brain edema or adhesion of the arachnoid membranes, a relatively normal part in the sulcus was dissected at first along the cortical artery, followed by extending the space to the lesion. At the brain surface, the subarachnoid membrane was cut with a minimal tension in the left applying gentle retraction onto a cottonoid sponge placed on the adjacent tissue. To open the sulcus, microscissors were used as much as possible to avoid cortical injures due to retraction and coagulation by bipolar forceps [4]. A self-retaining retractor placed over a cottonoid strip was used in the deep area but the use was limited to as short a time as possible.
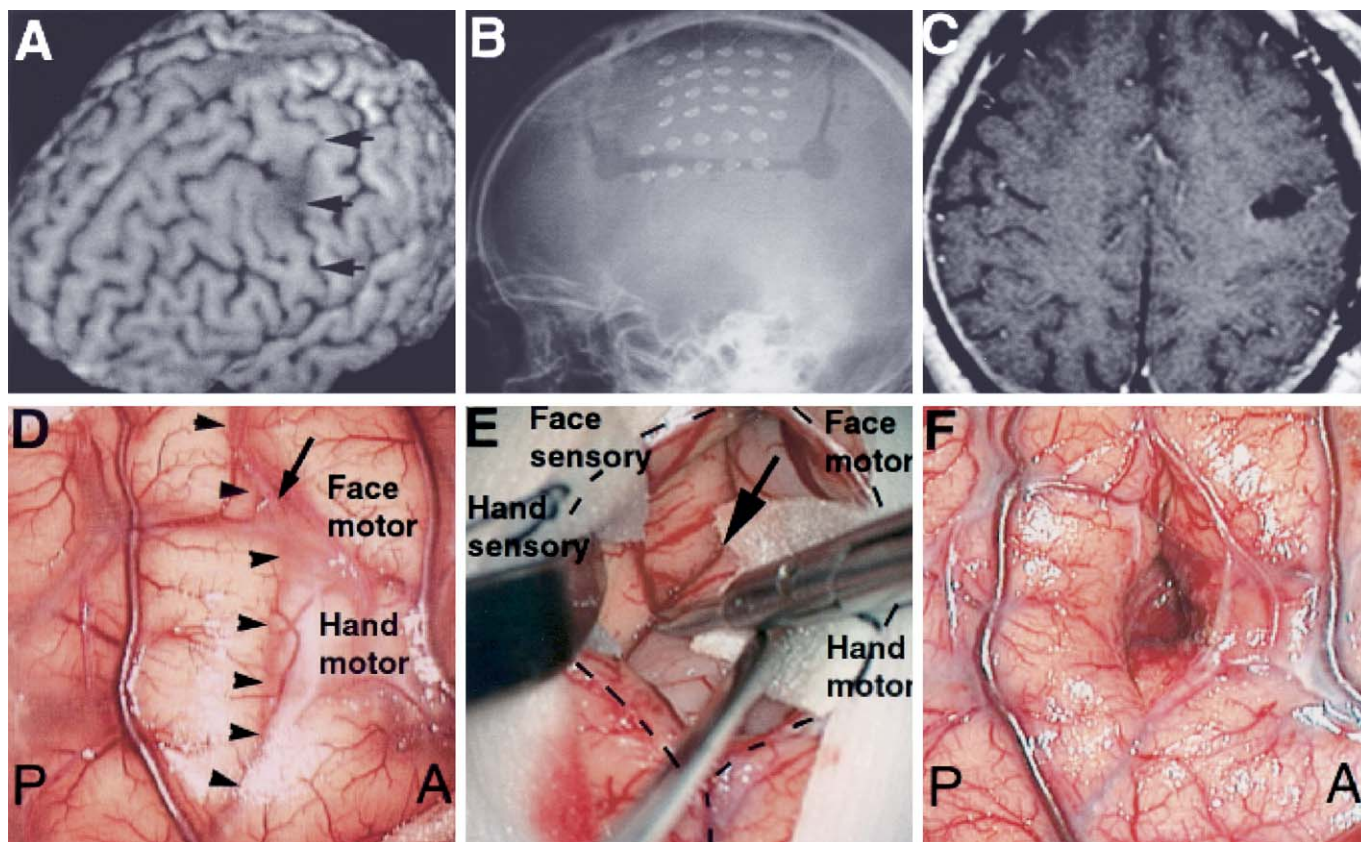
Fig. **1** Preoperative 3D MRI, craniogram with subdural grid electrodes, postoperative MRI, and operative views in patient 1 with anaplastic astrocytoma. **A** Cortical surface image on 3D MRI clearly shows location and shape of the central sulcus (arrows). **B** Implantation of 30 contact subdural grid electrodes for evaluation of cortical function over the tumor. **C** Postoperative MRI with gadolinium enhancement shows total removal of the enhancing lesion as compared with the preoperative MRI in Table **1**. **D** Intraoperative preresection view photograph shows that the central sulcus (arrow heads) over the tumor looks edematous. Note that a cortical artery (arrow) enters into the central sulcus with a little subarachnoid space. **E** According to the results of cortical function defined by electric stimulation and the anatomic considerations, the central sulcus (dot lines) is opened from the facial motor/sensory area. Dissection into the central sulcus is continued using microscissors towards the enhancing lesion located deeply in the hand motor/sensory area. Note that minimal brain retraction during the manipulation at the deep part of the sulcus is applied on the postcentral gyrus. **F** An operative view photograph after removal of the tumor. A = anterior, P = posterior.

Intraoperative neurological examination

General anesthesia was induced and maintained with intravenous propofol for the craniotomy. The patients lightened in 5 to 8 minutes on discontinuing the infusion of propofol. Awake microsurgery under continuous monitoring of motor and sensory function, was performed with approval by the Ethical Committee of Kyoto University Graduate School of Medicine (No. 542) and written informed consent was obtained from the patients. The bilateral abductor pollicis brevis, biceps, brachialis, deltoid, gastrocnemius, quadriceps femoris, and tibialis anterior muscles were chosen for electromyogram (EMG) recording by using neurological monitoring (Epoch XP, Axon Systems, NY, USA).

Results

The results of MRI and functional mapping showed that the lesions were located deep in the central sulcus at the hand/face area in patient 1, the hand area in patient 4, and the foot area in patient 2, and in the postcentral sulcus at the hand area in patient 3. Sulci over the astrocytoma and cavernoma accompanied by hemorrhage (patients 1, 2, and 4) were edematous and arach-

noid membranes were adhering with each other. In these three patients, the relatively normal sulcus corresponding to the face area was opened at first, followed by dissection to the lesion located under the hand area. The transsulcal approach to the lesions was successfully conducted without any neurological deficits in all cases. All the lesions were removed completely with intraoperative functional monitoring, and there were no further postoperative neurological deficits.

Illustrative case (patient 1) (Fig. 1)

A 53-year-old right-handed man had a history of simple partial seizures on his right hand and face progressing to complex partial seizures. Interictally, he had mild dysarthria due to central facial nerve palsy and clumsiness on his right hand. An MRI demonstrated low intensity on the T_1-weighted image, and high intensity on the T_2-weighted image in the precentral gyrus extending to the pyramidal tracts, while the surface cortex were preserved intact. Gadolinium enhancement showed an enhancing lesion at the bottom of the central sulcus (area 3a according to Brodmann's cortical classification). The 3D MR image showed that the tumor was adjacent to the precentral hand knob. Functional mapping by using subdural electrode grids demon-

strated that the tumor was located under the cortex of hand/face area. According to the results of MRI and functional mapping, we scheduled to remove the enhanced lesion through the central sulcus followed by additional removal of the tumor to the largest possible extent without further neurological deficits.

At the surface part of the central sulcus just above the enhanced lesion, the brain was edematous and arachnoid membranes were adhering with each other. To begin with, the lower part in the central sulcus corresponding to the face area was dissected along the cortical artery. Then, dissection was performed toward the enhanced lesion extending the space into the central sulcus at the hand area. Finally, the central sulcus was opened to its bottom to 2 cm in width and 2 cm in depth. Neurological examinations soon after the patient lightened demonstrated no further deficits. During continuous evaluation of motor/sensory function and MEP monitoring combined with fiber tracking of the pyramidal tracts on neuronavigation (functional neuro-navigation), the tumor was removed piece by piece. Subsequent histology of the resected tissue led to the diagnosis of anaplastic astrocytoma as the enhancing lesion.

Discussion

It is well known that Penfield and his colleagues stimulated the cortex for functional mapping and removed the epileptogenic area in the eloquent area with local anesthesia [6–8]. Subsequent development of anesthesia and intraoperative functional mapping has lead to more precise and safe identification of cortical functions than before [1, 8–13].

Intraoperative motor functions associated with the pyramidal tracts have been generally evaluated under general anesthesia quantitatively by the D-waves detected on cervical epidural electrodes or qualitatively by the electromyogram, although difficulty will be encountered in judging sensory functions [2, 3, 14, 15]. Both motor and sensory functions can be evaluated with local anesthesia [1, 13, 16]. By these anesthesia and intra-operative methods, some lesions at the cortical surface in the hand or foot primary motor/sensory area have been reported to be removable [1, 3]. Even so, small lesions located deep in the paracentral cortex are still challenging due to the risks accompanying surgical procedures. Theoretically, transcortical and remote approaches always involve cortical and subcortical injury, thus, the transsulcus approach is the best way to be considered. In our patients, lesions deep in the central or postcentral sulcus were removed completely without further neurological deficits by using MEP and continuous functional monitoring under local anesthesia, based on detailed preoperative functional mapping by cortical stimulation as well as functional MRI and fiber tracking.

Among several surgical procedures to remove brain tumors and arteriovenous malformations (AVMs), opening the sulcus/fissure preserving the surround cortices is a principle in our institute. Certainly, the transcortical approach should be considered according to the location of lesions and the spatial relationship between lesions and eloquent areas. In the present report, we have introduced our surgical procedures to deeply located para-central lesions for which the transsulcus approach is expected to be the most required and useful way. There are three important points to be considered in the transsulcal approach. The first one is to examine preoperative MRI for determining the entrance and direction of dissection, the shape and depth of the sulcus should be evaluated by 3D and axial images. The second point is to consider the results of functional mapping. Since paracentral topography in motor and sensory functions is variable, cortical electrical stimulation as well as functional MRI, MEG, and fiber tracking of the pyramidal tracts would be necessary for removal of the paracentral lesion [2, 11–13, 17, 18]. According to the cortical function over the deeply located lesions, the central or postcentral sulcus should be opened. If the facial area is close to the lesion, dissection should be started from the facial area to the hand area to avoid retraction to cortex in the hand area. The third point, which is necessary and most important, is to perform basic microsurgical techniques [4, 19]. It is of critical importance to take advantage of the natural sulci of the brain and to continue the furthest possible dissection in the natural pathways. After opening the arachnoid, dissection is continued using microscissors with the least coagulation so that even small veins running along and then down into the deep sulcus can be preserved. A microsiphon over the cotton on the superficial cortex is suitable for transient and minimal brain retraction. A feasible part of the sulcus, with relatively less edema and adhesion between arachnoid membranes, should be located and opened in the first place. Then, the working space in the sulcus can be extended deeply and widely to the lesions. Self-retractors, if necessary, could be applied on the postcentral gyrus, not on the precentral gyrus only during the manipulation at the deep part of the sulcus and should be loosened frequently.

We believe that microsurgical techniques based on anatomic and functional information allow surgeons to reach lesions deep in the sulcus at the paracentral hand or foot region.

References

1 Cohen-Gadol AA, Britton JW, Collignon FP, Bates LM, Cascino GD, Meyer FB. Nonlesional central lobule seizures: use of awake cortical mapping and subdural grid monitoring for resection of seizure focus. J Neurosurg 2003; 99: 1255–1262
2 Duffau H. Recovery from complete hemiplegia following resection of a retrocentral metastasis: the prognostic value of intraoperative cortical stimulation. J Neurosurg 2001; 95: 1050–1052
3 Duffau H, Capelle L, Denvil D, Sichez N, Gatignol P, Lopes M, Mitchell MC, Sichez JP, Van Effenterre R. Functional recovery after surgical resection of low grade gliomas in eloquent brain: hypothesis of brain compensation. J Neurol Neurosurg Psychiatry 2003; 74: 901–917
4 Hashimoto N. Microsurgery for cerebral arteriovenous malformations: a dissection technique and its theoretical implications. Neurosurgery 2001; 48: 1278–1281
5 Mikuni N, Shinji Ohara S, Ikeda A, Hayashi H, Nishida N, Taki J, Enatsu R, Matsumoto R, Shibasaki H, Hashimoto N. Evidence for a wide distribution of negative motor areas in the perirolandic cortex. Clin Neurophysiol 2006; 117: 33–40
6 Penfield W, Rasmussen T. The cerebral cortex of man: a clinical study of localization of function. New York, Macmillan, 1950
7 Penfield W, Welch K. The supplementary motor area of the cerebral cortex. A clinical and experimental study. Arch Neurol Psychiatry 1951; 66: 289–317
8 Penfield W, Jasper H. Epilepsy and the functional anatomy of the human brain. Little Brown, Boston, 1954

9 Danks RA, Rogers M, Aglio LS, Gugino LD, Black PM. Patient tolerance of craniotomy performed with the patient under local anesthesia and monitored conscious sedation. Neurosurgery 1998; 42: 28–36

10 Luders H, Lesser RP, Dinner DS, Morris HH, Wyllie E, Godoy J. Localization of cortical function: new information from extraoperative monitoring of patients with epilepsy. Epilepsia 1988; 29: 56–65

11 Luders H, Lesser RP, Hahn J, Dinner DS, Morris HH, Wyllie E, Godoy J. Basal temporal language area. Brain 1991; 114: 743–754

12 Maegaki Y, Yamamoto T, Takeshita K. Plasticity of central motor and sensory pathways in a case of unilateral extensive cortical dysplasia: investigation of magnetic resonance imaging, transcranial magnetic stimulation, and short-latency somatosensory evoked potentials. Neurology 1995; 45: 2255–2261

13 Taylor MD, Bernstein M. Awake craniotomy with brain mapping as the routine surgical approach to treating patients with supratentorial intraaxial tumors: a prospective trial of 200 cases. J Neurosurg 1999; 90: 35–41

14 Katayama Y, Fukaya C, Yamamoto T. Poststroke pain control by chronic motor cortex stimulation: neurological characteristics predicting a favorable response. J Neurosurg 1998; 89: 585–591

15 Taniguchi M, Cedzich C, Schramm J. Modification of cortical stimulation for motor evoked potentials under general anesthesia: technical description. Neurosurgery 1993; 32: 219–226

16 Whittle JR, Borthwick S, Haq N. Brain dysfunction following 'awake' craniotomy, brain mapping and resection of glioma. Br J Neurosurg 2003; 17: 130–137

17 Duffau H, Capelle L, Denvil D, Sichez N, Gatignol P, Taillandier L, Lopes M, Mitchell MC, Roche S, Muller JC, Bitar A, Sichez JP, van Effenterre R. Usefulness of intraoperative electrical subcortical mapping during surgery for low-grade gliomas located within eloquent brain regions: functional results in a consecutive series of 103 patients. J Neurosurg 2003; 98: 764–778

18 Skirboll SS, Ojemann GA, Berger MS, Lettich E, Winn HR. Functional cortex and subcortical white matter located within gliomas. Neurosurgery 1996; 38: 678–685

19 Yasargil MG. Microneurosurgery: AVM of the Brain – Clinical Considerations, General and Special Operative Techniques, Surgical Results, Nonoperative Cases, Cavernous and Venous Angiomas, Neuroanesthesia. Stuttgart, Georg Thieme Verlag, Vol. III B, 1987, pp 42–53

Original Article

295

Comparison between Transuncal Approach and Upper Vertebral Transcorporeal Approach for Unilateral Cervical Radiculopathy – A Preliminary Report

W. J. Hong[1]
W. K. Kim[1]
C. W. Park[1]
S. G. Lee[1]
C. J. Yoo[1]
Y. B. Kim[1]
H. D. Jho[2]

296

Abstract

Objective: The surgical treatments for unilateral cervical radiculopathy have been performed by either the anterior or posterior approach. The anterior approach has usually been used more than the posterior approach. The authors compared the results of newly advanced upper vertebral transcorporeal (UVTC) approach with those of the original transuncal (TU) approach in the anterior approach. **Methods:** The anterior cervical microforaminotomy was performed for 60 patients (male: female = 40:20) from June, 2000 to October, 2003. 40 patients were treated by the TU approach while 20 patients were operated on by the new UVTC approach. The authors analyzed postoperative changes of disc height, the spinal instability, the average length of hospital stay, the degree of patients' satisfaction and complications from each approach. The mean follow-up period was 9.5 months. **Results:** In the TU approach, postoperative intervertebral disc height was decreased from 7.1 ± 0.65 mm to 6.2 ± 0.61 mm. In the UVTC approach, postoperative intervertebral disc height was decreased from 6.6 ± 0.43 mm to 6.3 ± 0.41 mm. The average length of hospital stay was 5.2 days for the TU approach and 3.4 days for the UVTC approach. In the TU approach, 28 patients experienced excellent results, 11 patients experienced good results, one patient who experienced a fair result was operated by anterior cervical fusion because of a recurrent herniated disc. In the UVTC approach, 16 patients had excellent results and four patients experienced good results. **Conclusions:** This comparative study demonstrates that the UVTC approach is a better surgical technique than the TU approach considering the preservation of disc height, spinal stability, length of hospital stay, degree of satisfaction and complications.

Key words

Anterior microforaminotomy · cervical vertebra · radiculopathy · intervertebral disc

Introduction

In spite of the many operative methods for unilateral cervical radiculopathy, the cervical microforaminotomy through the anterior approach has been used widely due to the high possibility of directly removing bony spurs and herniated disc material causing nerve compression. However, there are some problems related to the original anterior cervical microforaminotomy through the anterior approach. With the anterior approach, there could be some side effects, cervical instability, fast degenerative changes [1], and nuchal pain due to kyphotic changes in the cervical spine [2, 3]. In the original anterior cervical microforaminotomy, the orifice of the microforaminotomy is situated slightly lower than the site of the lesion. So, as the size of microforaminotomy orifice is increased to expose the nerve roots exactly, the disc in the unco-vertebral juncture is removed more than is needed.
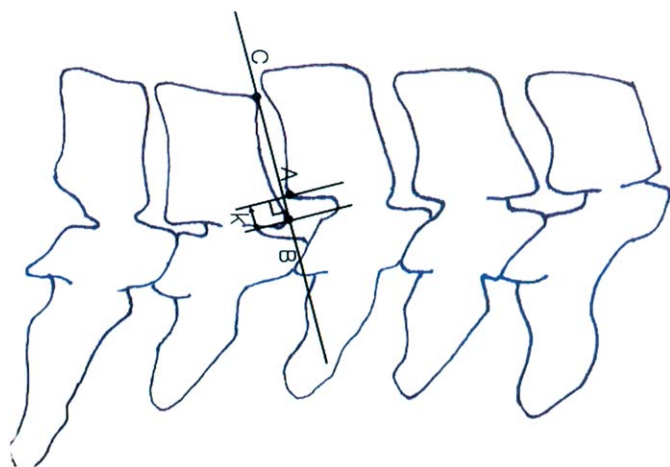
Fig. **1** The method for measuring translatory displacement. **A:** Postero-inferior angle of upper vertebral body. **B:** Posterosuperior angle of lower vertebral body. **C:** Anterosuperior angle of lower vertebral body. Linear distance k is the translatory displacement; if this is more than 3.5 mm, it is considered suggestive of instability.

Fig. **2** The method for measuring sagittal plane rotation in dynamic radiographs (left: flexion view, right: extension view). **a:** Anterosuperior angle of upper vertebral body. **b:** Posterosuperior angle of upper vertebral body. **c:** Anterosuperior angle of lower vertebral body. **d:** Posterosuperior angle of lower vertebral body. **S:** Extension line between a and b. **T:** Extension line between c and d. 'x' and 'y' are angle of S and T. Sagittal plane rotation = x + y. More than 20 degrees of sagittal plane rotation on the dynamic radiograph is considered suggestive of instability.

In order to overcome these problems, Jho developed the UVTC approach. We performed a microforaminotomy with this UVTC approach by moving the orifice of microforaminotomy cephalad rather than to the unco-vertebral juncture so the neural foramen where the nerve root is located could be exposed effectively. With this process, we could remove only one third of the posterior part of the uncinate process without resecting its anterior portion and could achieve decompression of the nerve root by removing bony spurs and herniated disc material compressing the nerve roots [4].

Although there have been studies on the surgical outcome of the transuncal approach [5, 6], no study has been reported on those of the upper vertebral transcorporeal approach. Thus, we compared surgical outcomes of the new upper vertebral transcorporeal approach with those of original transuncal approach and analyzed the outcome.

Materials and Methods

Of the 60 patients who underwent anterior cervical microforaminotomy with the diagnosis of a unilateral herniated disc of the cervical spine from June 2000 to October 2003, 40 patients underwent the microforaminotomy with the transuncal approach, and 20 patients underwent the microforaminotomy with through the upper vertebral transcorporeal approach.

Inclusion criteria for the anterior cervical microforaminotomy are as follows:
– unilateral cervical radiculopathy that had not responded to conservative treatment in more than three months
– imaging studies including magnetic resonance images and computed tomographs confirming pathoanatomic features such as protrusion of disc and bony spur corresponding to the clinical symptoms, and
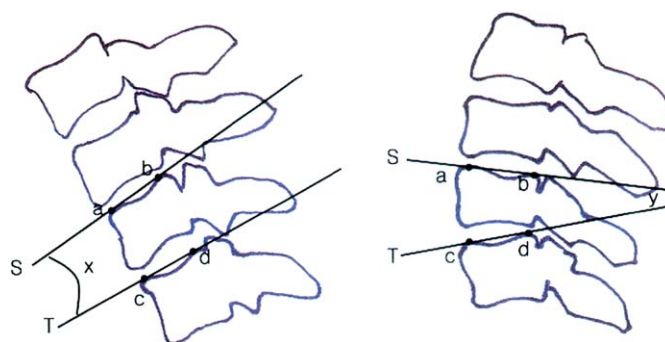– no previous cervical spine surgery.

Table **1** Preoperative clinical features

Clinical finding		Number of patients (%)
Pain	Nuchal	27 (46.5%)
	Radicular	40 (68.9%)
	Headache	1 (1.3%)
	Interscapular	5 (8.6%)
	Shoulder	11 (19%)
	Paresthesia	16 (27.6%)
Neurological sign	Sensory loss	25 (43.1%)
	Motor weakness	27 (46.6%)

Each surgical technique for the anterior cervical microforaminotomy has been discussed in many studies [4–7] so we do not mention it in this report.

Three-dimensional computed tomographs were taken from all patients immediately after surgery to confirm the location of the foraminotomy hole and the degree of decompression. Dynamic radiography of the cervical spine was taken to confirm cervical instability after surgery. The cervical instability was evaluated by the method of White and Panjabi [8]. The methods are as follows:
– The translatory distance between the upper and lower vertebra was measured on a lateral radiograph of the cervical spine. If it is more than 3.5 mm, it is considered suggestive of instability (Fig. **1**).
– The sagittal plane rotation in a dynamic radiograph was measured. If it is more than 20°, it is considered suggestive of instability (Fig. **2**).

The patients were followed up for one to three months after surgery. They were followed up every three months to examine the presence of cervical instability, the decrease in intervertebral disc space and the degree of nuchal pain or symptoms for compression of the nerve root. The average follow-up period
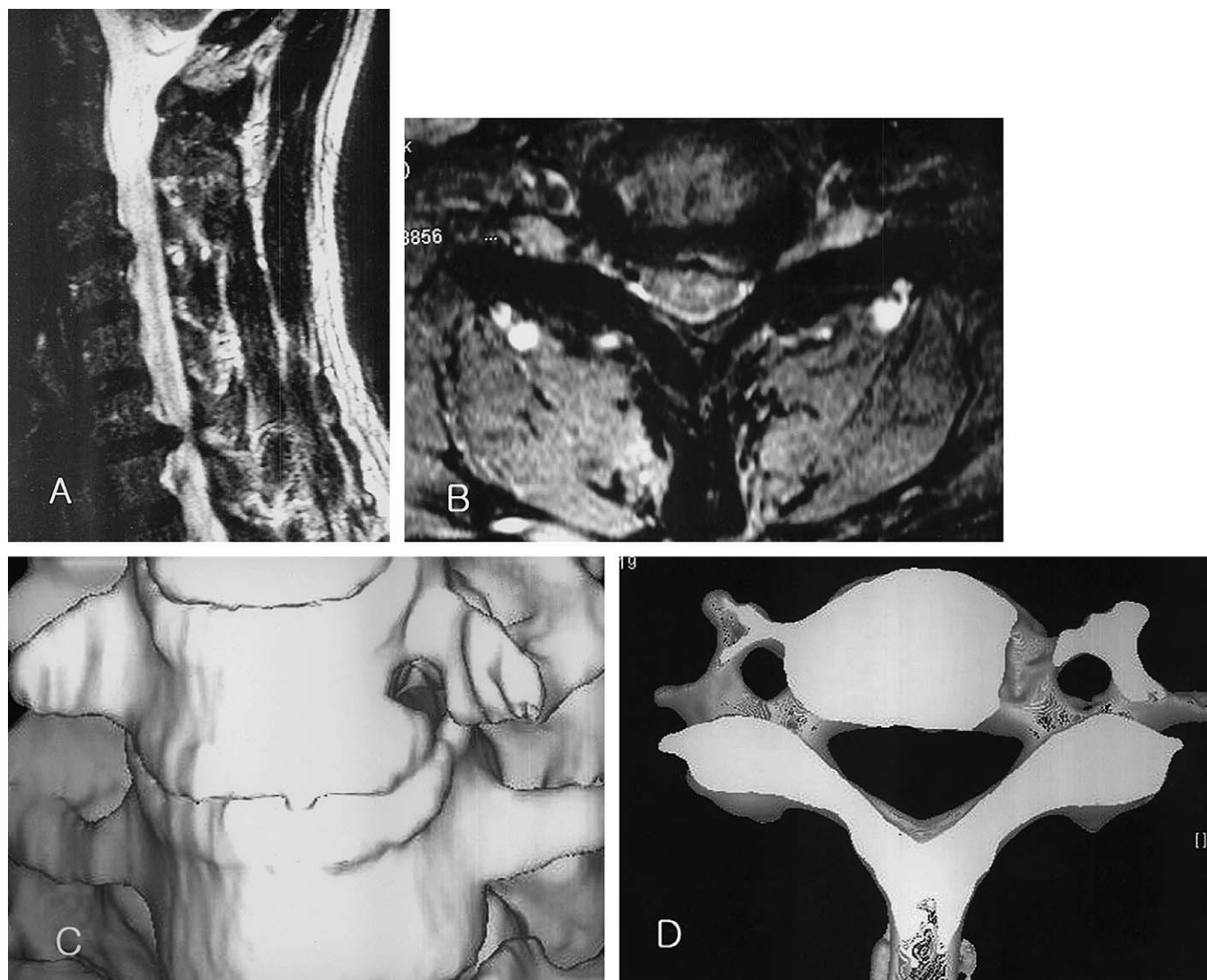
298

Fig. **3** Upper vertebral transcorporeal approach. Preoperative magnetic resonance images, sagittal (**A**) and axial (**B**) views showing the disc encroaching on the left C7 nerve root at the C6-C7 neural foramen. Postoperative three-dimensional computerized tomography of upper vertebral transcorporeal approach (**C**, **D**). **C** The anterior view demonstrating a left-sided anterior foraminotomy hole which was made more cephalad than that for the transuncal approach. **D** The inferior view demonstrating preserved uncinate process and the tunnel of bone removal through the anterior foraminotomy hole.

was 9.5 months. The patient's satisfaction was evaluated through a phone survey conducted by people not related to the surgery.

Results

A total of 60 patients were enrolled in this study. 40 underwent surgery through the transuncal approach, and 20 underwent through the upper vertebral transcorporeal approach. The average age of the patients was 46.6 years. The periods of symptoms experienced by the patients were: less than six months in 45 cases, six months to one year in seven cases, one to three years in six cases, and more than three years in two cases. Preoperative symptoms were radiating pain in all cases, nuchal pain in 27, paresthesia in 25 cases, and muscle weakness in 27 cases (Table **1**).

With the transuncal approach, the findings of preoperative magnetic resonance imaging demonstrated herniation of soft disc material in 23 cases, bony spurs in 10 cases and both in seven cases. With the upper vertebral transcorporeal approach (Fig. **3**), herniation of soft disc material was observed in 12 cases, bone spurs were observed in five cases, and both results were viewed in three cases.

The site of surgery was C5-C6 in most cases, followed by C6-C7. In 40 patients who underwent surgery with the transuncal approach, the average hospitalization stay was 5.2 days. In 20 patients who underwent surgery with the upper vertebral transcorporeal approach, it was 3.4 days.

With the transuncal approach, the average height of disc space was decreased from 7.1 ± 0.65 mm (before operation) to 6.3 ± 0.63 mm (at three months after operation). It was decreased to 6.2 ± 0.61 mm at 6 months after operation but there was little change afterwards. With the upper vertebral transcorporeal approach, it was decreased from 6.6 ± 0.43 mm (before operation) to 6.3 ± 0.41 mm (at three months after operation) and

Table 2 Intervertebral disc height

	TU approach	UVTC approach
Pre op	7.1 ± 0.65 mm	6.6 ± 0.43 mm
Post op 3 months	6.3 ± 0.63 mm	6.3 ± 0.41 mm
Post op 6 months	6.2 ± 0.61 mm	6.3 ± 0.45 mm
Post op 1 year	6.2 ± 0.71 mm	6.3 ± 0.35 mm

Repeated measures ANOVA test ($P > 0.05$).

Table 3 Postoperative surgical results

Surgical results	No. of patients TU approach	UVTC approach
Excellent	28 (70 %)	17 (85 %)
Good	10 (25 %)	3 (15 %)
Fair	2 (5 %)	0
Poor	0	0
Total	40 (100 %)	20 (100 %)

Odom's criteria: Excellent, patient exhibited complete resolution of all symptoms; Good, patient experienced relief of radiculopathy but still experienced occasional minimal/mild residual non-radicular discomfort. Fair, patient exhibited mild residual symptoms of radiculopathy, with or without mild/moderate residual non-radicular discomfort; Poor, patient continued to exhibit significant radicular symptoms, with or without non-radicular discomfort.

there was little change afterwards. Thus, we conclude that the upper vertebral transcorporeal approach is better than the transuncal approach in maintaining the height of the disc space after surgery. However, the superiority of the upper vertebral transcorporeal approach in change of disc height was not statistically significant (Repeated measures ANOVA test, p > 0.05) (Table **2**).

Three-dimensional computed tomography of the cervical spine taken after surgery showed the degree of decompression of the neural foramen. Dynamic radiographs of the cervical spine taken during follow-up demonstrated kyphotic changes in the cervical spine in one case treated with the transuncal approach in two sites; C4-C5 and C5-C6. But we think that the kyphotic changes might be due to surgery. We had removed too much of the intervertebral disc. However, a second surgery was not performed in this case since the patient had no pain and showed no evidence of spinal instability (Fig. **4**). All cases who underwent with the upper vertebral transcorporeal approach demonstrated stability of the cervical motion segment.

Odom's criteria were used to evaluate the patient's satisfaction [5]. With the transuncal approach, the satisfaction rate was excellent in 28 cases, good in 10 cases and fair in two cases, With the upper vertebral transcorporeal approach, the satisfaction rate was excellent in 16 cases and good in four cases (Table **3**).

With the transuncal approach, kyphotic changes in the cervical spine were seen in one case, and a herniated nucleus pulposus recurred in the same site at 12 months after operation in 1 case. There were no complications such as Horner's syndrome or hoarseness, vertebral artery injury, and damage to the nerve root.

Discussion

The surgery for herniated nucleus pulposus in the cervical spine is generally divided into two approaches: the posterior approach and the anterior approach [9]. At first, the posterior approach was used widely [10–12]. However, due to many problems related to the posterior approach, the anterior approach has been used since the 1950s and the approach has been used more extensively in recent times.

With the posterior approach, the damage to the spinal structures could be minimized with the development of various surgical instruments such as the endoscope [12]. However, this approach has the following drawbacks:
– persistent nuchal pain due to muscle injury

– the possibility of nerve root damage with the traction on the nerve root to remove lesion in the anterior portion of the spine
– frequent epidural hemorrhages during surgery
– discomfort to the patient during surgery due to the operative position, and
– especially, the difficulty in removing the bony spur in the unco-vertebral joint.

With the anterior approach, the patient feels comfortable during surgery. The surgical site is easy to access without injuring muscles because of the anatomy of the neck and direct removal of lesions to minimize the possibility of nerve root injury. Most lesions are located in the anterior portion of the spine. However, there are the risks of hoarseness, injury of recurrent laryngeal nerve, Horner's syndrome due to injury to the sympathetic nerve, injury of the longus coli and vertebral artery injury due to excessive traction [13]. Because there are not so many studies reporting the drawbacks that are related to the anterior approach, it has been used more frequently for herniated nucleus pulposus in the cervical spine as compared to the posterior approach. There is controversy about performing bone fusion after diskectomy with the anterior approach. Various studies comparing outcomes after performing bone fusion or anterior cervical fusion after diskectomy with those after performing only diskectomy have been published [2, 3, 14]. Some reports showed that results for each method were similar [15, 16], and other reports stated that performing only diskectomy would increase the cervical instability [15, 17, 18].

To preserve the stability and motion of the cervical spine, the anterior cervical microforaminotomy was developed. Various modifications have also been made with the anterior microforaminotomy [4, 5, 19, 20]. After Verbiest had reported on the lateral approach to the cervical spine during the 1960s, many neurosurgeons such as Hakuba et al. introduced modifications of it [21, 22].

Snyder and Bernhardt reported the method of nerve root decompression by making a round hole in the lateral 1/3 portion of disc in 1989 [18]. However, neurosurgeons were not impressed with this method since a poor outcome was seen in more than 1/3 of
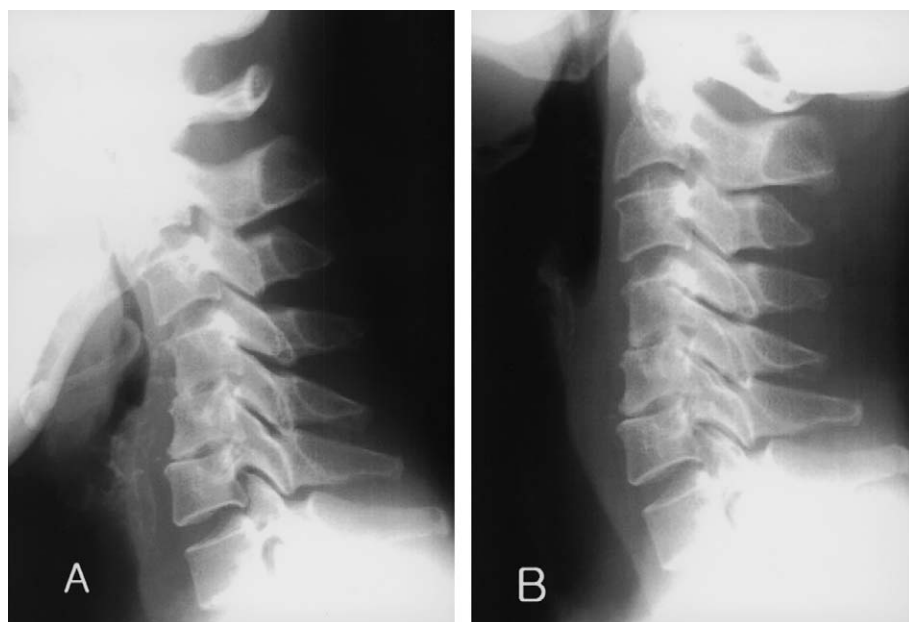
the patients due to non-removal of the posterior portion of the uncinate process, causing compression of nerve root.

Jho reported the method of expanding the intervertebral foramen by removing the uncinate process compressing the nerve root and minimizing removal of disc through the anterior approach in 1996, setting the stage for the anterior cervical microforaminotomy that is currently in use [6]. However, some authors reported that degenerative changes could be accelerated by invading the lateral portion of disc by accessing the uncovertebral juncture, and delayed the cervical instability [3]. It could be induced by removing the uncinate process when performing surgery through the previous transuncal approach [1, 2, 21, 23].

Johnson performed the operation as reported by Jho in 21 patients and presented the satisfactory results in 2000. Johnson observed improvements in 91% of the patients after following up the patients for three years [6, 24]. In 2002, Jho et al. reported excellent results and excellent recovery in 99% of 104 patients after a three-year follow-up period. Excellent outcomes have been reported with similar methods in many studies [5].

However, according to Hacker et al. in 2003, the second surgery was done in about 30% of 23 patients who underwent the anterior cervical microforaminotomy [25]. The satisfaction of patients was excellent and good in only 54%, thus they stated that this method was not good. But, when their data are examined in detail, the poor outcome may be due to removal of too much disc to decompress of the nerve root.

Concerning the biomechanical effect on anterior cervical decompression, Chen et al. reported that preserving much of the anterior structures including the uncinate process is better for the cervical stability if cervical fusion is not performed [16, 26]. Moreover; Kotani and Clausen emphasized the importance of maintaining the uncinate process [27, 28]. However, these biomechanical tests are not an accurate representation of the actual methods currently being used. Unlike the actual anterior cervical microforaminotomy, these results were obtained after removing

the uncinate process or much of the surrounding structures. Thus, accurate biomechanical tests should be performed.

In order to overcome these problems, the upper vertebral transcorporeal approach was used for removing the 1/3 posterior portion of the uncinate process and herniated disc material to achieve decompression of the nerve root by minimizing disc invasion by directly exposing the neural foramen with the nerve roots through making the hole of microforaminotomy in the rostral portion to the uncinate tip on the anterior aspect of the spine. Compared with the previous transuncal approach, the upper vertebral transcorporeal approach could minimize injuries in the uncovertebral joint and decompress the nerve root by minimizing disc invasion.

We performed the anterior cervical microforaminotomy as a minimally invasive surgery through the upper vertebral transcorporeal approach for the unilateral cervical radiculopathy to overcome problems related to the transuncal approach. When the two methods were compared, the upper vertebral transcorporeal approach has the following merits; a better access to the site of the lesion; better preservation in the height of the intervertebral disc space; and increased patient satisfaction by decreasing the average hospitalization stay and returning to normal daily life sooner. However, we need to perform actual biomechanical tests for this surgery, to examine more clinical cases, and to follow-up for longer periods.

References

1 Osti OL, Vernon RB. Annulus tears and intervertebral disc degeneration. An experimental study using an animal model. Spine 1990; 15: 762–767
2 Jacobs B, Krueger EG, Leivy DM. Cervical spondylosis with radiculopathy. Results of anterior diskectomy and interbody fusion. JAMA 1970; 211: 2135–2139
3 Park CH, Kim CJ, Chung KS et al. Results of anterior cervical discectomy without interbody fusion. J Korean Neurosurg Soc 1996; 25: 1371–1376

4 Kim DY, Kim WK, Lee SG et al. Technical evolution of anterior micro-foraminotomy for unilateral cervical radiculopathy. J Korean Neurosurg Soc 2004; 35: 23–28

5 Jho HD, Kim WK, Kim MH. Anterior microforminotomy for treatment of cervical radiculopathy: Part I – Disc-preserving "functional cervical disc surgery". Neurosurgery 2002; 51 (Suppl 2): 46–53

6 Jho HD. Microsurgical anterior cervical foramiotomy for radiculopathy: a new approach to cervical disc herniation. J Neurosurg 1996; 84: 155–160

7 Park SJ, Ha HG, Jung H et al. Anterior cervical microforaminotomy: a minimally invasive anterolateral approach for spondylotic lesions. J Korean Neurosurg Soc 2000; 29: 87–94

8 White AA, Johnson RM, Panjabi MM et al. Biomechanical analysis of clinical stability in the cervical spine. Clin Orthop 1975; 109: 85–96

9 Raynor RB. Anterior or posterior approach to the cervical spine: an anatomical and radiographic evaluation and comparison. Neurosurgery 1983; 2: 7–13

10 Aldrich F. Posterolateral microdiscectomy for cervical monoradiculopathy caused by posterolateral soft cervical disc sequestration. J Neurosurg 1990; 72: 370–377

11 Davis RA. A long-term outcome study of 170 surgically treated patients with compressive cervical radiculopathy. Surg Neurol 1996; 46: 523–530

12 Kim YS, Kuh SU, Jin BH et al. The result of posterior microforaminotomy for posterolateral herniation of cervical discs. J Korean Neurosurg Soc 2001; 30: 743–748

13 Kang DS, Ha YI, Choi SW et al. Clinical analysis of surgically managed cervical spondylosis by anterior approach. J Korean Neurosurg Soc 1998; 27: 1250–1256

14 Lee JC, Lee CY, Son EI et al. Comparison of surgical results between anterior cervical interbody fusion (ACIF) and microsurgical anterior cervical foraminotomy (MACF) for cervical disc herniation. J Korean Neurosurg Soc 1999; 28: 1173–1178

15 Jang WY, Kim KS, Lee JC et al. Results of microsurgical anterolateral tunnel approach for cervical disc herniation. J Korean Neurosurg Soc 2001; 30: 600–604

16 Chen TY, Crawford NR, Sonntag VK. Biomechanical effects of progressive anterior cervical decompression. Spine 2001; 26: 6–14

17 Smith GW, Robinson RA. The treatment of certain cervical spine disorders by anterior removal of the intervertebral disc and interbody fusion. J Bone Joint Surg [Am] 1958; 40: 607–624

18 Snyder GM, Bernhardt AM. Anterior cervical fractional interspace decompression for treatment of cervical radiculopathy. A review of the 66 cases. Clin Orthop 1989; 246: 92–99

19 Chung HY. A new technique for cervical simple discectomy through a small anterolateral exposure with emphasis on the importance of preserving the anterior soft tissue of the intervertebral space. Abstract of the 7th International Congress of Neurological Surgery in München, July 1981; pp 12–18, Supplement to Neurochirugia, Stuttgart: Georg Thieme Verlag, 1982; p 52

20 Lunsford LD, Bissonette DJ, Jannetta PF et al. Anterior surgery for cervical disc disease. Part 1: Treatment of lateral cervical disc herniation in 253 cases. J Neurosurg 1980; 53: 1–11

21 Verbiest H. A lateral approach to the cervical spine: technique and indications. J Neurosurg 1968; 28: 191–203

22 Hakuba A. Trans-unco-discal approach. A combined anterior and lateral approach to cervical discs. J Neurogurg 1976; 45: 284–291

23 Yoshihasa K, Patrick SM, Kuniyoshi A et al. The role of anteromedial foraminotomy and the uncovertebral joint in the stability of the cervical spine. Spine 1998; 20: 1559–1565

24 Johnson JP, Filler AG, McBride DQ et al. Anterior cervical foraminotomy for unilateral radicular disease. Spine 2000; 25: 905–909

25 Hacker RJ, Miller CG. Failed anterior cervical foraminotomy. J Neurosurg (Spine 2) 2003; 98: 126–130

26 Chen BH, Natarajan RN, An HS, Andersson GBJ. Comparison of biomechanical response to surgical procedures used for cervical radiculopathy: posterior keyhole foraminotomy versus anterior foraminotomy and discectomy with fusion. J Spinal Disord 2001; 14: 17–20

27 Kotani Y, McNulty PS, Abumi K et al. The role of anteromedial foraminotomy and the uncovertebral joints in the stability of the cervical spine: a biomechanical study. Spine 1998; 23: 1559–1565

28 Clausen JD, Goel VK, Traynelis VC. Uncinate processes and Luschka joints influence the biomechanics of the cervical spine: quantification using a finite element model of the C5-C6 segment. J Orthop Res 1997; 15: 342–347

Rational Management of Transient Obstructive Hydrocephalus Secondary to a Cerebellar Infarct

R. Ramos-Zuñiga
R. Jiménez-Guerra

302

Abstract

Introduction: Cerebrovascular disease is a common occurrence in adults with immediate as well as long-term neurological effects. Sequelae are disabling for patients and lead to a greater demand for healthcare infrastructure and search for treatment options. The acute phase in a cerebellar infarction may become complicated with transient obstructive hydrocephalus, subsequent intracranial hypertension, and the need for surgical management. Although many patients respond well to medical treatment, clinical findings and neuroimaging methods must be considered to determine whether the hydrocephalus can be surgically treated in a timely fashion. A series of cases is presented and a proposal is made for adding endoscopic third ventriculostomy to the available treatment armamentarium. **Clinical Cases:** Fourteen patients with cerebellar strokes and their clinical course are reported. Six required surgery for hydrocephalus management. Three of the cases had an endoscopic third ventriculostomy without complications, the rest were managed conservatively. As an average, patency was re-established in the aqueduct three months post ictus. **Conclusions:** Management of obstructive hydrocephalus in the acute phase of a cerebellar stroke must be individualized. In cases with transient obstructive hydrocephalus, endoscopic third ventriculostomy is a good surgical treatment option that avoids the risks of a long-term ventricular shunt.

Key words

Cerebellar infarction · endoscopic third ventriculostomy · intracranial hypertension · obstructive hydrocephalus · posterior fossa mass · stroke

Abbreviations

HSS	hypertensive skull syndrome
SCA	superior cerebellar artery
AICA	anterior inferior cerebellar artery
PICA	posterior inferior cerebellar artery
VPS	ventriculoperitoneal shunt

Introduction

Stroke is one of the most common conditions in adult age [1] and, because of immediate and long-term effects, an ever growing healthcare infrastructure is required that would provide patients with neurological sequelae and resulting disability with the necessary means to have a good quality of life.

The ischemic compromise of the vertebrobasilar system, with cerebellar manifestations, accounts for 1.5 – 5% of all cases [2, 3]. Mixed infarcts usually occur in this segment, where bleeding is added to the previous ischemic event after reperfusion. In about 10 – 25% of cases, besides the increased intracranial pressure in the posterior fossa from the mass effect of the lesion, a global intracranial hypertension results because of obstructive hydrocephalus and brainstem compression. During the acute stage, this specific territory is significantly affected from the occlusion of the sylvian aqueduct and the fourth ventricle, blocking CSF [2] and leading to a progressive subacute deterioration of the state of awareness once the infarct is installed [4, 5]. Under these conditions, the patient may progress to a coma or death. Thus, it is necessary to alleviate the transient obstructive hydrocephalus that may be reverted with surgical management. [6].

Affiliation
Departamento de Neurosciences, CUCS, Universidad de Guadalajara, Guadalajara, Jalisco, México

Correspondence
Rodrigo Ramos-Zuñiga, M.D., Ph.D. · Victoria · 1531 Colonia Providencia · Guadalajara · Jalisco · México · Fax: + 52/33/36 42 09 37 · E-mail: rodrigor@cencar.udg.mx

Table **1** Cases with transient hydrocephalus secondary to a cerebellar vascular lesion

Pathology	Territory	Age/Sex	Transient hydrocephalus	Hypertensive skull syndrome	Clinical sourse	Surgical procedure
Ischemic infarct	SCA	65 y/M	Yes	Yes	Improvement after VPS	VPS
Ischemic infarct	PICA	70 y/M	Yes	No	Stable	No
Ischemic infarct	SCA	67 y/M	Yes	No	Stable	No
Mixed infarct	PICA	62 y/M	Yes	Yes	Stable after DVP	VPS
Mixed infarct	AICA/SCA	65 y/F	Yes	No	Vertigo	No
Ischemic infarct	AICA/SCA	62 y/F	Yes	Yes	Vertigo	Third ventriculostomy
Ischemic infarct	SCA	57 y/M	Yes	Yes	Stable after surgical procedure	Third ventriculostomy
Ischemic infarct	PICA	64 y/M	No	No	Stable	No
Hemorrhagic infarct	Cerebellar cavernoma	15 y/F	yes	No	Stable	Suboccipital craniectomy/ cavernoma resection
Ischemic infarct	SCA	57 y/F	No	No	Stable	No
Massive hemorrhagic infarct	SCA/AICA/PICA	55 y/M	Yes	Yes	Fast and progressive neurological deterioration/death	No
Ischemic infarct	PICA	66 y/F	No	No	Stable	No
Ischemic infarct	SCA/PICA	60 y/F	Yes	Yes	Stable after surgical procedure	Third ventriculostomy
Ischemic infarct	PICA	75 y/M	No	No	Stable	No

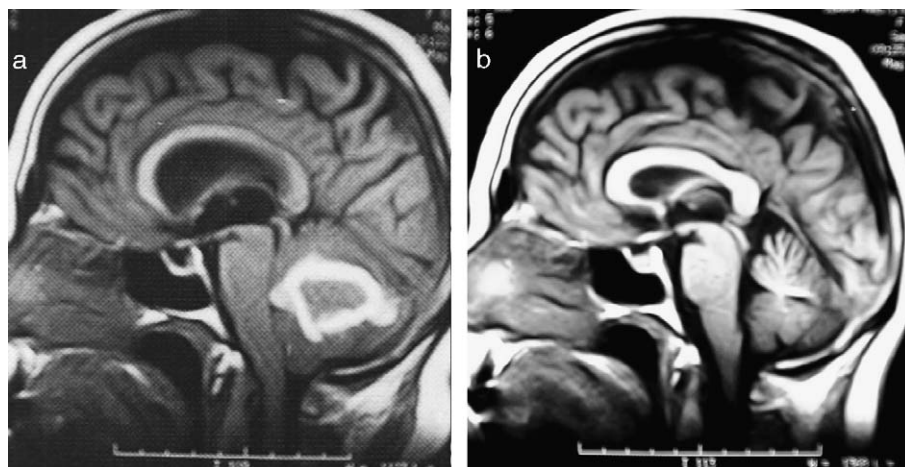Fig. **1** **a** MRI during the acute stage of a mixed cerebellar infarct, with perilesional edema and obstruction of the sylvian aqueduct and the fourth ventricle. Note the supratentorial ventricular dilatation. **b** MRI after three months shows aqueduct patency.

In view of all this, neurosurgical decisions should be considered as urgent, to compensate for the risk of the associated complications.

Most of the cerebellar infarcts that compromise a selective territory tend to compensate in the course of their own natural history without the need of corrective surgery. Generally, neurosurgical options are ventriculoperitoneal shunt (VPS), decompressive craniectomy in extreme cases, and recently, endoscopic third ventriculostomy.

We are presenting a series of representative cases with a different clinical course and therapeutic management, as well as the proposal of including endoscopic third ventriculostomy in selected situations. It is particularly stressed that the obstructive hydrocephalus condition in these cases is usually transient; as a relevant feature in the clinical course so that decisions should be made at short-term.

Patients and Methods

In a review of 14 patients with cerebellar infarct who were seen between 1998 and 2003 (Table **1**)**,** eight were males, with a median age of 60 years. The predominant symptoms at diagnosis were: vertigo, headache, vomiting, coordination disturbances and dysarthria.

The vascular territory of the superior cerebellar artery (SCA) and the posteroinferior cerebellar artery (PICA) was the most affected. Those patients who had no CSF flow impairment had a stable course, with a compensated ventricular dilatation, and no evidence of additional neurological damage besides the functional symptoms of the cerebellar infarct itself or the manifestations of a intracranial hypertensive syndrome. However, 5 of the 10 cases that were accompanied by obstructive hydrocephalus during the acute stage of the event developed an intracranial hypertensive syndrome that also required surgical treatment. A ventriculoperitoneal shunt was placed (VPS) in two of the patients with improvement of the clinical picture, and in the last 3

Fig. **2** Endoscopic view of the pre-mamilary region in one case of hydrocephalus secondary to the cerebellar infarct.

cases an endoscopic third ventriculostomy was performed with no complications and similar results. Only one patient died after a massive cerebellar hemorrhagic infarct in the acute stage. In every case, the aqueductal system regained its patency in an average of 3 months (Fig. **1**).

Discussion

In the last two decades mortality from cerebellar infarct has substantially changed [2, 7, 8]. As a result of multidisciplinary management, survival after this event is now 85% [5, 9], with an acceptable recovery at long-term [2].

Currently, surgical management is recommended for patients with secondary neurological deterioration [10–13]. Suboccipital craniectomy is still considered in extreme cases as a necessary procedure; however, considering the risk-benefit ratio, early management of hydrocephalus might be enough, and therefore avoid the need of posterior fossa decompression in some cases [5]. There are some reports that suggest early intervention with the procedure. [4, 6].

Conventional management of CSF flow obstruction, as a consequence of a cerebellar vascular event, has been the placement of an external ventricular shunt, which is not free of complications. Risk of infection is 10–20% due to manipulation and the time period that the catheter is in place [6, 14], aside from considering the inherent risks of a permanent ventriculoperitoneal shunt in cases where the obstructive phenomenon is not necessarily permanent.

Thus, this proposal of an endoscopic third ventriculostomy is an option that, in selected cases, may maintain proper control of the patient's course, without the complications or risks of deterioration due to a intracranial hypertension [15] (Fig. **2**), This is particularly valid if the transient nature of the obstruction during the acute and subacute stage is considered, as patency of the aqueduct is re-established at a later stage according to the natural history of the disease. Likewise, the cost-benefit ratio makes an external shunt system questionable, as well as the subsequent placement of a VPS [16].

To conclude, management of obstructive hydrocephalus during the acute stage of a cerebellar infarct must be individualized. Considering the transient nature of the phenomenon in many cases, the clinical neurological signs due to increased intracranial pressure must be distinguished from the primary signs of the ischemic event in the vertebrobasilar territory. Treatment may range from conservative medical management to suboccipital decompressive craniotomy. In those cases with transient obstructive hydrocephalus, third ventriculostomy is a good alternative to surgical treatment, without the risks involved in a long-term ventricular shunt.

References

1 Barinagarrementeria F, Amaya LE, Cantu C. Causes and mechanisms of cerebellar infarction in young patients. Stroke 1997; 28: 2400–2404

2 Kelly P, Stein J, Shafqat S, Eskey C, Doherty D, Chang Y et al. Functional recovery after rehabilitation for cerebellar stroke. Stroke 2001; 32: 530–534

3 Duncan J, Forman A. Hydrocephalus after cerebellar infarction. Br Med J (Clin Res Ed) 1984; 289: 1301–1302

4 Koh M, Phan T, Atkinson J, Wijdicks E. Neuroimaging in deteriorating patients with cerebellar infarcts and mass effect. Stroke 2000; 31: 2062–2067

5 Ganapathy K, Girija T, Rajaram R, Mahendran S. Surgical management of massive cerebellar infarction. J Clin Neuroscience 2003; 10: 362–364

6 Jensen M, St.Louis E. Management of acute cerebellar stroke. Arch Neurol 2005; 62: 537–544

7 Greenberg J, Skubick D, Shenkin H. Acute hydrocephalus in cerebellar infarct and hemorrhage. Neurology 1979; 29: 409–413

8 Taneda M, Ozaki K, Wakayama A, Yagi K, Kaneda H, Irino T. Cerebellar infarction with obstructive hydrocephalus. J Neurosurg 1982; 57: 83–91

9 Tengs T, Yu M, Luistro E. Health-related quality of life after stroke: a comprehensive review. Stroke 2001; 32: 964–972

10 Prat R, Conde FJ, Febles P, Cortes S, Millan-Corada AM. Infarto cerebeloso expansivo: tratamiento quirurgico o conservador? Rev Neurol 2004; 38: 133–136

11 Seelig JM, Selhorst JB, Young HF, Lipper M. Ventriculostomy for hydrocephalus in cerebellar hemorrhage. Neurology 1981; 31: 1537–1540

12 St Louis E, Wijdicks E, Li H. Predicting neurologic deterioration in patients with cerebellar hematomas. Neurology 1998; 51: 1364–1369

13 Shenkin HA, Zavala M. Cerebellar strokes: mortality, surgical indications, and results of ventricular drainage. Lancet 1982; 429–432

14 Lozier A, Sciacca R, Romagnoli M, Conolly S. Ventriculostomy-related infections: a critical review of the literature. Neurosurgery 2002; 51: 170–182

15 Boschert J, Hellwig D, Krauss J. Endoscopic third ventriculostomy for shunt dysfunction in occlusive hydrocephalus: long term follow up and review. J Neurosurg 2003; 98: 1032–1039

16 Garton H, Kestle J, Cochrane D, Steinbok PA. Cost-effectiveness analysis of endoscopic third ventriculostomy. Neurosurgery 2002; 51: 69–78

W.-Y. Cheng[1]
S.-C. Chao[1]
W.-H. Chen[2]
C.-C. Shen[1]

Minimally Invasive Keyhole Approach for Removal of a Migratory Balloon Complicated by Endovascular Embolization of a Carotid-Cavernous Fistula

Abstract

Purpose: This report presents our experience in using a minimally invasive keyhole approach to remove a migratory balloon in the cerebral artery in one patient. **Case Report:** A 19-year-old male suffered from carotid-cavernous fistula after craniofacial trauma two months previously. The patient received endovascular embolization of a carotid-cavernous fistula with detachable balloons. Unfortunately, migration of one balloon to the right middle cerebral artery (MCA) at the M1-M2 junction was noted after detaching the balloon during this procedure. Volume expansion, anticoagulation therapy and an emergency pterional keyhole approach with removal of the displaced balloon were performed successfully. Transient left hemiparesis due to temporary occlusion of the right middle cerebral artery by the balloon was promptly alleviated. There was no definite neurological sequel after the operation. **Conclusions:** Although detachable balloon embolization is the best initial treatment of direct carotid-cavernous fistulas, it is likely to migrate to downstream cerebral arteries. We recommend a minimally invasive pterional keyhole approach as a good alternative for treating such endovascular complications to improve outcome.

Key words

Carotid-cavernous fistula · keyhole · migratory balloon · pterion

Introduction

A carotid-cavernous fistula (CCF) is an aberrant vascular communication between the carotid artery system and the venous channels within the cavernous sinuses of the sphenoid. In 1985, Barrow and his colleagues formulated a classification system of CCF (type A, B, C, D) based on angiographic studies [1]. Direct type CCF (type A) is usually associated with trauma and the current standard therapy is endovascular detachable balloon occlusion [2]. Migration of balloon is one of the complications of detachable balloon embolization. Management of the migratory balloon includes volume expansion, anticoagulation therapy and embolectomy. For embolectomy, the traditional pterion craniotomy is frequently used. As an alternative we report here the case of a migratory balloon during the endovascular procedure that was successfully treated by the pterional keyhole approach. The advantages of the pterional keyhole approach for removal of the migratory balloon during anticoagulation therapy and possible complications of the detachable balloon technique are discussed.

Case Report

A 19-year-old man had presented with redness and proptosis of the right eye, double vision, and progressive deterioration in visual acuity after craniofacial trauma two months previously. Four-vessel cerebral angiography revealed a Barrow type A CCF.

Affiliation
¹Department of Neurosurgery, Taichung Veterans General Hospital, Taichung, Taiwan, R.O.C.
²Department of Radiology, Taichung Veterans General Hospital, Taichung, Taiwan, R.O.C.

Correspondence
Chinng-Chyi Shen, M.D. · Department of Neurosurgery · Taichung Veterans General Hospital · 160, Sec. 3, Taichung-Kang Road · Taichung · Taiwan · Republic of China · Tel./Fax: +886/4/23 74 12 18 · E-mail: ns@vghtc.gov.tw

Fig. **2** Illustration of the pterional keyhole approach. An oblique skin incision (curved black line) about 5 cm in length was first made in the right frontotemporal region. A burr hole (inset, black dot) was made at the temporal base and a small craniotomy (inset, shadowed area) about 2 cm in diameter at the right pterional region just below the temporal line was performed.

Fig. **3** A picture showing the displaced balloon trapped at the MI-M2 junction of the right middle cerebral artery.

Fig. **1** Angiograms showing the locations of the detachable balloon embolization. **a** Gauge-7 (arrow) and gauge-9 (arrowhead) detachable balloons mounted with a 3F/2Fr microcatheter were placed into the right cavernous sinus through the carotid-cavernous fistula but complete occlusion of the fistula could not be achieved, suggestive of balloon trapping in the right internal carotid artery (proximal and distal locations of the fistula). **b** After detachment of the gauge-7 balloon, it deflated immediately. The shrunken balloon (arrow) flowed to and lodged in the right middle cerebral artery.

Initial treatment of the fistula was performed by detachable latex balloon (Acta Vascular System Inc., Paris, France) embolization. Unfortunately, just after detaching the last balloon (gauge 7), it deflated immediately (Fig. **1**). The shrunken balloon flowed to and lodged in the right middle cerebral artery (MCA). The valve of the balloon did not function as usual and leakage of contrast media happened immediately after detachment. Shortly after-
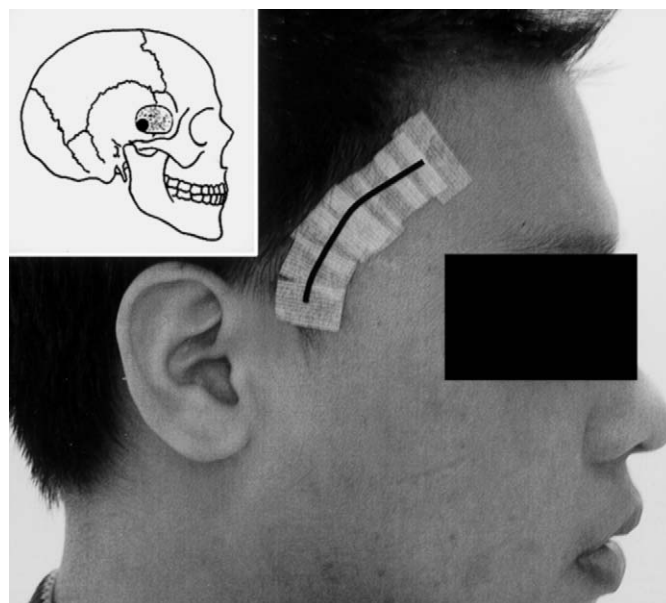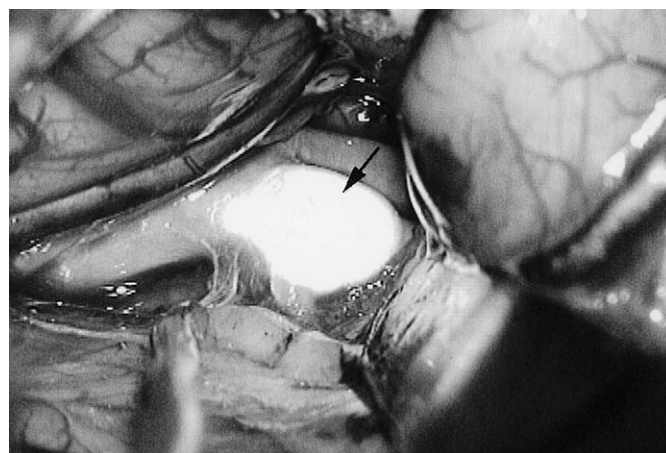
ward, a follow-up angiogram showed a total obstruction of the right MCA at the MI-M2 junction. Progressive weakness of the left limbs was noted after the accident. A pterional keyhole approach with removal of the displaced balloon was then performed as an emergency operation and a sufficient volume supply to maintain cerebral perfusion as well as intravenous heparin were given during operation.

A curved incision of the scalp about 5 cm in length over the right frontotemporal region was made and a small craniotomy of about 2 cm in diameter in the right pterional region was performed (Fig. **2**) as we previously reported [3]. Frequent oozing of the operative field was noted. Under the microscope, microsurgical dissection was done to open the sylvian fissure and to identify the MCA at the MI-M2 junction. The displaced balloon
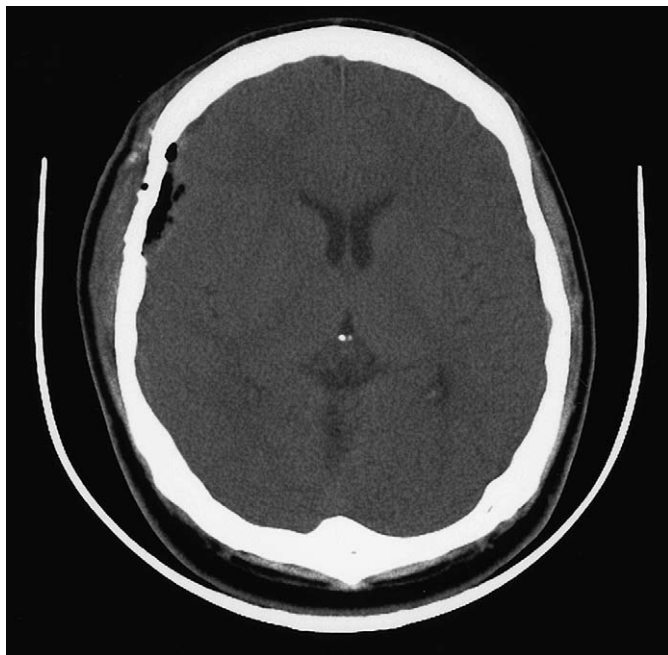
Fig. **4** Postoperative computed tomographic scan of the brain showed no definite infarction in the territory of the right middle cerebral artery.

Fig. **5** Postoperative angiogram of the detachable balloon embolization. The right internal carotid artery was totally occluded with preservation of the right middle cerebral artery and anterior cerebral artery. Complete obliteration of the carotid-cavernous fistula was also confirmed.

was found (Fig. **3**) and the main trunk and branches of the MCA were temporarily clipped. The vessel was opened and the balloon was removed smoothly. A thrombus was also found at M2 and embolectomy was performed. Then the vessel from Ml to M2 was sutured with 10–0 nylon thread. After that, the blood flow of the MCA was measured with Doppler flowmetry to ensure its patency. The time spent from occlusion of the MCA to re-establishment of blood flow was about 2.5 hours. After operation, enoxaparin was given to the patient for two days. Postoperative computed tomography (CT) of the brain showed no definite infarction in the right MCA territory (Fig. **4**). Transient left hemiparesis due to the temporary occlusion of the right MCA by the migratory balloon was promptly alleviated.

Two weeks after the operation, another detachable balloon embolization was performed smoothly. One week after this embolization, the patient's orbital symptoms except for diplopia were resolved. Angiography confirmed the complete obliteration of the fistula (Fig. **5**). The follow-up magnetic resonance (MR) angiography revealed no evidence for recurrence of the fistula 3 months later.

Discussion

Occlusion of direct carotid-cavernous fistulas (CCFs) with the detachable balloons was first described by Serbinenko in 1974 [4]. Since then Debrun et al. have popularized their use for the treatment of direct CCFs [5]. Currently, several studies have shown that transarterial embolization of direct CCFs by detachable balloons is the best option for initial treatment [6–8]. Although this technique can be performed with minimal risks, there are potential complications.

The most common complication is oculomotor nerve palsy. Debrun et al. reported that oculomotor nerve palsy occurred in 20 % of 54 patients with traumatic carotid-cavernous fistulas treated with detachable balloons and the occurrence rate was 16 % in the series reported by Tsai et al. [9]. Lewis et al. reported complications associated with this procedure, including cerebral infarction, intracerebral hemorrhage, loss of vision, transient cerebral ischemia and pseudoaneurysm formation [10]. Lee et al. reported that a ruptured balloon lodged in the cavernous sinus [11] and Peeters et al. also reported rupture of the balloon during the embolization procedure [12]. The balloon may deflate prematurely and become lodged in the carotid artery or its branch [9]. In our case, the balloon deflated immediately just after it was detached. The shrunken balloon then flowed to and lodged in the right MCA. Thus, migration of balloon may be also a complication of detachable balloon embolization. Most of the patients with migratory balloons were complicated with cerebral infarction and/or mortality after the endovascular procedure [10]. Only a few cases of migratory balloon during endovascular embolization were successfully treated by a traditional pterion craniotomy and embolectomy [13–15]. In the present case, the migratory balloon was also successfully removed by a minimally invasive pterion keyhole approach.

The keyhole concept is defined by two principles including widening of the intracranial optical field with increased distance from the keyhole and visualization of the contralateral structures. Perneczky proposed the concept of keyhole surgery and the supraorbital keyhole approach for aneurysm clipping or tumor removal. We modified the method as a pterional keyhole approach in which a small craniotomy of about 2 cm in diameter was made in the pterional region [3]. The advantages of our method are minimal brain retraction, minimal surgical trauma, better cosmetic results, easy approach, less approach-related surgical morbidity and shortened hospitalization. From March 1999 to December 2004, we have gained experienced in this minimally invasive approach to treat anterior cranial base lesions such as pituitary adenomas, arachnoid cysts, parasellar meningiomas, craniopharyngiomas, cavernous neurilemmomas,

cavernous hemangiomas, metastatic adenocarcinomas, gliomas, interpeduncular lipomas and intracranial aneurysms (data unpublished). In the present case, we also used this minimally invasive approach to remove the migratory balloon in the MCA. This keyhole approach can avoid large craniotomy-related intracranial hemorrhage, especially in patients under heparinization during endovascular procedures or other operations. Swann et al. reported a case of MCA embolism by a detachable balloon treated with embolectomy [13]. They spent about 3 hours from occurrence of embolism to re-establishment of blood flow by reopening a recent craniotomy. They thought that patient outcome was related to the degree of cerebral ischemia and time interval to re-establish the blood flow, and that it appeared difficult to re-establish the blood flow by embolectomy within 3 hours of vessel occlusion [13]. In our case, we only required 2.5 hours by the keyhole approach. We think that it is more time-saving than a traditional craniotomy with similar or even better improvement of clinical outcome. The authors consider that in selected groups of patients the pterional keyhole approach is a valuable alternative to the traditional pterion approach.

Conclusion

Although detachable balloon embolization is the best initial treatment of direct carotid-cavernous fistulas, there are potential complications. We report a case of a migratory balloon as a complication of detachable balloon embolization for the treatment of a direct carotid-cavernous fistula. The displaced migratory balloon was removed smoothly by the pterional keyhole approach. We recommend this minimally invasive approach as a good choice for treating such endovascular complications to improve outcome.

References

1 Barrow DL, Spector RH, Braun IF, Landman JA, Tindall SC, Tindall GT. Classification and treatment of spontaneous carotid-cavernous sinus fistulas. J Neurosurg 1985; 62: 248–256
2 Fattahi TT, Brandt MT, Jenkins WS, Steinberg B. Traumatic carotid-cavernous fistula: pathophysiology and treatment. J Craniofac Surg 2003; 14: 240–246
3 Cheng WY, Shen CC. Minimally invasive approaches to treat simultaneous occurrence of glioblastoma multiforme and intracranial aneurysm – case report. Minim Invas Neurosurg 2004; 47: 181–185
4 Serbinenko FA. Balloon catheterization and occlusion of major cerebral vessels. J Neurosurg 1974; 41: 125–145
5 Debrun G, Lacour P, Vinuela F, Fox A, Drake CG, Caron JP. Treatment of 54 traumatic carotid-cavernous fistulas. J Neurosurg 1981; 55: 678–692
6 Berthelsen B, Svendsen P. Treatment of direct carotid-cavernous fistulas with detachable balloons. Acta Radiol 1987; 28: 683–691
7 Negoro M, Kageyama N, Ishigauchi T. Cerebrovascular occlusion by catheterization and embolization: clinical experience. AJNR 1983; 4: 362–365
8 Tress BM, Thomson KR, Apsimon HT, King I, Brownbill D, Klug GL, Crawford B. Treatment of caroticocavernous fistulae with detachable balloons introduced by percutaneous catheterization. Med J Aust 1983; 4: 373–377
9 Tsai FY, Hieshima GB, Mehringer CM, Grinnell V, Pribram HW. Delayed effects in the treatment of carotid-cavernous fistulas. AJNR 1983; 4: 357–361
10 Lewis AI, Tomsick TA, Tew JM Jr, Lawless MA. Long-term results in direct carotid-cavernous fistulas after treatment with detachable balloons. J Neurosurg 1996; 84: 400–404
11 Lee ST, Hsu HH, Ng SH, Wong HF. Recurrent traumatic carotid-cavernous fistula caused by rupture of the detachable balloon. J Trauma 1998; 45: 969–971
12 Peeters FL, van der Werf AJ. Detachable balloon technique in the treatment of direct carotid-cavernous fistulas. Surg Neurol 1980; 14: 11–19
13 Swann KW, Heros RC, Debrun G, Nelson C. Inadvertent middle cerebral artery embolism by a detachable balloon: management by embolectomy. Case report. J Neurosurg 1986; 64: 309–312
14 Chalif DJ, Flamm ES, Berenstein A, Choi IS. Microsurgical removal of a balloon embolus to the internal carotid artery. Case report. J Neurosurg 1983; 58: 112–116
15 Langford KH, Vitek JJ, Zeiger E. Migration of detachable mini-balloon from the ICA causing occlusion of the MCA. Case report. J Neurosurg 1983; 58: 430–434

J. A. González-Garcia[1]
J. R. Garcia-Berrocal[1]
A. Trinidad[1]
J. M. Verdaguer[2]
R. Sanz[3]
R. Ramirez-Camacho[1]

Endonasal Endoscopic Management of a Large Meningocephalocele in a Patient with Concomitant Middle Skull Base Defect

Case Report

309

Abstract

The presence of a skull base defect can lead to major complications such as cerebrospinal fluid leak, meningocele, encephalocele and meningitis. It is exceptional to find the existence of two concomitant defects in the skull base. We present the case of a patient with concomitant spontaneous defects of the anterior and middle skull base that were surgically repaired. After 18 years of right rhinorrhea the patient was referred after being diagnosed with a large right nasal fossa meningoencephalocele, which was surgically removed by functional endoscopic sinus surgery. Following the surgery the patient complained about unilateral ear fullness. A paracentesis revealed a highly suspicious cerebrospinal fluid collection. High resolution scans revealed a defect in the mastoid tegmen; subsequently a transmastoid approach was carried out. Greater defects or those lying around the internal auditory canal, are best treated via the middle fossa approach. In the anterior cranial fossa the treatment of choice is provided by endoscopic procedures, but frontal bone craniotomy should be considered if the defect is in the frontal sinus or greater than 5 cm in size.

Key words

Cerebrospinal fluid · meningocele · encephalocele · skull base

Introduction

Congenital malformations of the skull base are rare. The presence of a skull base defect can lead to major complications such as cerebrospinal fluid leak, meningocele, encephalocele and in approximately 25% of patients it can present itself as meningitis. It is not unusual to experience a major complication or even recurrent episodes of meningitis as the only symptom. The origin of skull base defects lies in the embryological development of the neurocranial region. At the sixth week of gestation, the fusion in the midline of the paired craniofacial structures begins. The maxillary and the frontonasal processes start to move towards the midline to fuse on each side. Failure of these mesenchymal clefts to close leads to skull base bone defects [1]. The temporal bone is formed from a triad of parts. The petrous part of the temporal bone was seen to come via endochondral ossification, while the rest of the temporal bone, and the parietal and frontal bones ossify via the intramembranous route [2, 3]. A failure in the ossification process, beginning during the seventh to eighth week of gestation and following after birth especially in the temporo-occipital or the petrosquamous sutures, gives rise to defects in the middle or posterior fossa [4]. We present the case of a patient with concomitant anterior and middle skull base defects that were surgically repaired.
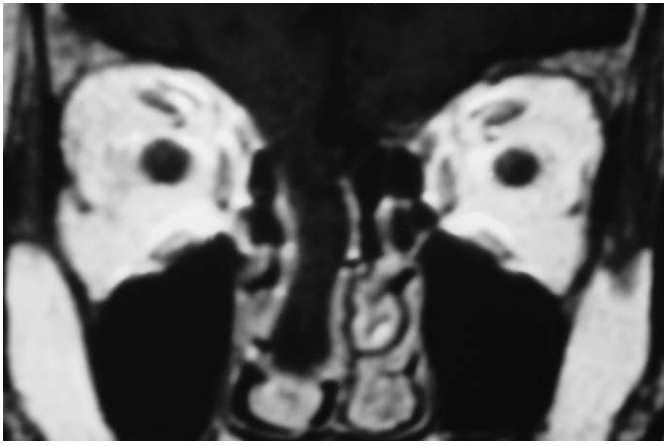
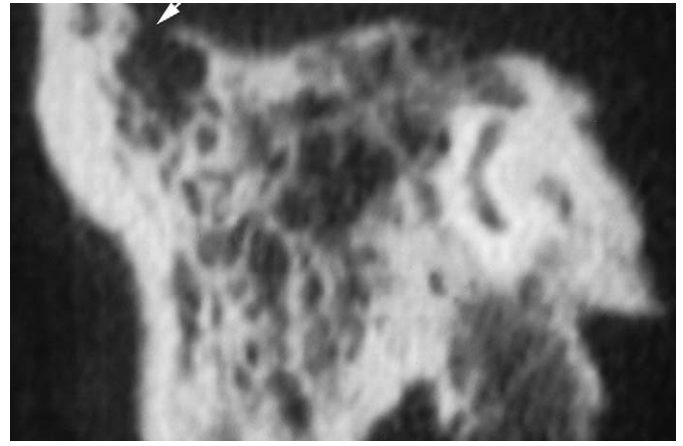Fig. **1** Coronal MRI showing basal meningoencephalocele occluding the right nasal cavity.

Fig. **3** A defect is seen in the most lateral portion of the mastoid tegmen in the coronal CT. Note the cerebrospinal fluid filling unremodelled mastoid cells.
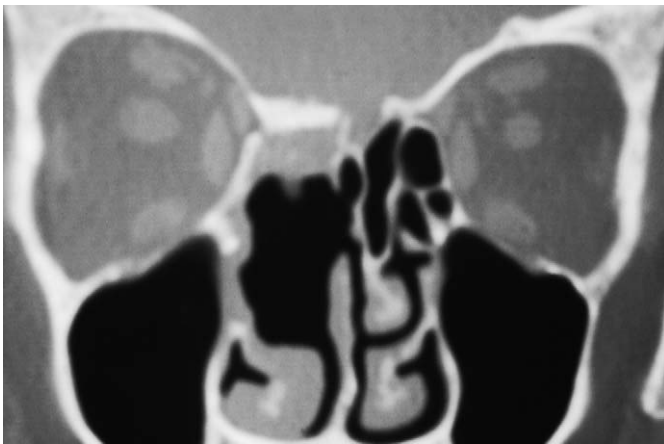

310

Fig. **2** Two years postoperative appearance in coronal CT. The middle turbinate bone covers the defect.

Pathology revealed normal brain tissue. The patient left the hospital after three weeks. Following the surgery she complained about right ear fullness, an otoscopic examination showed a light liquid collection in the middle ear. An audiogram revealed conductive hearing loss and low compliance tympanometry confirmed the occupation. Suspecting a secretory otitis media as a result of the surgery, a paracentesis was done revealing a highly suspicious cerebrospinal fluid collection. DTPA-^{111}In cisternography revealed an isotopic deposit in the right middle ear. A defect in the mastoid tegmen was found in high resolution computed tomography (Fig. **3**) and a transmastoid approach was carried out to repair the 6-mm defect in the middle cranial fossa with a temporal muscle graft. Two years and five months after the first surgery there is no evidence of a recurrence of the cerebrospinal fluid leak in the anterior cranial fossa or in the middle ear. Both nasal patency and audition were restored.

Case Report

A 62-year-old woman was referred with the spontaneous onset of a right-side cerebrospinal fluid rhinorrhea, which had been recurring for 18 years. She also complained about anosmia. There was no history of head or facial trauma, possible iatrogenic damage, inflammatory or neoplastic process, elevated intracranial pressure, sella turcica pathology or other intraoperative findings, so, as other authors, we assumed the lesions found were congenital [3]. Clinical examination revealed a pulsatile mass dropping from the right superior meatus and in contact with the inferior turbinate accompanied by a possible cerebrospinal fluid leak confirmed by biochemical procedures (immunofixation of beta-2-transferrin). High-resolution CT scan and MRI of the sinuses and anterior cranial fossa defined a bony defect in the cribiform plate through which a hypointense mass invaded the right nasal cavity (Fig. **1**). Functional endonasal sinus surgery was performed and the meningoencephalocele was removed. The defect was covered, overlaid with bone from the vomer and underlaid with a right middle turbinate mucous, osteal and periosteal flap (Fig. **2**).

Discussion

The coexistence of more than one spontaneous defect in the skull base is very uncommon. Published case reports have shown a relationship between anterior cranial fossa defects and a malformation in the inner ear or the middle cranial fossa skull base [5]. Congenital forms of cerebrospinal fluid fistulas account for approximately 10% of the cases. Possible complications justify the surgical treatment of this pathology. Precise localisation of the dural lesion is a prerequisite for surgical repair, without which the patient will continue to be at risk for potentially fatal meningitis. The treatment of the second defect shown by our patient could be deferred, approaching first the greater defect, the one with associated meningocele or cephalocele or the one that has probably caused a concurrent complication [6,7].

Cerebrospinal fluid can be identified by various methods. The determination of the albumin-prealbumin ratio in the suspicious liquorrhea compared to peripheral blood levels has usually been used to identify the cerebrospinal fluid. Beta-2-transferrin is a specific cerebrospinal fluid protein and its identification by immunofixation or qualitative methods is now used. In the referred patient there was no problem with the identification of

the skull base defect. In other cases there are no anatomic findings in the imaging. Isotopic cisternography does not provide anatomic images but is able to grossly identify the possible localisation of the fistula. Application of intrathecal fluorescein before surgery can be helpful when managing an occult cerebrospinal fluid leak. It was not used in this case as we had a good anatomic location of the defect. Moreover in our country there are still some legal problems to obtain and dispense intrathecal fluorescein. Although multiple defects are very rare, both the frontal and the lateral skull base should be carefully evaluated when managing spontaneous cerebrospinal fluid rhinorrhea. It is particularly important to consider a defect in the middle ear as a potential source in the differential diagnosis of cerebrospinal fluid rhinorrhea when spontaneous defects are found. In the middle cranial fossa, an extralabyrinthine transmastoid approach could be performed when the defect lays on the mastoid tegmen or the tegmen tympani and it is possible to have a complete exposure [7]. Greater defects or those surrounding the internal auditory canal are best treated via the middle fossa approach. In the anterior cranial fossa, the treatment of choice is provided by endoscopic procedures, but frontal bone craniotomy should be considered if the defect is in the posterior wall of the frontal sinus or greater than 5 cm in diameter.

References

[1] Anson BJ, Donaldson JA. The temporal bone. In: Anson BJ, Donaldson JA (eds). Surgical anatomy of the temporal bone. 3rd edn, Philadelphia, Saunders, 1981, pp 13–19

[2] Sadler TW. Sistema esqueletico. In: Langman Embriologia Medica 8th edn, Mexico DF, William and Wilkins-Panamericana, 1990, pp 151–155

[3] Schick B, Draf W, Kahle G et al. Occult malformations of the skull base. Arch Otolaryngol Head Neck Surg 1997; 123: 77–80

[4] Maniglia AJ. Embryology, teratology and arrested developmental disorders in otolaryngology. Otolaryngol Clin North Am 1981; 14: 25–39

[5] Claros P, Guirado C, Claros A, Claros Jr A, Claveria A, Wienberg P. Association of spontaneous anterior fossa CSF rhinorrhea and congenital perilymphatic fistula in a patient with recurrent meningitis. J Pediatr Otolaryngol 1993; 27: 65–71

[6] Raghavan U, Majumdar S, Jones NS. Spontaneous cerebrospinal fluid rhinorrhoea from separate defects of the anterior and middle cranial fossa. J Laryngol Otol 2002; 116: 546–547

[7] Ramirez-Camacho R. Cierre de fistula dural (Dural fistula closing). In: Ramirez-Camacho R, ed, Atlas de Cirugia del Oido (Ear Surgery Atlas). Madrid, Mosby-Doyma, 1994, pp 193–194

H. Akdemir[2]
I. S. Oktem[1]
B. Tucer[1]
A. Menkü[1]
K. Başaslan[1]
Ö. Günaldı[2]

Intraoperative Microvascular Doppler Sonography in Aneurysm Surgery

Abstract

Objective: The goal of this study was to evaluate the efficacy and reliability of intraoperative microvascular Doppler sonography (MDS) for the assessment of cerebral haemodynamics in aneurysm surgery. **Methods:** For 40 patients (21 men, 19 women, mean age 54.0 years, range 23–73 years) who underwent surgery for the treatment of 48 intracranial aneurysms, microvascular Doppler sonography with a 20-MHz microprobe was used before and after clip application, to confirm the complete obliteration of the aneurysm. Postoperative angiography was performed to assess the complete occlusion of the aneurysm and the patency of adjacent vessels. The findings of MDS were analysed and compared with the postoperative angiography. **Results:** A 1-mm diameter microprobe was able to insonate all vessels of the circle of Willis and their major branches and perforating arteries were reliably insonated. The aneurysm clip was repositioned on the basis of the MDS findings in 12 out of 48 patients (25 %). For 9 aneurysms (18.7 %) MDS exposed a relevant stenosis of an adjacent vessel induced by clip positioning that had escaped detection by visual inspection. Clip repositioning resulted in complete occlusion of the aneurysms in 7 of 9 cases (14.5 %). In two cases, additional wrapping became necessary as it was not possible to achieve complete clipping. The mean duration of MDS investigations was 5.3 minutes. There were no complications of intraoperative MDS probe use. **Conclusion:** Intraoperative MDS should be used routinely in cerebral aneurysm surgery, especially for large, complicated and giant aneurysms. Intraoperative MDS is a feasible, safe, and very reliable technique in aneurysm surgery. This technique is a valuable tool, in many instances, in place of intraoperative angiography for the surgical treatment of aneurysms.

Key words

Aneurysm · intraoperative · microvascular · Doppler

Introduction

The outcome of surgical treatment of cerebral aneurysms may be severely impaired by local cerebral ischemia, or by infarction resulting from the inadvertment occlusion of an adjacent vessel. On the other hand, incomplete aneurysm occlusion increases the risk of rebleeding after aneurysmal subarachnoid haemorrhage. Despite great attempts to preserve patency at the time of the clip application, intraoperative three-dimensional visual inspection of the entire vascular complex may not reveal arterial compromise or occlusion. Total obliteration of the punctured sac of the aneurysm can be tested intraoperatively by angiography [1–5]. In addition, an intraoperative microvascular Doppler sonography system has been used for this purpose in the past few years [6–9].

The present study was performed to investigate the reliability and practicability of intraopertive microvascular Doppler sonography during cerebral aneurysm surgery.

Table **1** Patient details

	Male		Female		Total	
	N	%	N	%	N	%
No. of patients	21	53	19	47	40	100
Single aneurysm	17	42	16	40	33	73
Multiple aneurysm	4	10	3	7	7	17
Total number of aneurysm	26	54	22	46	48	100
SAH grade (Hunt & Hess)						
Grade 0	6	15	5	12.5	11	22.9
Grade I − V	20	50	17	42.5	37	77.1

N = number, SAH = subarachnoid haemorrhage.

Patients and Methods

Forty patients, 21 men, mean age 53. 1 years (range 26–73), 19 women, mean age 54.1 years (range 38–70) with cerebral aneurysms treated by clipping from July 2003 until January 2004 were included in this prospective study. All of the patients underwent preoperative four-vessel angiography and computed tomography. Computed tomographic scanning was also performed for all patients within 6 hours after the surgery. Thirty-five patients (87.5 %) underwent postoperative angiography within 1 week after the surgery, which served as the gold standard to assess complete occlusion of the aneurysm and patency of adjacent vessels. Forty-six aneurysms were succesfully clipped and 2 aneurysms were wrapped because of an inability to directly clip the aneursym. The patients' data are shown in Table **1**. Intraoperative MDS recordings were performed with microvascular Doppler sonography equipment consisting of a 1-mm diameter, 20-MHz microprobe (ΔWL, Elektronische Systeme GmbH, Sipplingen, Germany). The Doppler probe was inserted through a surgical suction cannula, secured at the base with bone wax, and directly applied to all segments of the vessels. It was also applied to all exposed vessels adjacent to the aneurysm as well as to the aneurysmal sac proper with an insonation angle of 30 to 60 degrees. Intraoperative MDS signals were evaluated not only as flow velocities but also as visual and acoustic assessments for comparing findings before and after the placement of the clip.

The MDS signals were distinguished as three categories:

– Signal appeared regular (*normal signal*) in the parent and brancing vessels (laminar flow);
– Signal appeared irregular (*weak signal*) within the sac of the aneurysm (turbulent flow)
– Signal could not be obtained (*absent signal*) within sac of the aneurysm (total obliteration) or in the parent and branching vessels (occlusion or stenosis).

Detection of complete aneurysm obliteration
An absent signal on MDS with multiple projections on the aneurysm sac was considered to be indicative of complete aneurysm obliteration (Fig. **1**).
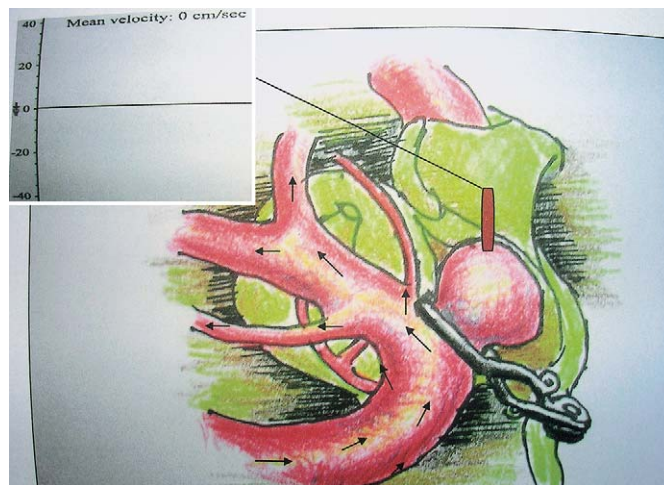

Fig. **1** Absent signal on MDS within the sac of the aneurysm after correct clipping.

Detection of incomplete aneurysm obliteration
A weak signal on MDS within the sac of the aneurysm was considered to be indicative of incomplete aneurysm obliteration (Fig. **2**).

Detection of adjacent vessel occlusion
An absent signal in the parent and branching vessels was considered to be indicative of adjacent vessel occlussion (Fig. **3**).

Statistical analysis was performed using the χ^2 test.

Results

Intraoperative MDS assessment demonstrated the patency of all arterial branches at the time of final clip placement. The presence, direction, and velocity of flow were determined for each patient. Successful insonation was performed on all major vessels or on perforators including the recurrent artery of Heubner, the lateral lentriculostriate artery, thalamoperforators, and the superior hypophyseal artery. The mean duration of the evaluation of MDS was 5.3 min (range from 2.5 to 7.2 min). There were no complications attributable to the use of the intraoperative MDS probe.

Postoperative angiography was performed in 35 out of 40 (87.5 %) patients. In five (12.5 %) patients, no postoperative angiography could be performed due to the critical condition or refusal by the patients. Findings from MDS were confirmed by the postoperative angiography in all 35 examined patients.

The clip was repositioned based on the MDS results in 12 of 48 (25 %) all aneurysms. There was a remarkable higher incidence of clip repositioning in aneurysms of the middle cerebral artery in 5 out of 21 patients (23.8 %) compared with aneurysms in other locations. These findings were not found to be statistically meanful (p > 0.05). Clip repositioning resulted in complete occlusion of the aneurysms in 7 of 9 cases (14.5 %). In two cases, additional wrapping became necessary as it was not possible to achieve complete clipping (Table **2**).
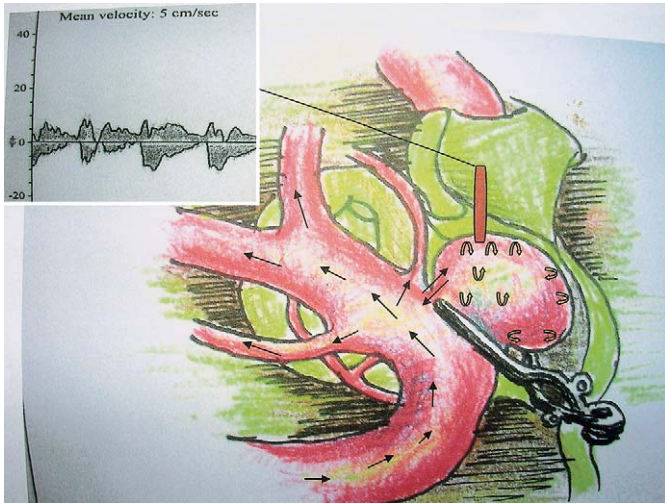
Fig. **2**   Weak signal on MDS after incomplete aneurysm clipping.
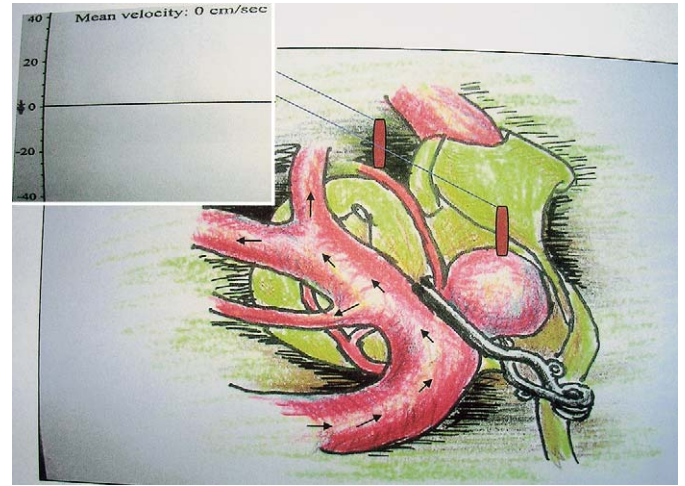

Fig. **3**   Absent signal in branching vessel and sac of the aneurysm after incorrect clipping.

Table **2**   MDS findings according to aneurysm location

Aneurysm location	No. of aneurysms		Insufficient aneurysm closure		Repositioning of aneurysm clip		Stenosis of adjacent vessel	
	N	%	N	%	N	%	N	%
ACA	11	22.9	2	4.1	2	4.1	2	4.1
MCA	21	43.9	5	10.4	5	10.4	4	8.3
ICA, PcoA, ACohA	13	27.1	2	4.1	4	8.3	2	4.1
BA, AIC, PICA	3	6.2	0	0	1	2.1	1	2.1
Total	48	100.0	9	18.7	12	25.0	9	18.7

ACA = anterior cerebral artery, MCA = middle cerebral artery, ICA = internal carotid artery, PcoA = posterior communicating artery, AcohA = anterior choroidal artery, BA = basilar artery, AICA = anterior inferior cerebellar artery, PICA = posterior inferior cerebellar artery.

The results of MDS flow analysis showed that primary insufficient aneurysm closure was found in 9 out of 48 (18.7%) all aneurysms. An initial stenosis of an adjacent vessel induced by the clip positioning that had escaped detection by visual inspection on microscopic magnifigation was verified during the surgery by using MDS in 9 of 48 (18.7%) aneurysms. The problem was solved by clip repositioning in 7 cases, and by repositioning plus wrapping in two.

Discussion

Doppler sonography was first used for the assessment of cerebral haemodynamics in extracranial vessels. Aaslid et al. [10] modified this technique for transcranial investigation of cerebral vessels. Further studies of Nornes et al. [11] and Gilsbach [12,13] led to the development of microprobes for the direct investigation of small cerebral vessels. These small Doppler probes of 0.3 or 1 mm in diameter have a high frequency of 20 MHz which allows them to be used for the direct intraoperative measurement of Doppler signals even from perporating vessels of the circle of Willis [14]. Intraoperative MDS provides a functional and non-invasive intraoperative examination of the haemodynamics of cerebral vessels. It can help to identify the aneurysmal sac by typical flow patterns even under complicated anotomic conditions. Intraoperative MDS also allows the determination of the flow direction and the detection of cerebral vasospasm with a high degree of sensitivity. Microprobes, as in the present study, allow the examination of not only the circle of Willis but also the small vessels such as the perforating arteries [15]. In the literature, a few studies have demonstrated [14–18] the usefulness of microvascular Doppler sonography in the practice of aneurysm surgery.

Bailes et al. [15] investigated 35 patients who underwent surgery for the treatment of 42 intracranial aneurysms by using intraoperative Doppler sonography at 20 MHz and a 1-mm diameter microprobe. They found an incidence of 31% for unexpected stenosis of adjacent arteries. However, they did not provide quantitative data on the incidence of insufficient aneursym closure and its relation to aneurysm location. The findings of Doppler sonography correlated with the findings of intra- or postoperative angiograhy in all cases. The authors concluded that microvascular Doppler sonography can be replaced intraoperative angiography and, in many cases, with postoperative angiography. Stendel et al. [19] reported on 75 patients who underwent surgery for the treatment of 90 intracranial aneurysms by using intraoperative Doppler sonography at 16 MHz and a microprobe diameter of 1 mm. They found incidences of 12.2%, 18.9%, 28.8% for insufficient aneurysm closure, stenosis of an adjacent vessel, and reposition of aneurysm clip, respectively. The authors concluded that their data demonstrate a statistically significant higher influence of the MDS results on the surgical procedure in aneurysms of the middle cerebral artery after

aneurysmal subarachnoid haemorrhage. Laborde et al. [18] showed 22 patients who underwent surgery for the treatment of 24 large and giant intracranial aneurysms at 20 MHz and microprobe diameters of 0.3 and 1 mm. They found five cases with severely disturbed flow after aneurysm clipping. They had to change their strategy; they resected the aneurysms and stured the neck, performed an end-to-end anastomosis, coated the aneursym, or repositioned the clips. Firsching et al. [20] used a 1-mm, 16 MHz intraoperative microprobe during aneurysm surgery in 50 patients and compared them retrospectively with 50 patients who were operated on without micro-Doppler sonography. The aneurysm clip was repositioned on the basis of MDS findings in 12 out of 50 patients (24%). Marchese et al. [9] reported on 130 patients harboring 136 aneuryms were operated on using MDS. They found that complete exclusion resulted in 129 aneurysms (94.9%). In 5 cases (3.7%) in which MDS revealed a persistent blood flow in the aneurysm, the clip was repositioned. In 25 cases (18.3%) in which MDS data documented a severe flow reduction in the vessel harboring the aneurysm or in the vessel originating very close to the aneurysm neck, the clip was repositioned. In 20 patients (15%) in whom MDS revealed arterial spasm by surgical manipulation topical sodium nitroprusside was followed by resolution of the spasm. In the present study, the incidences of insufficient aneurysm closure, repositioning of the aneurysm clip and stenosis of adjacent vessels were 18.7% (9 out of 48 cases), 25% (12 out of 48 cases), and 18.7% (9 out of 48 cases), respectively. Intraoperative MDS was paticulary helpful in MCA aneurysm surgery where the anatomy is critical because of several main vessels. For our cases of MCA (8.3%) aneurysms, MDS was essential to rapidly understand the real anatomy of the surgical field, favoring a safe and correct clip placement. However, intraoperative MDS may be unable to detect the persistence of a minimal blood flow after aneurysm clipping. In two cases (4.1%), the routine cut of the sac will reveal such incomplete exclusion of the aneurysm permitting a comfortable addition of another clip.

Intraoperative angiography has gained popularity at most large centres because of its relatively rapid evaluation of clip placement and its ability to guide appropriate changes in clip application. Intraoperative angiography has been advised [21] to improve outcome, as postoperative angiography has revealed unexpected major vessel occlusion and incompletely clipped aneurysms [21–25]. MacDonald et al. [23] reported a series of 78 patients who underwent surgery for intracranial aneurysm. They found that there was a 12% incidence of unexpected major vessel occlusion, as determined by postoperative angiography, resulting in disabling stroke or death. Furthermore, in the same study there was a 4% incidence of residual aneurysm and an additional 4% incidence of insufficient aneurysm closure. Intraoperative angiography is associated with a small but significant morbidity rate. Aside from a significant morbidity, however, the major drawback of intraoperative angiography is the time necessary as angiography requires 30 or 45 minutes of extra time. In the present study, the results of postoperative angiography were correlated with the findings of MDS.

Although the theoretical limitations of intraoperative MDS relate to the inability to detect aneurysmal rests or residual necks, MDS takes no more than altogether 5 minutes to investigate all related vessels prior to and after clipping of the aneurysm. Although intraoperative MDS is able to verify the complete closure of the aneurysm sac, it cannot detect a residual neck. However, if visual inspection suggests an unexpected vessel occlusion, MDS can verify or preclude perfusion within the vessel. The prospective angiographic study of Sindou et al. [26] involving the clipping of 305 aneurysms 18 out of 305 were considered as incomplete aneurysm closure (5.9%).

Our results are smillar with those of other series puplished in the literature [13–17]. Although, personal skill and experience play an important role in achieving undisturbed patency after aneurysm surgery, intraoperative MDS is able to increase the safety of the procedure, especially if less experienced surgeons operate on aneurysms.

In conclusion, we think that intraoperative MDS seems to offer an advantage by assisting surgeons in making difficult intraoperative decisions, especially, when a compromise is necessary between complete obliteration of the aneurysm neck and maintenance of adequate parent and adjacent vessel patency.

References

1 Hillmann J, Johansson I. Peroperative angiography – a useful tool in cerebral aneurysm surgery. Acta Neurochir (Wien) 1987; 84: 39–42
2 Lazar ML, Watts CC, Kilgore B, Clark K. Cerebral angiography during operation for intracranial aneurysms and arteriovenous malformations. Technical note. J Neurosurg 1971; 34: 706–708
3 Loop JW, Foltz EL. Applications of angiography during intracranial operation. Acta Radiol Diagn (Stockh) 1966; 5: 363–367
4 Parkinson D, Legal J, Holloway AF, Walton RJ, Lafrance RR, MacEwan DW, Johnson J. A new combined neurosurgical headholder and cassette changer for intraoperative serial angiography. Technical note. J Neurosurg 1978; 48: 1038–1041
5 Parkinson D. Rapid serial simultaneous biplane stereoscopic angiography; an aid in the surgical management of the cerebral arteriovenous malformations. Clin Neurosurg 1969; 16: 170–184
6 Gilsbach JM, Harders A, Mohadjer M. The microvasculer Doppler an intraoperative tool for aneurysm surgery. In: Advances in Neurosurgery, vol 16 1988; 42: 75–80
7 Gilsbach JM, Harders AG. Microvascular and transcranial Doppler sonographic evaluation of cerebral aneurysm flow pattern. Neurol Res 1989; 11: 41–48
8 Gilsbach JM. Intraoperative Doppler sonography in neurosurgery. Springer Wien, New York, Neurosurg Rev 1984; 7: 199–208
9 Marchese E, Albanese A, Denaro L, Vignati A, Fernandez E, Maira G. Intraoperative microvascular Doppler in intracranial aneurysm surgery. Surg Neurology 2005; 63: 336–342
10 Aaslid R, Markwalder TM, Nornes H. Noninvasive transcranial Doppler ultrasound recording of flow velocity in basal cerebral arteries. J Neurosurg 1982; 57: 769–774
11 Nornes H, Grip A, Wikeby P. Intraoperative evaluation of cerebral hemodynamics using directional Doppler technique. Part 2: Saccular aneurysms. J Neurosurg 1979; 50: 570–577
12 Gilsbach JM, Hassler WE. Intraoperative Doppler and real time sonography in neurosurgery. Neurosurg Rev 1984; 7: 199–208
13 Gilsbach JM. Microvascular intraoperative Doppler sonography. Ultraschall Med 1984; 5: 246–254
14 Gilsbach JM, Harders A. Early aneurysm operation and vasospasm. Intracranial Doppler findings. Neurochirurgia (Stuttg) 1985; 28 (Suppl 1): 100–102
15 Bailes JE, Tantuwaya LS, Fukushima T, Schurman GW, Davis D. Intraoperative microvascular Doppler sonography in aneurysm surgery. Neurosurgery 1997; 40: 965–970
16 Bailes JE, Deeb ZL, Wilson JA, Jungreis CA, Horton JA. Intraoperative angiography and temporary balloon occlusion of the basilar artery as

an adjunct to surgical clipping: technical note. Neurosurgery 1992; 30: 949–953

[17] Giller CA, Meyer VJ, Batjer HH. Hemodynamic assessment of the spinal cord arteriovenous malformation with intraoperative microvascular Doppler ultrasound: Case report. Neurosurgery 1989; 25: 270–275

[18] Laborde G, Gilsbach J, Harders A. The microvascular Doppler an intraoperative tool for the treatment of large and giant aneurysms. Acta Neurochir Suppl (Wien) 1988; 42: 75–80

[19] Stendel R, Pietila T, Al Hassan AA, Schilling A, Brock M. Intraoperative microvascular Doppler ultrasonography in cerebral aneurysm surgery. J Neurol Neurosurg Psychiatry 2000; 68: 29–35

[20] Firsching R, Synowitz HJ, Hanebeck J. Practicability of intraoperative microvascular Doppler sonography in aneurysm surgery. Minim Invas Neurosurg 2000; 43: 144–148

[21] Martin NA, Bentson J, Vinuela F, Hieshima G, Reicher M, Black K, Dion J, Becker D. Intraoperative digital substraction angiography and the surgical treatment of intracranial aneurysms and vascular malformations. J Neurosurg 1990; 73: 526–533

[22] Karhunen PJ. Neurosurgical vascular complications associated with aneurysm clips evaluated by postmortem angiography. Forensic Sci Int 1991; 51: 13–22

[23] Macdonald RL, Wallace MC, Kestle JR. Role of angiography following aneurysm surgery. J Neurosurg 1993; 79: 826–832

[24] Selman W, Tarr R, Lanzieri C, Ratcheson R. Intraoperative angiography in the management of neurovascular disorders. Neurosurgery 1992; 31: 163

[25] Wrobel CJ, Meltzer H, Lamond R, Alksne JF. Intraoperative assessment of aneurysm clip placement by intravenous fluorescein angiography. Neurosurgery 1994; 35: 970–973

[26] Sindou M, Acevedo JC, Turjman F. Aneurysmal remnants after microsurgical clipping: classification and results from a prospective angiographic study (in a consecutive series of 305 operated intracranial aneurysms). Acta Neurochir (Wien) 1998; 140: 1153–1159

Gradual Formation of an Operative Corridor by Balloon Dilation for Resection of Subependymal Giant Cell Astrocytomas in Children with Tuberous Sclerosis: Specialized Minimal Access Technique of Balloon Dilation

N. B. Levine[1]
J. Collins[2]
D. N. Franz[2]
K. R. Crone[3]

317

Abstract

Background: Major sources of morbidity and mortality in patients with tuberous sclerosis who develop subependymal giant cell astrocytomas (SEGAs) relate to tumor growth and resultant hydrocephalus. We describe a modification of a specialized minimal access resection technique in which an operative corridor is formed with balloon dilation over the course of a week prior to tumor resection. **Methods:** Three patients with tuberous sclerosis who had an enlarging SEGA and concomitant hydrocephalus underwent surgical resection with this modified technique. A frontal craniotomy was performed and the optimal trajectory for tumor resection was confirmed by image guidance. After initial insertion of the deflated balloon into the ventricle and removal of the peel-away sheath, inflation of the balloon with a 1-mL saline injection sealed the tract. Additional 1-mL saline injections were continued during the next week until the balloon reached a 15-mm diameter, thus creating the operative corridor. One week after the first operation, the balloon was deflated and removed, and the patient underwent tumor resection via the newly formed operative corridor. **Results:** Three patients with tuberous sclerosis underwent gross total resections of SEGAs and experienced subsequent resolution of ventricular dilation. Postoperative imaging confirmed minimal cortical disruption. **Conclusions:** Use of balloon dilation for the gradual formation of an operative corridor eliminated the need for additional retraction during SEGA resection, potentially decreasing injury to the surrounding neural tissue. In our three patients, the dilation tract retained its integrity during the operation and had sealed completely on postoperative imaging.

Key words

Balloon dilation · operative corridor · tuberous sclerosis · subependymal giant cell astrocytoma

Introduction

Tuberous sclerosis is an autosomal dominant phakomatosis with low penetrance. Historically, it was characterized by sebaceous adenomas, mental retardation, and epilepsy, collectively referred to as Vogt's triad [1]. Neurological symptoms account for the primary source of morbidity. Up to 90 % of patients with tuberous sclerosis develop seizures, 50 to 70 % have mental retardation, and 20 to 60 % are autistic. Both hamartomatous lesions (e.g., cortical tubers, cardiac and renal rhabdomyomas) and locally invasive tumors (e.g., subependymal giant cell astrocytomas [SEGAs] and renal angiomyolipomas) may occur. Neuro-axis lesions include tubers, subependymal nodules, and subependymal giant cell astrocytomas. Five to 14 % of patients with tuberous sclerosis also have SEGAs [1–4].

Major sources of morbidity and mortality associated with tuberous sclerosis are related to the growth of SEGAs and the resultant

[1]Department of Neurosurgery, The Neuroscience Institute, University of Cincinnati College of Medicine, Cincinnati, OH, USA
[2]Department of Neurology, Cincinnati Children's Hospital Medical Center, Cincinnati, OH, USA
[3]Departments of Neurosurgery, Cincinnati Children's Hospital Medical Center and the University of Cincinnati College of Medicine, Cincinnati, OH, USA

Correspondence

Kerry R. Crone, M.D. · c/o Editorial Office · Department of Neurosurgery · ML 0515 · 231 Albert Sabin Way · Cincinnati, Ohio 45267-0515 · USA · Tel.: + 1/513/558/35 63 · Fax: + 1/513/558/77 02 · E-mail: editor@mayfieldclinic.com

hydrocephalus. Resection was typically undertaken in patients when radiographic and/or clinical evidence confirmed that hydrocephalus was present. Surgical approaches for the resection of intraventricular lesions include transcortical or transcallosal. Image guidance, coupled with microneurosurgical techniques has improved tumor resection. However, microneurosurgical dissection techniques require a cortical incision and varying degrees of cortical excision. Blunt dissection, bipolar electrocautery, and suction are used to approach deep brain or intraventricular lesions. Additional techniques to minimize damage to the cortex, specialized minimal access resection techniques (SMART), are imperative for the resection of deep brain or intraventricular lesions. Two such techniques include sequential cylindrical retractors and balloon dilation [5–9].

Some authors have reported the use of balloon dilation to create an operative corridor at the time of resection of deep brain or intraventricular lesions [5–7, 9, 10]. We modified this balloon dilation technique by forming the operative corridor before resection during the course of a week. We report our findings using SMART for the resection of lateral ventricle SEGAs in three patients with tuberous sclerosis, thus avoiding the development of symptomatic hydrocephalus.

Materials and Methods

Formation of the operative corridor

The patient undergoes a preoperative magnetic resonance imaging (MRI) scan with fiducial placement. The patient is positioned supine and rigid fixation of the head is achieved for frameless image guidance registration using BrainLAB (Vector Vision, Heimstetten, Germany). On the basis of the tumor location within the anterior horn of the lateral ventricle, a right or left skin incision is marked using the image guidance pointer. After a 3.5-cm skin incision is made, a high-speed drill (Medtronic, Minneapolis, MN) is used to create a 3-cm craniotomy that is 1 cm anterior to the coronal suture. The dura is opened and a small cortical incision is made after bipolar electrocautery.

A 12.5-French peel-away sheath introducer is registered with a navigational star and used to confirm the optimal trajectory. The introducer is placed through the frontal lobe, no more than 5 cm, with its tip at the frontal horn of the lateral ventricle. A mark is placed on the balloon catheter (Z-Med Peripheral Balloon Dilatation Catheter, B. Braun Medical Inc.), 15 cm distal to the tip, corresponding to the length of the introducer. The balloon catheter is inserted into the introducer. As the peel-away sheath is removed, the catheter is left in place and inflated with 1 mL of saline to seal the tract; the catheter is tunneled beneath the scalp away from the incision. A postoperative CT scan confirms the position of the catheter. Antibiotics are administered postoperatively during the next 7 days. On postoperative day 1 and each succeeding day (total 5 days), additional injections of 1-mL saline injections were continued until the balloon reached a diameter of 15 millimeters, thus creating the operative corridor (Fig. 1).

Tumor resection

One week after the first operation, the patient undergoes resection of the tumor. After the previous incision is opened, deflation and removal of the balloon leaves a cylindrically shaped operative corridor (1.5×4.0 cm). Use of a self-retaining halo retractor system maintains the dilation tract. Tumor removal is performed with an operative microscope. After gross total resection of the tumor, the ventricle is inspected and a septostomy is performed. An external ventricular drainage catheter is placed under direct visualization. Serial CT scans are obtained to follow ventricular size. When serial CT scans show neither an increase in ventricular size nor any indication of hydrocephalus, the catheter can be removed.

Clinical results

Three patients with tuberous sclerosis and MRI evidence of an enlarging SEGA and concomitant hydrocephalus underwent formation of an operative corridor with balloon dilation in preparation of surgical resection (from 2000 to 2003) (Table 1). Gross total resection with subsequent resolution of ventricular dilation was achieved in each patient. The average number of days of drainage in the three patients was 6.7 days. The balloon tract remained patent during the resection and postoperative imaging showed little to no evidence of the tract (Fig. 2).

Discussion

Gradual formation of an operative corridor via balloon dilation before resection of a SEGA eliminated the need for additional retraction during resection and presumably decreased potential retraction injury to the surrounding neural tissue in our three patients. In an attempt to reduce the damage to normal cortical neurons, balloon dilation to create an operative corridor has been described previously. Shahbabian et al. first described the technique in an experimental model using dogs [10]. Balloon dilation was demonstrated, both clinically and histologically, to incur less damage to the cortex than blunt dissection. Several groups subsequently used this balloon technique via a ventricular approach for brain grafting in the treatment of Parkinson's disease, a transcortical approach for deep cortical lesions, and a transcortical/transventricular approach for intraventricular lesions [5, 6, 7, 9].

Unlike previous applications in which balloon dilation was performed during resection, we modified this technique to form the operative corridor during the course of a week before performing the SEGA resection in children with tuberous sclerosis. The balloon dilation tract retained its integrity during the operation and sealed completely as seen on follow-up postoperative scans. Furthermore, the slow formation of the tract may reduce possible damage to the surrounding brain parenchyma incurred by rapid balloon dilation at the time of the operation.

Resection of deep brain and intraventricular lesions, such as SEGAs, remains a challenge by virtue of the critical structures that surround these lesions and the brain that must be transgressed to reach them. Damage to the cortex and white matter inevitably occurs. The transsulcal approach, advocated by Yasargil, decreases the extent of damage by reducing the area of cortex
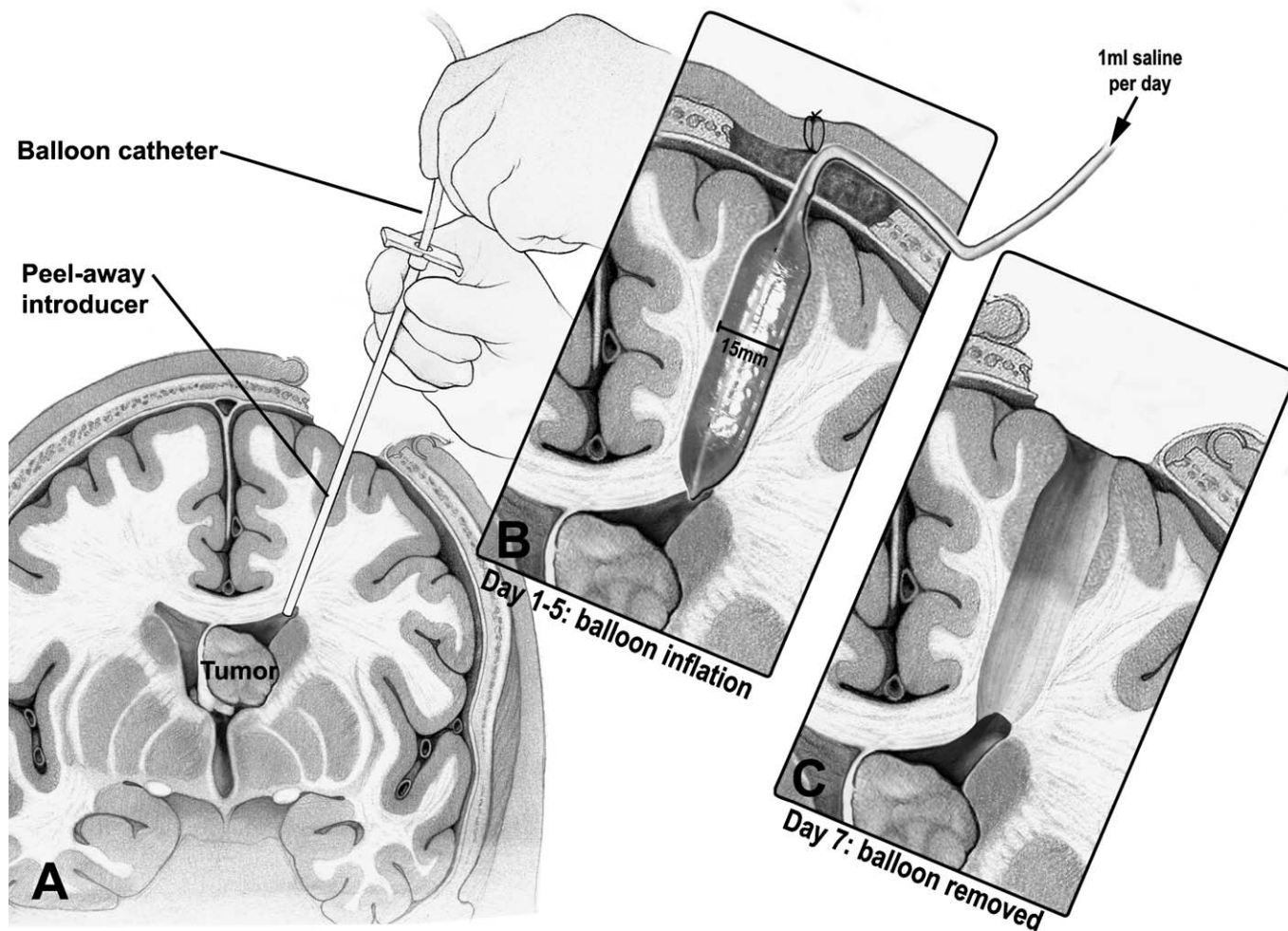
Fig. 1 Gradual formation of an operative corridor by balloon dilation over 7 days. **A** A small craniotomy performed on day 1 allows placement of a peel-away introducer into the frontal horn of the lateral ventricle through which a balloon catheter is inserted. The peel-away introducer is removed leaving the catheter in place. The catheter tube is tunneled to an exit point beyond the craniotomy and secured to the skin. **B** The balloon catheter is inflated with 1 mL of saline per day over 5 days to a maximum diameter of 15 mm. **C** The craniotomy is reopened on Day 7. After deflation and removal of the balloon, a 15-mm operative corridor to the lesion is formed (with permission from the Mayfield Clinic).

Table **1** Three children with tuberous sclerosis who underwent resection of subependymal giant cell astrocytomas (SEGAs) through an operative corridor created by gradual balloon dilation

Age (years), sex	Hydrocephalus	SEGA location and size (AP/transverse–cranial–caudal, cm)	Symptoms	Follow–up
5.5, m	yes	left foramen of Monro 2.4×1.4×2.2	asymptomatic	gross total resection
8, f	yes	right foramen of Monro 3.3×1.4×2.5	increased seizure activity	gross total resection
18, m	dilation of left frontal horn	left foramen of Monro 1.2×1.2×1.3	asymptomatic	gross total resection

and white matter transgressed to resect the lesion [5]. A trans-sulcal approach is not always possible and when used may not preclude postoperative sequelae, including seizures. Additional attempts at minimizing cortical destruction include approaches through "non-eloquent cortex." Transcortical approaches require limited resection of normal brain to reach the ventricle and necessitate increased retraction on normal surrounding cortex to maintain an operative corridor. Contusions and infarction secondary to intraoperative brain retraction have an incidence of approximately 10% in cranial base procedures and 5% in intracranial aneurysm procedures [11]. Delayed parenchymal injury can occur after excessive retraction and postoperative hematomas can be seen several days after an operation. Brain

deformation caused by retractor blades can result in a reduction or cessation of local perfusion and direct injury to neurons, neuronal processes, and/or glial cells. The shape and number of retractors, as well as the pressure and duration of retraction contribute to focal ischemia and subsequent parenchymal injury.

Transcallosal approaches have been advocated for the resection of intraventricular tumors, including SEGAs. The transcallosal approach not only avoids a cortical incision but also provides natural planes for dissection and anatomic landmarks for orientation. Complications of transcallosal surgery include venous infarction from disruption of bridging veins, thrombosis of the superior sagittal sinus from retraction, pericallosal artery injury,
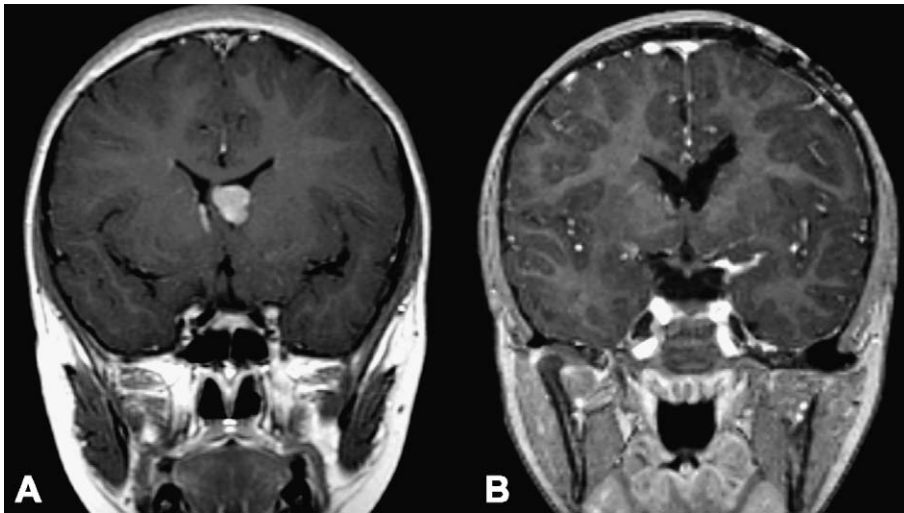
Fig. **2** Resection of SEGA in a child with tuberous sclerosis (coronal views). **A** MR scan showing evidence of a growing SEGA at the left foramen of Monro. After the child underwent a staged procedure with balloon catheter dilation over a week, the tumor was resected. **B** Follow-up scan shows no evidence of tumor recurrence, hydrocephalus, or cortical damage secondary to the operative corridor (with permission from the Mayfield Clinic).

cortical infarction, disconnection syndromes, and damage to the fornices and subcortical nuclei impairing memory and learning. With respect to SEGAs, which usually originate from the lateral ventricular wall at the level of the foramen of Monro, this approach may preclude a gross total resection by preventing adequate visualization of the tumor origin. Gross total resection is desirable to reduce recurrence and the need for reoperation [1, 4, 12].

Previous studies have established criteria for surgical resection of SEGAs, including hydrocephalus, tumor growth, new focal neurological deficits secondary to the tumor, and/or symptoms of increased intracranial pressure [1, 3, 12, 13, 14]. When surveillance imaging shows a growing SEGA, a minimally invasive resection can be undertaken before the development of tumor growth sequelae. The technique of using balloon dilation to form an operative corridor enables the surgeon to achieve gross total tumor resection in a less traumatic manner. Postoperative MRIs demonstrate little evidence of cortical damage.

Conclusions

In our three children with tuberous sclerosis who first underwent the gradual formation of an operative corridor, all then achieved gross total resection of SEGAs. We speculate that the slow dilation of the adjacent parenchyma capitalizes on the viscoelastic properties of the brain, thus resulting in less cortical damage and reducing surgical trauma during tumor resection via a generous surgical tract. Image-guided microcraniotomies can be successfully coupled with specialized minimal access resection techniques to minimize surgical trauma to surrounding cortex when approaching deep brain tumors.

References

[1] Abraham RG, Shyam Kumar NK, Chacko AG. A minimally invasive approach to deep-seated brain lesions using balloon dilatation and ultrasound guidance. Minim Invas Neurosurg 2003; 46: 138–141

[2] Andrews RJ, Bringas JR. A review of brain retraction and recommendations for minimizing intraoperative brain injury. Neurosurgery 1993; 33: 1052–1063

[3] Beems T, Grotenhuis JA. Subependymal giant-cell astrocytoma in tuberous sclerosis: endoscopic images and the implications for therapy. Minim Invas Neurosurg 2001; 44: 58–60

[4] Couillard P, Karmi MZ, Abdelkader AM. Microsurgical removal of an intraventricular meningioma with ultrasound guidance, and balloon dilation of operative corridors: case report and technical report. Surg Neurol 1996; 45: 155–160

[5] Cuccia V, Zuccaro G, Sosa F, Monges J, Lubienieky F, Taratuto AL. Subependymal giant cell astrocytoma in children with tuberous sclerosis. Childs Nerv Syst 2003; 19: 232–243

[6] Di Rocco C, Iannelli A, Marchese E. On the treatment of subependymal giant cell astrocytomas and associated hydrocephalus in tuberous sclerosis. Pediatr Neurosurg 1995; 23: 115–121

[7] Hirsch J-F, Sainte-Rose C. A new surgical approach to subcortical lesions: balloon inflation and cortical gluing. J Neurosurg 1991; 74: 1014–1017

[8] Kelly PJ. Principles of stereotactic surgery. In: Youmans JR (ed): Neurological Surgery. Phildaelphia, W. B. Saunders, 1990, pp 4208–4209

[9] Kim SK, Wang KC, Cho BK, Jung HW, Lee YJ, Chung YS, Lee JY, Park SH, Kim YM, Choe G, Chi JG. Biological behavior and tumorigenesis of subependymal giant cell astrocytomas. J Neuro-Oncol 2001; 52: 217–225

[10] Madrazo I, Franco-Bourland R, Aguilera M, Reyes P, Guizar-Sahagun G. Balloon needle for the atraumatic transcortical ventricular approach: technical note. Surg Neurol 1990; 33: 226–227

[11] Nabbout R, Santos M, Rolland Y, Delalande O, Dulac O, Chiron C. Early diagnosis of subependymal giant cell astrocytoma in children with tuberous sclerosis. J Neurol Neurosurg Psychiatry 1999; 66: 370–375

[12] Narayanan V. Tuberous sclerosis: genetics to pathogenesis. Pediatr Neurol 2003; 29: 404–409

[13] Shahbabian S, Keller JT, Gould HJ, Dunsker SB, Mayfield FH. A new technique for making cortical incisions with minimal damage to cerebral tissue. Surg Neurol 1983; 20: 310–312

[14] Sinson G, Sutton LN, Yachnis AT, Duhaime AC, Schut L. Subependymal giant cell astrocytomas in children. Pediatr Neurosurg 1994; 20: 233–239

320